Study of SiO_2- B_2O_3 based glass ceramics as sealants

A THESIS

SUBMITTED FOR THE AWARD OF DEGREE OF

Doctor of Philosophy

By

Vishal Kumar

Under the Supervision of

Dr. Kulvir Singh & Dr. O. P. Pandey

School of Physics & Materials Science

Thapar University

Patiala 147004

DECLARATION

I hereby certify that the work which is being presented in the thesis entitled, **"Study of SiO_2-B_2O_3 based glass ceramics as sealants"** in partial fulfillment of the requirements for the award of degree of Doctor of Philosophy in School of Physics & Materials Science at Thapar University, Patiala, is an authentic record of my own work carried out under the supervision of Dr.Kulvir Singh and Dr O.P.Pandey. The matter presented in this thesis has not been submitted by me for the award of any other degree of this or any other University.

(Vishal Kumar)

This is to certify that the above statement made by the candidate is correct and true to the best of my knowledge.

7/6/10

(Dr O. P. Pandey)

Professor & Head
School of Physics & Materials Science
Thapar University
Patiala- 147004

7/6/10

(Dr. Kulvir Singh)

Associate Professor
School of Physics & Materials Science
Thapar University
Patiala- 147004

ACKNOWLEDGEMENTS

At this momentous occasion of binding my thesis I would like to acknowledge the contribution of all those benevolent people who helped me during my PhD work. Knowledge is imparted through the developing relationship between the guru and the disciple. It is considered that this relationship, based on the genuineness of the guru, and the respect, commitment, devotion and obedience of the student, is the best way for subtle or advanced knowledge to be conveyed. I have been blessed to associate with. Dr. Kulvir Singh (Associate. Prof) and Dr. O.P.Pandey (Prof. & Head). They provided me a chance to work under their guidance and supervision, assisting with all kind of support and inspiration, wide counsel, constant encouragement, sincere criticism, valuable suggestions, expertise and fruitful advice which they proffered throughout this investigation and preparation of the thesis.

I am profoundly obliged to Prof. K.K. Raina, Deputy Director, Thapar University, Patiala for his constant encouragement and needful help during various stages of the work.

I am very thankful to Prof S.Mittal (Dean Research & Sponsored Projects) and Prof N. K. Verma, (Dean of Students Affairs) for their whole hearted support and blessings.

I am highly thankful to Department of Science and Technology for providing the financial support to carry out this work under the scheme SR/S2/CMP-48/2004. I would also like to acknowledge CSIR for their financial assistance.

My special thanks to Anu Arora and Ashutosh Goel for their valuable help at the initial stage of my work.

Words are inadequate in expressing my sincere thanks to my friends Dr. Ankush Pathania, Dr. Zinki Jindal, Dr. Birbikram Singh, Dr. Shefali Kanwar, Manmeetpal Singh and Amit Awasthi for their support in every moment of difficulty. I can never forget to mention the names of Dr.

Mohit Sharma, Himani Sharma and Navinder Singh, my best friends who stood by me during hard times through all thick and thin. I thank almighty for blessing me with friends like them.

I am also indebted to Dr. Pankaj Kumar, Dr. Ravi Kant, Manoj Kumar, Kamalpreet Kaur, Jasmeet Kaur, Bhupinder Kaur, Akshay Kumar, Kapil Sood, Neeraj Sharma, Sanjeev Kumar, Sarita Sharma, Indu Bala, Poonam Sharma and Sanjeev Kumar for their kind help and valuable suggestions whenever I needed.

I am especially grateful to Dr. C.P Khatter for helping me in designing of some tedious experiments.

I also thank Mr Ravi Sukhla and Mr. Dinesh for their help and precious time which they devoted for my cause.

My special thanks to Mr. Purushottam, Mr Vijay, Mr S. P. Yadav, Mrs Praveen, Mr. Indermani, Mr. Jant Singh and Mr. Gurmeet Singh for providing all kinds of help. All the faculties and staff of School of Physics and Materials Science are acknowledged who never turned me down whenever I approached for any help.

My wife Mrs. Gurbinder and my family deserve the special thanks and great appreciation for their patience, persistent moral support and capability to rejuvenate me during the course of the Ph.D. work at each step. Special thanks to my brother Mr. Ashish who stood by me all the times.

Last but not least my father Mr. Surinder Kumar and my mother Mrs. Sneh Lata are the two guiding pillars of my success. Especially my father whose constant motivation and financial assistance has been the sole source of inspiration and strength to carry out my work.

Above all, hidden force by Almighty God steered me in the right direction to achieve the goal.

Vishal Kumar

PUBLICATIONS:

1. Vishal Kumar, Anu Arora, O.P. Pandey and K. Singh, Studies on Thermal and Structural Properties of Glass Sealants for Solid Oxide Fuel Cell**, International Journal of Hydrogen Energy, *33*(2008) 434-438.**
2. Vishal Kumar, Sarita Sharma, O.P.Pandey and K. Singh, Thermal and physical properties of 30SrO-40SiO_2-20B_2O_3-10A_2O_3 (A=La, Y, Al) glasses and their chemical reaction with bismuth vanadate for SOFC, **Solid State Ionics 181 (2010) 79–85.**
3. Vishal Kumar, O.P.Pandey and K. Singh, Structural and optical properties of barium borosilicate glasses, **Physica B 405 (1) (2010) 204-207.**
4. K. Singh, Indu Bala, Vishal Kumar, Structural and optical properties of calcium borosilicate glasses**, Ceramics International, 35 (2009) 3401-3406.**
5. Vishal Kumar, O.P.Pandey and K. Singh, Effect of A_2O_3 (A = La, Y, Cr, Al) on thermal and crystallization kinetics of borosilicate glass sealants for solid oxide fuel cells**, Ceramics International, 36 (2010) 1621-1628.**
6. Anu Arora,Vishal Kumar, K. Singh and O.P.Pandey Thermal, structural and crystallization kinetics of ZnO-BaO-SiO2-of A_2O_3 based glass sealants for solid oxide fuel. (**Accepted**)
7. Vishal Kumar, O.P.Pandey and K. Singh, Study on nucleation of crystalline phases in lanthanum borosilicate glass, **(Press) Transactions of Indian Ceramic Society.**
8. Vishal Kumar, Rupali, O.P. Pandey and K.Singh Thermal and crystallization kinetics of yttrium and lanthanum calcium silicate glass sealants for solid oxide fuel **(Accepted) International Journal of Hydrogen Energy.**

9. Gurbinder Kaur, Vishal Kumar, O.P. Pandey and K. Singh Thermodynamical and configurational stability of disordered systems. (**Under Review**).
10. Sachin Tyagi,Vishal Kumar and K. Singh Al_2O_3 addition effect on invitro bioactive properties of sodium silicate glasses. **(Communicated).**

Presented at Conferences

1. Studies on thermal and structural properties of glasses as sealants for solid oxide fuel cells, Vishal Kumar, O.P. Pandey and K.Singh International Workshop on Hydrogen Energy, Jaipur (2006)
2. Thermal and structural properties of Sr based glasses as sealants for SOFC, Vishal Kumar, K.Singh and O.P. Pandey Punjab Science Congress, Thapar University, Patiala, YSA-B7, Pg 151 (2008)
3. Study on nucleation of crystalline phases in lanthanum borosilicate glass, Vishal Kumar, K.Singh and O.P. Pandey 72nd Annual session of Indian Ceramic Society, Jaipur Pg 65 (2009)
4. Thermal and structural analysis of Mg based glasses as sealants for solid oxide fuel cell Vishal Kumar, K.Singh and O.P. Pandey NIT (Hamirpur) (2009)
5. Thermal and crystallization kinetics of yttrium and lanthanum calcium silicate glass sealants for solid oxide fuel cellsVishal Kumar, Rupali, O.P. Pandey and K.Singh FUCETECH 2009 Symposium on Fuel Cell Technology, Mumbai.

INDEX

Chapter 2: Literature Review

Chapter 3: Experimental Techniques

Chapter 4: Results and Discussion

Part I

A. Barium borosilicate glasses

B. Calcium borosilicate glasses

Part II

B. Strontium and Magnesium borosilicate glasses

List of Figures **Page No**

Chapter 1

Chapter 2

Chapter 3

Chapter 4

Chapter 4 Part II

List of Tables Page No

Chapter 4 Part II

Preface

Glass and glass ceramics are being used in many fields of engineering and technology. Recently, glass and glass ceramics are also finding application in the field of renewable energy especially as a sealing material in solid oxide fuel cells as conventional sealing materials cannot work at the operating temperature (800-1000°C) of solid oxide fuel cells (SOFCs).

In order to check the feasibility of various glasses as sealing materials it is necessary to understand the crystallization kinetics, thermal and structural properties of the glasses. In addition, chemical interaction study with other components of SOFC is must for its end application as sealing material for longer duration. Basically, glass and glass ceramics must be chemically stable, mechanically rigid after sealing and thermodynamically nonreactive to meet the prerequisite condition as required for sealing material during operation of SOFC.

Based on literature survey and requirement for sealant, a series of glass compositions was selected and synthesized by melt quench technique. These glasses were characterized and studied for their thermal, structural and crystallization kinetics to check their suitability and feasibility as sealant for SOFC. The present thesis deals with the synthesis and characterization of SiO_2- B_2O_3-A_2O_3-MO, A= (Y, La, Al, Cr), M= (Mg, Sr, Ca, Ba) glasses. The entire work is presented in **four chapters**. In the **first chapter** general introduction of the present work is given. The historical origin of glasses, their evolution up to twenty first century is described in the first section of this chapter. The development process of flat glass (1905), sheet glass (1914), float process (1959) which enhanced the utility of glasses for their advanced applications has been given in second section. In the last section of this chapter the recent application of glasses as sealants in solid oxide fuel cells has been described.

Chapter 2 gives a detailed account of the literature survey in context of the solid oxide fuel cell. The work done on the glasses developed as sealing material for SOFC has been presented in this chapter. After reviewing all segment of literature the need to select this series was felt and accordingly the reason for it is given. In the last section of this chapter gaps in the study so far with aims and objectives of the work of the thesis is presented.

Chapters 3 describe about experimental procedure followed in this present work. On the basis of literature, glasses of desired composition were synthesized by melt quenching technique. The as prepared glasses were characterized by X-ray diffraction (XRD) studies, Scanning electron microscopy (SEM), Dispersive Analysis of X-rays (EDAX), Fourier Transform Infra-Red Spectroscopy (FTIR), Differential Thermal Analysis (DTA), Thermogravimetric Analysis and Dilatometery test. The details of glass preparation with characterization techniques are described in this chapter.

Chapter 4 The first part of this chapter describes the detailed thermal, structural analysis and crystallization kinetics of Barium and Calcium glass compositions i.e. BaO/CaO-SiO_2-B_2O_3-A_2O_3 (A=La, Y, Al, Cr). The thermal expansion and viscosity parameters were calculated to check their suitability as sealants. Apart from this interaction study of BaO-SiO_2-B_2O_3-Cr_2O_3 glass with Crofer 22 APU (interconnect) was done for 1h and 20h at 950°C. The detail of structural analysis including SEM of this interaction study has been presented in this chapter.

In second part Strontium and Magnesium glass series SiO_2- B_2O_3-A_2O_3-MO, A= (Y, La, Al, Cr), M= (Mg, Sr) have been discussed. After thermal analysis these glasses were heat treated at

different temperatures (800 °C, 900°C and 950°C) for different time durations (1h, 10h, 100h). The structural analysis of heat treated glasses was done with XRD and SEM. The details of this analysis are presented in this chapter.

Strontium based glasses were also studied for their chemical interaction with bismuth vanadate as electrolyte at 800 °C for 1h, 10h and 100h. The outcome of interaction results are also presented in this chapter.

Chapter 5 gives the conclusions for all the work.

1.1 Historical background of glasses:

Glasses have been used by the humans for thousands of years for different applications. The term glass is derived from a latin term “Glaseum” which means lustrous and transparent materials. Obsidian the natural glass made from sand melted by the intense heat of a volcanic eruption was used by human being as spear tips. Egyptian made first synthetic glass in the form of bead sand called it “faience”. The first colorless glass was produced in first century A.D. It can be defined as an inorganic product of fusion which has been cooled through its glass transition to the solid state without crystallizing [1-6]. A major milestone in the history of glass was the invention of lead crystals by George Raven Scroft. In later stages these glasses proved invaluable especially to optical industry. First time in 1851, the glass was used as a building material which opened new area for glass industry. Later on, glass manufacturing techniques improved with advancement of science and technology with time. The First glass bottle was made by Ashley in 1887 using fully automated process technique. There was acceleration in technological development in glass by various scientists during late nineteenth century.

In modern age, glass plays an essential role in science and industry. The optical and physical properties of glass make it suitable for different applications such as utensils, optoelectronic materials, laboratory equipment, thermal insulator (glass wool), reinforcement fiber in composites thermo chemical, nuclear and solar energy technologies etc. [7-12]. In addition to these, it is also being used as a decorative material since long back. Now a day, it features in almost every aspect of our lives.

1.2 Glassy state and its formation

The properties of luster, transparency are neither sufficient nor necessary to describe glass. Morey stated that "glass is an inorganic substance in a condition with, analogous to, the liquid state of that substance, but which as the result of a reversible change in viscosity during cooling has attained so high degree of viscosity as to be for all practical purpose rigid". According to American Society of Testing and Materials (ASTM), the glass is an inorganic product of fusion, which has been cooled to rigid condition without crystallization. However, these definitions do not include glass formation by chemical vapour deposition, sol-gel, ball milling and neutron irradiation of crystalline materials. Therefore in general, glass is defined as "solid with liquid like structure" or an amorphous solid. The long range order characteristic of crystalline solids is absent in glass and liquids, however, they may have short range order [13]. On the other hand Shelby [14] has defined the glass as any materials like organic, inorganic or metallic formed by any technique that exhibits glass transformation behavior is a glass.

During processing of materials, cooling rate plays very important role to decide the nature of the product. A slow cooling rate gives rise to a crystalline state with an abrupt reduction in the volume of the materials whereas a rapid cooling of the melts gives rise to a glassy state without the abrupt changes in volume. Crystallization can be prevented if the cooling rate is faster than the rate of crystallization. Basically, due to very fast cooling, the atoms and molecules are quenched in a disorder state during a continuous transformation temperature range leading to their arrangement becoming more like liquid although they become progressively more immobile.

There are several theories of glass formation such as Goldschmidt's radius ratio criterion, Zachariascn's, sun's single bond strength criterion, Smekal's mixed bonding rule and Stanworth's electro negativity rule. Modern theories of glass formation deal with glass formation by changes in processing known as kinetic theory of glass formation. The above mentioned theories are described in many standard text books on glasses for example Varshnaya (1994) [13] and Shelby (1997) [14]. However, it is worthwhile to give brief account of super cooled liquid and glassy state

1.2.1 Glass versus super cooled liquid

Glass is generally categorized as an amorphous solid rather than a liquid [15, 16]. Glass displays all the mechanical properties like a solid. On the other hand the notion that glass flows like a liquid to an appreciable extent over extended periods of time is not supported by empirical research or theoretical analysis. Therefore, glass can be considered as a solid since it is rigid according to everyday experience [17].

Contrary to above mentioned view, some researchers consider glass to be a liquid due to its lack of a first-order phase transition [16] where certain thermodynamic variables such as volume, entropy and enthalpy are continuous through the glass transition range. So, the glass transition may be described as analogous to a second-order phase transition where the intensive thermodynamic variables such as the thermal expansion and heat capacity are discontinuous [18]. Despite this, the equilibrium theory of phase transformations of solids does not entirely hold for glasses. Thus, the glass transition cannot be classified as one of the classical equilibrium phase transformations like solids [4].

Although the atomic structure of glass looks like structure of a super cooled liquid, however, it behaves as a solid below glass transition temperature [19]. A super cooled liquid behaves as a liquid, below the freezing point of the material, and will crystallize. The change in heat capacity at a glass transition and melting temperature are typically of the same order of magnitude, as observed for crystalline materials with similar structure. It indicates that the change in active degrees of freedom is similar in both the cases i.e**.** amorphous and crystalline state of the materials.

1.3 Basic components of glasses

The initial glass composition plays an important role in the formation of glasses and their structural, thermal and other properties. Therefore, selection of initial constituents and their molar ratio is very vital to optimize the glass properties as required for different applications. Based on single bond strength theory the common glass forming oxides can be categorized as glass former, glass modifier and intermediate oxides as given in table 1.1. The basic properties of these components are given in the following section of this chapter.

1.3.1 Glass network former

According to Goldschmidt theory oxides of general formula R_nO_m form glass easily when the ionic radius ratio of cation (R) to the oxygen ion lies in the range between 0.2 and 0.4. Cation form tetrahedron with anions when radius ratio of cations to anions lies between 0.2 and 0.4. In other words, materials containing tetrahedrally coordinated cations can work as a glass former. For example in silicate structure silicon cation forms covalent bonds with four oxygen

anions. These tetrahedrons connect in such a way that an intricate network of silicon and oxygen atoms is formed in which each oxygen atom acts as a bridge between two adjacent silicon atoms. Because of its interlinking structure, silicon dioxide is often called a network former [20]. Generally, the cation–oxygen bond strength in case of network formers is greater than 80 k cal/mol. Besides SiO_2, other glass network formers are P_2O_5, B_2O_3, GeO_2, TeO_2, SeO_2, As_2O_3, Sb_2O_3, V_2O_5, etc. All the above oxides form tetrahedral units, which share corners in their crystalline forms except B_2O_3, which forms triangular structure.

1.3.2 Glass network modifier

Alkali metal oxides are termed network modifiers, because these ions take up random positions in the glass network and thus "modify" or change the structure of the glass network. The network modifier bond strength usually lies in the range 10 - 40 k cal/mol. Similarly, alkaline earth elements locate into cavities of the glass network. However, bonds between alkaline earth ions and oxygen are stronger than alkali metals so neither a rapid decrease in viscosity nor a significant increase of the thermal expansion coefficient of the glasses is observed in alkaline earth based glasses.

Alkali metal oxides modify the glass network in such a way that every alkali ion creates one new non bridging oxygen (NBO) and every alkali oxide 'molecule' creates two NBO's. The modifier in network leads to change in various properties of glass. Therefore the properties of glass depend upon the ratio of BO's and NBO's. Modifying oxides create lower 'Qx' (x = 0, 1, 2, 3) tetrahedral structures by replacing bridging oxygens with nonbridging oxygens. It can be understood by the following scheme.

• Q3 tetrahedra: 3 bridging, 1 nonbridging oxygens per silicon

• Q2 tetrahedra: 2 bridging, 2 nonbridging oxygens per silicon

• Q1 tetrahedra: 1 bridging, 3 nonbridging oxygens per silicon

• Q0 tetrahedra: 0 bridging, 4 nonbridging oxygens per silicon

1.3.3 Role of intermediate oxides

Some oxides can either work as a network former or network modifier which depends on their chemical nature. Aluminum, titanium and zirconium oxides are classified as intermediate glass formers when they form the tetrahedron due to their higher coordination state in glass. They modify the glass network. Therefore, aluminum, titanium and zirconium are classified as intermediate oxides. The bond strength of these oxides usually lies in the range between 10 to 40 k cal mol^{-1}.

Table 1.1 Major Glass network formers, modifiers and intermediate oxides. (13)

Role of oxide	M in MO_x	Valence electrons	Dissociation Energy E_d per MOx (kcals)	Coordination number	Single bond strength (kcals)
Glass former	B	3	356	3	119
	Si	4	424	4	106
	Ge	4	431	4	108
	Al	3	402-317	4	101-79
	B	3	356	4	89
	P	5	442	4	111-88
	V	5	449	4	112-90
	As	5	349	4	87-70
	Sb	5	339	4	85-68
	Zr	4	485	6	81
Intermediate	Ti	4	435	6	73
	Zn	2	144	2	72
	Pb	2	145	2	73
	Al	3	317-402	6	53-67
	Th	4	516	8	64
	Be	2	250	4	63
	Zr	4	485	8	61
	Cd	2	119	2	60
Modifier	La	3	406	7	58
	Y	3	399	8	50
	Sn	4	278	6	46
	Ga	3	267	6	45
	In	3	259	6	43
	Th	4	516	12	43
	Pb	4	232	6	39
	Mg	2	222	6	37
	Li	1	144	4	36
	Pb	2	145	4	36
	Zn	2	144	4	36
	Ba	2	260	8	33
	Ca	2	257	8	32
	Sr	2	256	8	32
	Cd	2	119	4	30
	Na	1	120	6	20
	K	1	15	9	13
	Rb	1	115	10	12
	Hg	2	68	6	11
	Cs	1	114	12	10

1.4 Fuel cells and their types:

Fuel cells are electrochemical devices that convert the chemical energy directly into electrical energy, via an electrochemical reaction. Because there is no intermediate thermal conversion step, so these devices provide a highly efficient means of electrical power generation. In addition, high-temperature fuel cells such as solid oxide fuel cells (SOFCs) offer a great deal of fuel flexibility. They have the potential to directly utilize a wide variety of commercial fuels, such as natural gas, methanol, coal gas and liquid hydrocarbons. Hence, capable of bringing a significant reduction in pollution emissions relative to present-day combustion power plants. Other attractive features include the modular design of fuel cell stacks, which offers expanded capacity, the potential for distributed power generation, and noise-free operation.

The basic physical structure or building block of a fuel cell consists of an electrolyte layer in contact with a porous anode and cathode on either side. A schematic representation of a fuel cell with the reactant/product gases and the ion conduction flow directions through the cell is shown in Figure 1.1.

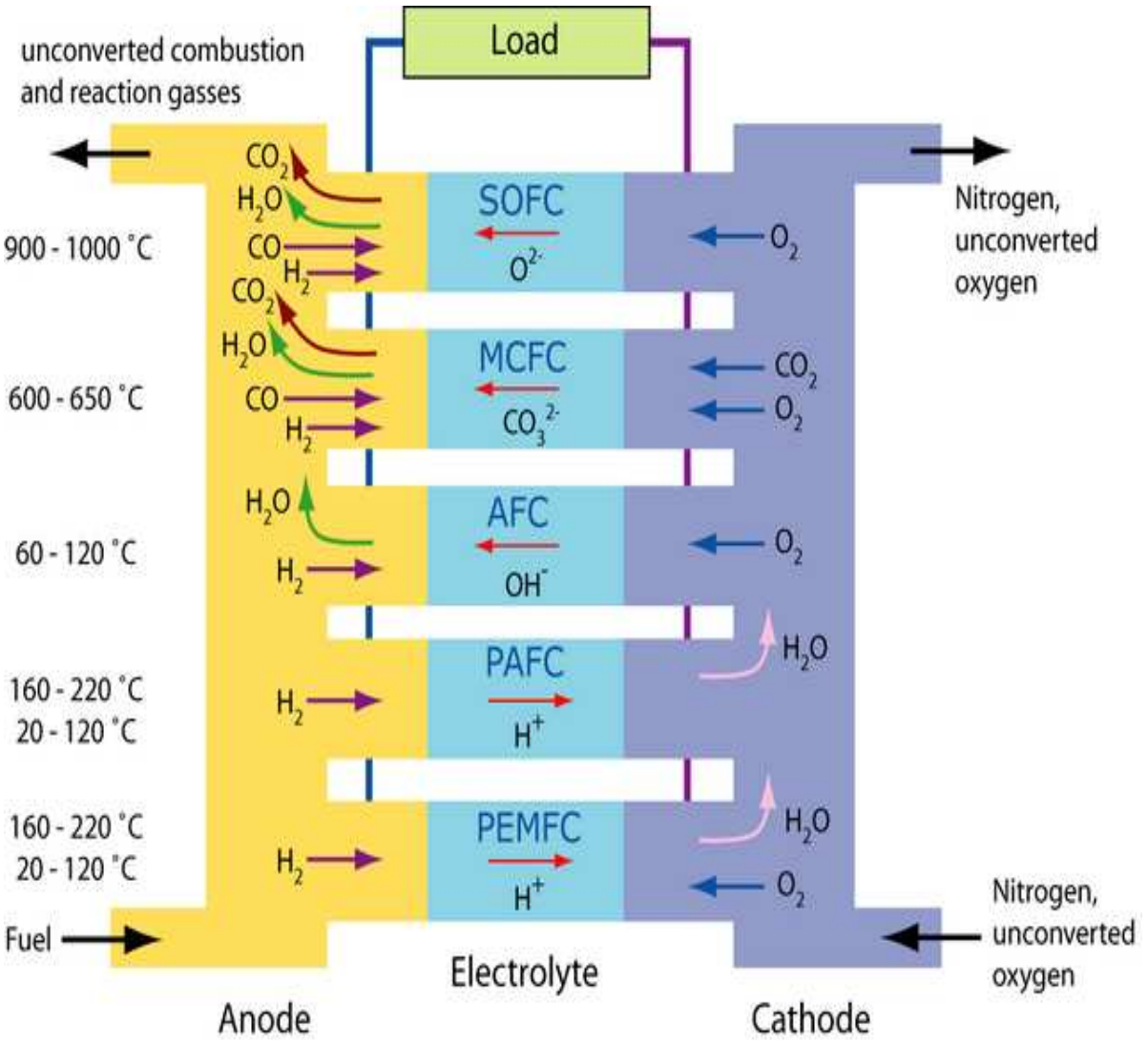

Figure 1.1: Working mechanism of different types of fuel cell [10].

In a typical fuel cell, gaseous fuels are fed continuously to the anode (negative electrode) compartment and an oxidant (i.e., oxygen from air) is fed continuously to the cathode (positive electrode) compartment; the electrochemical reactions take place at the electrodes to produce an electric current. Theoretically, the fuel cell is an energy conversion device that has the capability of producing electrical energy for as long as the fuel and oxidant are supplied to the electrodes. In reality, degradation, primarily corrosion, limits the practical operating life of

fuel cells due to degradation in fuel cell components. The transport ion can be either a positive or a negative ion, meaning that the ion carries either a positive or negative charge. The fuel or oxidant gases flow past the surface of the anode or cathode opposite the electrolyte and generate electrical energy by the electrochemical oxidation of fuel, usually hydrogen, and the electrochemical reduction of the oxidant, usually oxygen. Gaseous hydrogen has become the fuel of choice for most of fuel cell applications, due to its high reactivity with suitable catalysts. Moreover, it can be produced from hydrocarbons for terrestrial applications. Additionally, it can be stored cryogenically in compressed form for closed environment applications, such as in space. Similarly, the most common oxidant is gaseous oxygen, which is readily and economically available from air for terrestrial applications, and again easily stored in a closed environment. During fuel cell operation, a three phase interface is formed by the reactants, electrolyte, and catalyst in the region of the porous electrode. The nature of this interface plays a critical role in the electrochemical performance of a fuel cell, particularly in those fuel cells where liquid electrolytes are being used. In such fuel cells, the reactant gases diffuse through a thin electrolyte and react electrochemically on electrode surface. If the porous electrode contains an excessive amount of electrolyte it restricts the transport of gaseous species in the electrolyte phase to the reaction sites. Consequently, it reduces electrochemical performance of the porous electrode. Thus, a delicate balance must be maintained among the electrode, electrolyte, and gaseous phases in the porous electrodes. Much of the recent effort in the development of fuel cell technology has been devoted to reducing the thickness of cell components while refining and improving the processing of electrodes and electrolyte, with the aim of obtaining a higher and more stable electrochemical performance. The electrolyte not only transports dissolved reactants, but also conducts ionic

charge between the electrodes and thereby completes the cell electric circuit, as illustrated in Figure 1. It also provides a physical barrier to prevent the fuel and oxidant gas mixing. The functions of porous electrodes in fuel cells are as follows:

1 To provide a site where gas/liquid ionization or de-ionization reactions can take place.

2 To conduct ions away from or into the three-phase interface after formation of ions (so an electrode must be made of materials that have good electrical conductance.

3 To provide a physical barrier that separates the bulk gas phase and the electrolyte.

Based on these points, it can be concluded that in order to increase the rates of reactions, the electrode material should be catalytic as well as conductive and porous rather than solid for effective working of fuel cells. The catalytic function of electrodes is more important for lower temperature fuel cells. The most common classification of fuel cells is made on the basis of their electrolytes. The most common fuel cells are given below

1) Proton exchange membrane (polymer) electrolyte fuel cell (PEFC)

2) Alkaline fuel cell (AFC)

3) Phosphoric acid fuel cell (PAFC)

4) Molten carbonate fuel cell (MCFC)

5) Solid oxide fuel cell (SOFC).

Operating temperature, charge carriers, efficiency and the application of these are summarized in table 1.2. Similarly, their operating mechanisms are also shown in Figure 1.2. All types of fuel cells show some limitations and advantages over each other. For example aqueous electrolytes are limited to temperatures of about 200°C or lower because of their high water vapor pressure and/or rapid degradation at higher temperatures. Additionally, operating temperature also plays an important role in dictating the type of fuel that can be utilized in a

fuel cell. The low-temperature fuel cells with aqueous electrolytes are, restricted to hydrogen as a fuel. On the other hand high-temperature fuel cells, CO and even CH_4 can be used because of the inherently rapid electrode kinetics and the lesser need for high catalytic activity at high temperature. A brief description of various fuel cells and their working is given in the following sections.

1.4.1 Polymer electrolyte fuel cell (PEFC):

The electrolyte in this fuel cell is an ion exchange membrane. It is made by fluorinated sulfonic acid polymer or other similar polymers which is an excellent proton conductor. The only liquid in this fuel cell is water; thus, corrosion problems in this fuel cell are minimal. Water management in this fuel cell is critical for efficient performance. PEFC must operate under such conditions that the byproduct water does not evaporate faster than its production because the membrane must be hydrated. Due to the limitation, H_2 with minimal CO (a poison at low temperature) is used as a fuel in these Fuel Cells. Moreover, during fuel cell operation costly catalyst (usually Pt) is required in both anode and cathode side.

1.4.2 Alkaline fuel cell (AFC):

The electrolyte in this fuel cell is either concentrated (85 wt %) KOH or dilute KOH (35-50 wt %) depending upon the working temperature of the cell. In the cell wide range of catalysts (e.g., Ni, Ag, metal oxides, spinels, and noble metals) can be used for catalytic activity. The fuel flexibility is not possible in this fuel cell, only H_2 can be used. The fuel impurities (CO and CO_2) will react with the KOH to form K_2CO_3 and modify the electrolytes which deteriorates the performance of the cell. Even, the small amount of CO_2 will reduce the efficiency of fuel cell drastically.

1.4.3 Phosphoric acid fuel cell (PAFC):

Phosphoric acid is used for the electrolyte in this fuel cell. At lower temperatures, phosphoric acid is a poor ionic conductor. Moreover, CO poisoning of the Pt electrocatalyst in the anode side becomes severe. The relative stability of concentrated phosphoric acid is high as compared to other common acids; consequently the PAFC is capable of operating at 100 to 220°C. In addition, the use of concentrated acid (100%) minimizes the water vapor pressure so water management in the cell is not difficult. The universally accepted matrix material is silicon carbide which is used to retain the acid. The appropriate catalyst is Pt which can work on both sides of electrolyte.

1.4.4 Molten carbonate fuel cell (MCFC):

The electrolyte in this fuel cell is usually alkali carbonates or combination of Na and K, which is retained in a ceramic matrix of $LiAlO_2$. The operating temperature of this fuel cell is 600 to 700°C. At that temperature molten alkali carbonates exhibit high ion conductivity due to mobile carbonate ions. Due to high operating temperatures of MCFCs, Ni (anode) and nickel oxide (cathode) adequately promote the reaction even without catalyst. In other words, catalyst is not required in these fuel cells.

1.4.5 Solid Oxide Fuel Cell (SOFC):

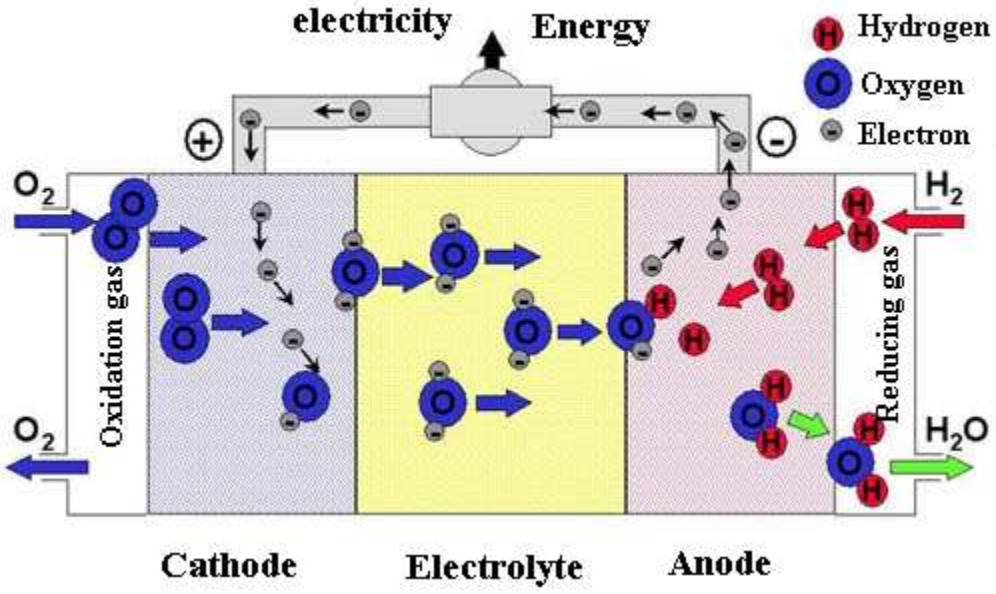

Figure 1.2: Schematic diagram of an Individual Fuel Cell [11].

The electrolyte in this fuel cell is a nonporous metal oxide, usually Y_2O_3-stabilized ZrO_2. The operating temperature of this cell is 650 to 1000°C. Typically, the anode is made by Co-ZrO_2 or Ni-ZrO_2 cermets. On the other hand, Sr doped $LaMnO_3$ is being used as cathode. The ionic conduction is taking place by oxide ions. Due to high working temperature individual catalyst is not required during cell operation. Another important advantage of SOFC over other fuel cells is its higher efficiency, less noise and emissions. Additionally, hydrocarbons like CH_4 can be used as a fuel after internal reforming. Detailed description of the components and their role in working of SOFC are described in next section.

Table 1.2 Details of different fuel cells [**10**]

Types of Fuel cell	**DMFC**	**PEMFC**	**AFC**	**PAFC**	**MCFC**	**SOFC**
Electrolyte type	Polymeric ion exchange membrane	Polymeric ion exchange membrane	Immobilized alkaline salt solution	Immobilized liquid phosphoric acid	Immobilized liquid molten carbonate	Ceramics
Operating temperature (°C)	20 – 90	30 – 100	50 – 200	~220	~650	800 – 1000
Charge carrier	H^+	H^+	OH^-	H^+	CO_3^{2-}	O^{2-}
Power range ()	1 – 100 W	1 – 100 kW	500 – 10 kW	10k – 1MW	100k – 10MW	1k – 10MW

As mentioned in previous section, SOFCs operating temperature is higher than other fuel cells (600-1000°C). Operating at high temperature is beneficial in the sense of internal fuel reforming and promotes rapid kinetics without precious catalyst. All parts of SOFC are made of either ceramics or high temperature alloys. Moreover, the involvement of liquid is negligible. Additionally high quality byproduct heat further enhances its efficiency up to ~85%. On the other hand high operating temperature of SOFC places stringent requirements on different components and their materials. The development of suitable cost effective materials is presently the key technical challenges being faced to commercialize the SOFCs [21]. The solid state character of all SOFC components means that, in principle, there is no restriction on the cell configuration. Instead, it is possible to shape the cell according to criteria required for different application. Figure 1.3 shows the working principle of solid oxide fuel cells.

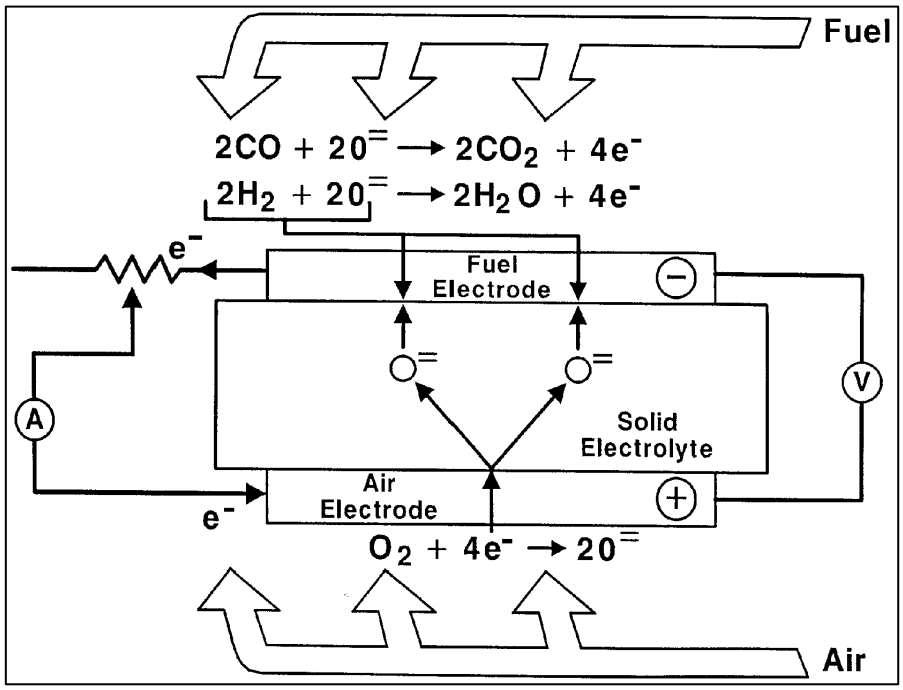

Figure 1.3: Operating Principle of Solid Oxide Fuel Cell [Siemens Westinghouse]

1.5 Components of solid oxide fuel cells

Due to high operating temperatures of SOFCs (approximately 1000°C), the materials used in the cell components are limited due to their chemical stability in oxidizing and reducing environments. Apart from this conductivity and thermo mechanical compatibility is also required. These limitations have prompted to develop and investigate different compositions of oxide and metals that can work and operate at intermediate temperatures range (650°C) [22]. The requirements of different components of SOFC are summarized in next subsections:

1.5.1 Cathode (air electrode)

The air electrode operates in an oxidizing environment of air or oxygen at 1000°C and participates in the oxygen reduction reaction. The air electrode in solid oxide fuel cells has to meet the following requirements [22, 23].

(a) High electronic conductivity.

(b) Chemical and dimensional stability in environments encountered during cell operation.

(c) Matching thermal expansion with other cell components.

(d) Compatibility and minimum reactivity with the electrolyte and interconnect/separator.

(e) Sufficient porosity to facilitate transport of molecular oxygen to the air electrode /electrolyte interface.

Cathodes are generally made of lanthanum compounds. $LaMnO_3$ is a p-doped perovskite structure which can undergo atomic distortion changing the shape of unit cells [24, 25]. It can easily acquire excesses or deficiencies in either lanthanum or oxygen. However, particular attention must be given to temperature variations as defects are functions of temperature. $LaMnO_3$ has intrinsic cation vacancies resulting in its p-type nature. Its conductivity can be further enhanced by replacing some atoms with lower- valence cations such as strontium, barium, nickel, magnesium or calcium. The substitution of La^{3+} with Sr^{2+} allow for a higher concentration of Mn^{4+} ions favoring conductivity. Furthermore, the reactivity and inter diffusion studies between doped lanthanum manganite and yttria stabilized zirconia electrolyte have shown any interactions between these two materials at 1000°C to be minimal [25]. Other materials of the same class as $LaMnO_3$ are investigated, such as $LaCrO_3$, which

has large oxygen deficiencies at high temperatures. This particular compound has a better conductivity under similar conditions, but is much less stable against reduction reactions. Tin-doped indium oxide has also been considered but was deemed too costly. For SOFC substantially lower operating temperature, such as 600-800 ° C, alternative cathode material has been developed and optimized since $LaMnO_3$ does not appear to be a satisfactory choice at lower temperature, owing to its low conductivity and slower oxygen transfer kinetics. Due to these shortcomings, other perovskite structure materials containing Co, Fe or Ni has received greater attraction but there are certain limitations such as TEC mismatching of Co with electrolyte, and electrical conductivity of Fe is low.

1.5.2 Anode (fuel electrode)

The requirements for the fuel electrode are similar to that of cathode [26, 22]. The main function of the anode is to facilitate the adsorption and oxidation of hydrogen from the fuel stream, thus permitting the oxygen ions from the electrolyte to combine with the hydrogen to form water and release electrons to the external circuit. Presently a common cheap material is being used as an anode for SOFCs. It is a Nickel-YSZ cermets, where the excellent electrical conductivity of nickel is combined with a porous YSZ powder and sintered at 1400°C, resulting in a highly porous, conductive electrode with many three-phase contact points. Nickel however, tends to catalyze the formation of carbon filaments in the absence of added steam and Ni-YSZ cermets are thus not an optimal choice in SOFCs where the use of carbon-based gases is often considered [27]. There is a thermal expansion coefficient mismatch between nickel and YSZ causing cracks in either the electrode or the electrolyte material. Copper and cobalt are two other materials that are beginning to see a wider use in fuel cell anodes. Although copper, and cobalt even more so, are expensive than nickel however, they

are cost effective than platinum. These metals can also withstand the high temperatures of a SOFC without being oxidized. Copper-ceria cermets based anode has been studied for the direct oxidation of hydrocarbon fuels. Copper suppresses carbon formation during direct oxidation while ceria improves the reaction kinetics. Unlike nickel, copper does not catalyze the carbon formation in CH_4 operated fuel cell.

1.5.3 Solid electrolyte

The electrolyte for solid oxide fuel cell must be stable in both reducing and oxidizing environments and must have sufficiently high ionic with low electronic conductivity at cell operating temperature. In addition, the material must be able to be formed into a thin strong film with no gas leaks. The required properties for these materials, fixed by both electrochemical constraints and high operating temperature, are the following [23]:

1. High ionic conductivity ($\geq 0.1 Scm^{-1}$ at $900^{\circ}C$)
2. Phase stability from room temperature to 1100°C approximately.
3. Thermal expansion coefficient compatible with other cell components.
4. Chemical compatibility with electrode and interconnection materials and with oxygen and fuel gas as well.
5. Gas tightness
6. Fracture toughness (>400MPa $m^{1/2}$ at room temperature)
7. Moderate cost of materials and fabrication

Based on these requirements the most promising candidate for fuel cell application is Yttria-stabilized zirconia (YSZ). The selection of YSZ as an electrolyte material is due to higher conductivity and desirable stability in both oxidizing and reducing atmospheres [28, 29]. High-temperature zirconia (ZrO_2) has the cubic fluorite structure. On cooling from its melting point (2680°C), it transforms to a tetragonal form at 2370°C and then to a monoclinic form at 1170°C. The high-temperature structure can be stabilized to room temperature by substitution of larger cations of lower valence (e.g.,$Zr_{1-x}Ca_xO_{2-x}$ or $Zr_{1-x}\ Y_xO_{2-0.5x}$) for Zr^{4+}, which also introduces oxygen vacancies on the normal sites and therefore lead to higher oxide-ion conductivity. The amount of dopant required to fully stabilize the cubic structure is about 12–13 mol% for CaO, 8–9 mol% for Y_2O_3 and Sc_2O_3, and 8–12 mol% for other rare-earth oxides.

The tetragonal phase is stabilized with low-dopant content, i.e., about 2 to 2.5 mol% for Y_2O_3 and several other rare-earth oxides. The cubic phase has low strength, toughness, and thermal shock resistance, whereas the tetragonal phase has extremely high strength and toughness due to a stress-induced phase transformation to monoclinic zirconia. Stabilized zirconia, however, requires an operating temperature of ~ 1000°C due to desirable conductivity requirements. Various problems are associated with such a high temperature: thermal stresses at the electrolyte-electrode and electrode-interconnect interfaces, inter diffusion between electrodes and electrolyte [30]. A substantial effort has been made to develop electrolytes, alternative to stabilized zirconia, with higher ionic conductivity at lower temperatures.

1.5.4 Inter connector or separator

Interconnect or separator is required to connect one unit of cell to other to increase the output voltage. Additionally, it serves as separator to prevent the mixing of fuel and air for smooth running of SOFCs [23, 22].

(a) Nearly 100% electronic conductivity.

(b) Stability in both oxidizing and reducing atmospheres at the cell operating temperature.

(c) Low permeability for oxygen and hydrogen to minimize direct combination of oxidant and fuel during cell operation.

(d) A thermal expansion close to that of the air electrode and the electrolyte.

(e) Non-reactivity with the electrodes, and easy to be fabricated.

(f) Low volatility and moderate cost.

Cell interconnects provide cell-to-cell electrical connection and separate fuel and oxidant gas atmospheres in a cell stack. Two most common interconnects extensively used in high-temperature and intermediate-temperature SOFCs are lanthanum chromite and different iron based metallic alloys.

Doped lanthanum chromite ($LaCrO_3$) ceramic is currently the most common candidate material for SOFCs for cells operating at temperature above 800°C. The dopants are Sr, Ca, Mg, Ni etc. Lanthanum chromite is a p-type conductor. This can be enhanced by doping of lower valence ions (e.g. Ca, Mg, Sr, etc). The substitution could be done either on La^{3+} or the

Cr^{3+} sites [22]. Chromite interconnects suffer from processing difficulties and high cost (high-temperature sintering, reactive powder synthesis, liquid phase additives, etc.).

As an alternative to ceramic interconnects, corrosion-tolerant conductive oxide scale forming commercial and experimental metallic alloys are also currently being investigated for use as current collectors in intermediate-temperature SOFCs. Metals and alloys offer the potential for lower cost, ease of fabrication and joining, excellent thermal conductivity, and commercial availability. Corrosion behaviors of Fe- and Ni-base alloys have been extensively studied under simulated fuel cell interconnect exposure conditions [31]. Metal loss and scale morphology results show that Fe-based austenitic or ferritic alloys experience accelerated localized corrosion under a dual atmosphere or bi-polar (simultaneous exposure to fuel and oxidant gases) conditions as compared to exposure to air environment. Therefore, these alloys are least preferred under a dual atmosphere.

1.6 Most common configuration of solid oxide fuel cell

The single unit of SOFC produces only 1volt direct current. So, it is necessary to stack SOFCs to increase the output voltage. The solid state character of all SOFC components means that, in principle, there is no restriction on the cell configuration and the cell can be designed into flexible shapes [32-33]. Instead, it is possible to shape the cell according to best suitable criteria from application point of view. Presently, cells are being developed in two different configurations namely sealless tubular and planar design. Both the designs have some advantages and disadvantages. The merit and demerit of both the designs are discussed below.

1.6.1 Sealless tubular configuration*:* The most advanced tubular solid oxide fuel cell is shown in fig 1.4. In this design seal is not required between adjacent cells and among the cell

components. A major advantage of this design over other designs is that relatively large single tubular cell can be constructed in which the successive active layers can be deposited without chemical or material interference with previously deposited layers. All the components of tubular cells can be deposited simultaneously on the one end closed support tube [34]. The fuel gas flows past the anode on the exterior of the cell and in a parallel direction to the oxidant. However, the seal-less tubular design results in a relatively long current path around the circumference of the cell to interconnect, limiting performance. Apart from this, the manufacturing of this design is costly and complicated due to requirement of highly sophisticated devices and instrumentation.

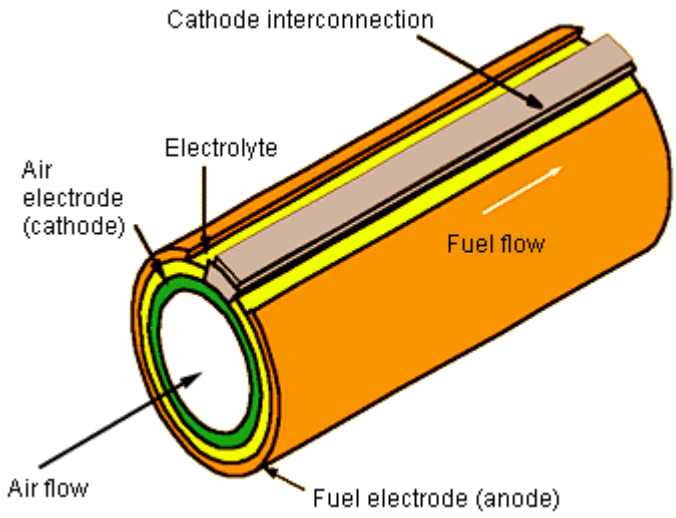

Figure 1.4: Tubular design of SOFC.

1.6.2 Bipolar (flat plate) configuration*:* The planar design offers improved power density relative to the tubular design. However, it requires high temperature gas seals at the edges of the plates as shown in fig 1.5. Compressive seals have been proposed; but these can lead to a non uniform stress distribution on the ceramic leads to cracks among the cell components. Further, seals may limit the height of a cell stack and there is a higher probability for

mismatches in tolerances creating unacceptable stress levels. It has structural ruggedness, concealed electrodes, ease of heat removal and low- stress assembly [35]. Moreover, their fabrication and assembly is simple as compared with tubular designs. Second concept of sealing is rigid sealing using glass and glass ceramics as a sealing material. Conventional sealing materials cannot work at that temperature (>600°C).

1.7 Role of glasses in planar design:

It is very clear that one of the technological problems in the development of planar solid oxide fuel cell (SOFCs) is the sealing of the stack. In a SOFC, the purpose of sealing is to prevent the mixing of air and fuel gasses (H_2, CO_2, CH_4) during cell operation. Leakage of fuel into air will lead to direct combustion and may cause local overheating with decreasing efficiency. An appropriate sealing material for planar SOFC is required to commercialize this technology.

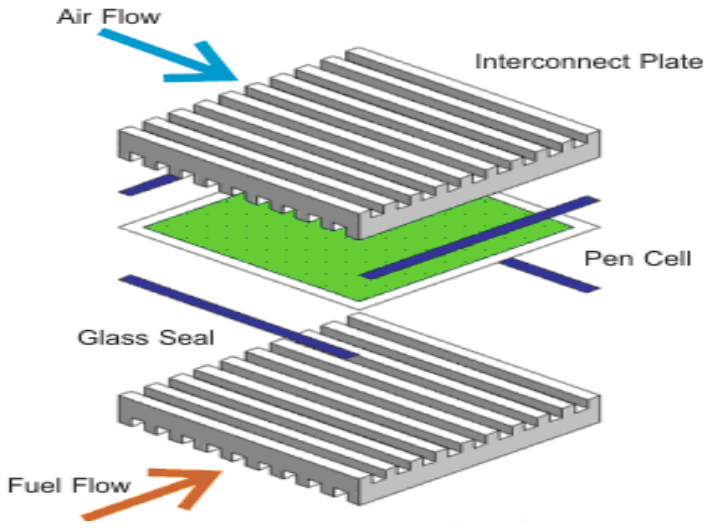

Figure 1.5: Exploded view of planar SOFC.

Figure 1.6: Stack of planar SOFC (Global Thermoelectric, Inc).

The stringent requirements of sealing material are such that good air tightness, adhesion with adjoining components, chemical compatibility, matching thermal expansion coefficient and electrical insulation. The sealing material should be in intimate contact with the stack components of SOFC in order to achieve the required good wetting capability with electrolyte and interconnect. It is necessary to ensure tight seal and limited chemical reactivity which is an essential parameter [36]. A variety of seals, such as metal-metal, metal-ceramic and ceramic-ceramic are used for the SOFCs. These seals must function for long times (5000-40,000 h) at high temperatures. The different mechanical, electrical, chemical and designing properties which are required for sealing are given in the following sections.

1.8 Properties required for sealing materials

As mentioned in previous section, sealing materials should have different properties so that it can withstand longer duration in stringent condition without deteriorating SOFC components by excess reactions.

1.8.1 Mechanical

- Hermetic sealing or marginal, non-localized leak rate
- TEC matching or mitigation of TEC mismatch stresses
- Acceptable bond strength or compressive loading requirement (i.e., load frame design)
- Resistant to degradation due to thermal cycling/thermal shock
- Robust under external static and dynamic forces [37]

1.8.2 Design/Fabrication

- Low cost and easy processing
- High reliability with respect to achieving initial hermeticity (seal conforms to non-flat substrate surfaces)
- Acceptable sealing environment/temperature i.e. has little effect on the subsequent performance of the stack)
- Design flexibility (e.g., allows use of Ni-based alloys in the interconnect)

1.8.3 Chemical

- Long-term chemical stability under simultaneous oxidizing/wet fuel environments
- Long-term chemical compatibility with the adjacent sealing surfaces
- Resistant to hydrogen embrittlement

1.8.4 Electrical

- Non-conductive

1.9 Different sealing options for SOFCs

The selection of sealing materials/techniques is closely tied to the specific application in which the stack will be used. Thus, it is dependent on a number of design factors, including individual assembly sequence, thermal gradients expected across the seal and other stack components, maximum weight and/or volume of the power plant, anticipated external forces, and required heating and/or cooling rate of the device [38]. Most common sealing concepts are glass joining or compressive sealing. Inherent advantages and limitations are found with each method. For example, glass joining is a cost-effective and relatively simple method of bonding ceramic to metal. However, the final seal is typically brittle and non-yielding, making it particularly susceptible to fracture when exposed to tensile stresses such as those encountered during non-equilibrium thermal events or due to thermal expansion mismatches between the glass and joining substrates [39, 40]. In addition, as the initial glass seal begins to devitrify during the first few hours of high temperature exposure, its engineered thermal expansion properties change significantly [41] ultimately limiting the number of thermal cycles and the rate of cycling that the stack is capable of surviving. Over time, additional problems arise as the sealing material reacts with other components forming a scale on the surface of the different components and resulting in mechanically weak phase formations at the interface [42]. In compressive sealing a compliant, high temperature material is captured between the two sealing surfaces and compressed, using a load frame external to the stack. Because the sealing material conforms to the adjacent surfaces and is under constant compression during use, it forms a dynamic seal. That is, the sealing surfaces can slide past one another without disrupting the hermeticity of the seal, and matching TEC is not required between the ceramic cell components and the metal separator. Unfortunately, this technology

remains incomplete, because of the lack of a reliable high-temperature sealing material that would form the basis of the compressive seal. Several materials have been considered, including mica, nickel and copper, but each has been found deficient for various reasons, such as oxidation resistance in the case of the metals to poor hermeticity and through-seal leakage in case of mica [43]. An additional difficulty is in designing the load frame, as it must be capable of delivering moderate-to-high loads in a high-temperature with oxidizing environment over the entire period of stack operation. Material oxidation and load relaxation due to creep, as well as added expense and additional thermal mass, are all issues of concern with this seal design. Other high-temperature joining techniques that have been considered include diffusion bonding, reaction bonding and active metal brazing. The extreme conditions required for diffusion bonding generally make this technique incompatible with planar stack fabrication. While reaction bonding has been used to join non-oxide ceramics such as SiC, less success has been demonstrated with forming hermetic ceramic-to-metal joints. The joints formed by this technique often contain residual porosity, shrinkage-induced cracks, unconverted reactants, and undesired secondary product phases, each of which can reduce the overall joint strength [44]. Active metal brazing employs a reactive element such as titanium to facilitate wetting between the filler metal and the ceramic faying surface [45]. However, two problems are encountered when using this technique to seal solid state electrochemical devices:

• The joint is not sufficiently resistant to oxidation, and will degrade under high-temperature operation [46].

• Joining must be conducted in a high-temperature, reducing gas environment, a condition that is too demanding for many of the pO_2-sensitive oxides used in the fuel cell [47].

1.10 Glasses as sealants:

Among SOFC designs, the planar stack (pSOFC) has received growing attention because its compact nature affords high volumetric power density – a design feature of particular importance in transportation applications. With the advent of anode-supported cells that employ thin yttrium-stabilized zirconium (YSZ) electrolytes, these devices can be operated at reduced temperature (700–800°C) and yet still achieve the same current densities exhibited by their high temperature, thick electrolyte-supported counterparts [48]. The lower operating temperature not only makes it possible to consider inexpensive, commercially available high-temperature alloys for use in the stack and balance-of plant, but also expands the range of materials that can be considered for device sealing. Because SOFCs function under an oxygen ion gradient that develops across the electrolyte, hermeticity across this membrane is paramount. In a planar design, this means that the YSZ layer must be dense, must not contain interconnected porosities, and must be connected to the rest of the device at high-temperature. One of the fundamental challenges in fabricating pSOFCs is how to effectively seal the thin, electrochemically active YSZ membrane against the metallic body of the device, in order to create a hermetic, rugged and stable stack.

Two important criteria for selection of a suitable glass sealant are the glass transition temperature (T_g) and the coefficient of thermal expansion (TEC). The glass transition temperature is important because the glass must flow sufficiently to provide an adequate seal, while maintaining sufficient rigidity for mechanical integrity. The softening temperature (T_s) is defined by the viscosity, and is thus a more direct measurement of flow characteristics of the glass. However, the trends in T_s typically follow those for T_g, which is easier to measure, so T_g data is available for a wider range of glass compositions. The thermal expansion

coefficient must match other cell components, such as (YSZ) electrolyte and the interconnect material, to minimize thermal stresses during the SOFC operation. Many glass sealant formulations are designed to soften and flow at a temperature above that required for stack operation in order to form a hermetic seal through a combination of mechanical and chemical bonding. When cooled to the stack operating temperature, the glass partially or fully crystallizes to form a rigid, bonded seal.

Typical conditions under which these devices are expected to operate and to which the accompanying YSZ-to-metal seal will be exposed in various conditions.

• An average operating temperature of 750°C.

• Continuous exposure to an oxidizing atmosphere on the cathode side and a wet reducing gas on the anode side.

• An anticipated device lifetime of more than 10 000 h.

The requirements allow specific oxide components of a sealing glass-ceramic, which form a systematic pattern in the periodic table of the elements. The elements of oxides that may show promising sealing properties for SOFC seals are marked yellow and given in fig.1.7.

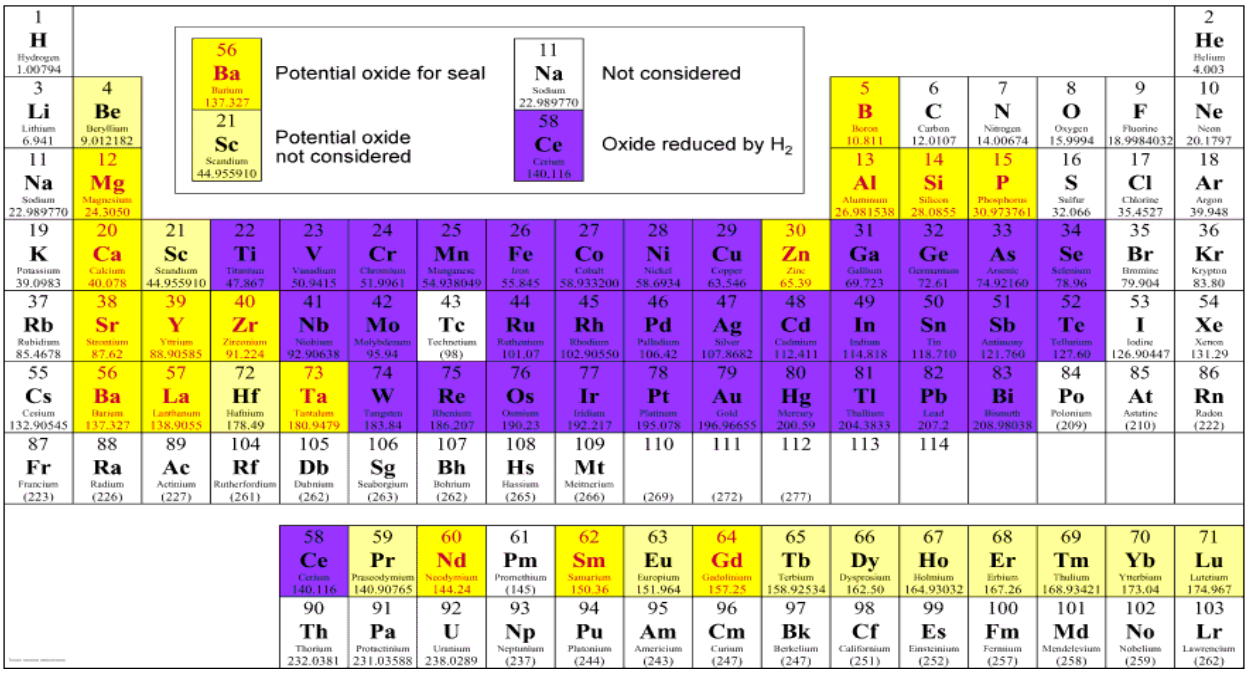

Figure 1.7: Potential oxides for sealing glass-ceramics.

Many glasses and glass–ceramics generally used for sealants contain alkali metals. Although some alkali metal containing glasses have been used for sealants in SOFCs, they are generally avoided because they react with other fuel cell components and can enhance the volatility of chromium which can lead to poisoning of the cathode. The advancement in field of glass will be given in chapter 2.

REFERENCES

[1] ASTM definition of glass from 1945; also: DIN 1259, Glas – Begriffe für GlasartenundGlasgruppen, September 1986

[2] Zallen, R. The Physics of Amorphous Solids. New York: John Wiley. (1983) ISBN 0471019682.

[3] Cusack, N. E. The physics of structurally disordered matter: an introduction. Adam Hilger in association with the University of Sussex press. (1987) ISBN 0852748299.

[4] Elliot, S. R. Physics of Amorphous Materials. (1984) Longman group ltd.

[5] Horst Scholze. Glass – Nature, Structure, and Properties. Springer. (1991) ISBN 0-387-97396-6.

[6] Werner Vogel Glass Chemistry (2 ed.). Springer-Verlag Berlin and Heidelberg GmbH& Co. K. (1994) ISBN 3540575723.

[7] V. Rajendaran , N. Palanivelu N, H.A El-Batal, F.A Khalifa and N.A Shafi Acoust.Letter.23 (1999), p.113.

[8] H.Hirashima, D. Arari and T.Yohida J.Am.Ceram.Soc 68 (1985), p.486.

[9] Vishal Kumar, O.P. Pandey and K. Singh Physica B 405 (2010) p.204.

[10] www.doitpoms.com. Department of Materials Science and Metallurgy, University of Cambridge .

[11] www.iwe.uni-karlsruhe.de

[12] A. Khanna, S.S Bhatti, K J Singh and K.S. Thind Nucl.Instrum.Methods B 114 (1996), p. 217.

[13] A.K Varshnya (1994), Fundamentals of inorganic glasses. Academic Press, San Diego.

[14] J. E Shelby (1997) Introduction to glass science and technology, The royal society of Chemistry, Cambridge.

[15] S. A. Baeurle, T Usami, A.A. Gusevet, Polymer 47 (2006) 6243.

[16] S.R.Elliott, Physics of amorphous materials London, longman group limited (1983) II nd Edition.

[17] Philip Gibbs Glass Worldwide, (2007) 14–18.

[18] M.I. Ojovan, W.E. Lee .J. Phys.: Condensed Matter 18 (2006) 11507–11520.

[19] **H. Rawson Glasses and their applications Royal Institute of metals, London, 499 (1991)166 ISBN 0901462896.**

[20] **Robert H Brill J. Glass studies 4 (1962) 127- 138.**

[21] N.Q. Minh, J. Am. Ceram. Soc., 76 (1993) 563-88.

[22] Battelle PNNL 17764 MST Handbook, U.S Department of Energy Pacific Northwest Laboratory (1994) 6.2.

[23] B. H. W. S. de Jong, "Glass"; in "Ullmann's Encyclopedia of Industrial Chemistry" 5th edition, vol. A12, VCH Publishers, Weinheim, Germany, (1989) pp 365–432.

[24] Horst Scholze Glass – Nature, Structure, and Properties. Springer. (1991).

[25] Hans-Heinrich Mobius, J. Solid State Chemistry 1(1997), 2-16

[26] Werner Vogel (1994). Glass Chemistry (2 ed.). Springer-Verlag Berlin and Heidelberg GmbH & Co. K. ISBN 3540575723.

[27] J. C. W Folmer, Franzen, Journal of Chemical Education 80 (7) (2003) 813.

[28] S.C. Singhal , MRS Bulletin 25 (3) 2000 16-21.

[29] Ivers-Tiffee, A. Weber, and D. Herbstritt, J. Eur. Ceramic Soc, 21(10-11) (2001), 1805- 1811.

[30] Ruifang Wang , Zhe Lu , Chaoqian Liu , Ruibin Zhu, Xiqiang, Huang, Bo Wei , Na Ai, Wenhui Su, J. Alloys and Compounds 432(1-2) (2007) 189-193.

[31] Prabhakar Singh, N.Q. Minh, Int. J of App. Ceram. Tech. 1 (1) (2004) 5-15.

[32] J. H. Hirschenhofer, D. V. Stauffer, R.R. Engleman and M. G. Klett Fuel Cell Handbook Parsons Corp (1998) 134.

[33] T.H. Etsell, S.N. Flengas, *J*. Electrochem. Soc, 1890 (1971) 118.

[34] A.O. Isenberg, in Proceedings of the Symposium on Electrode Materials and Processes for energy Conversion and Storage, edited by J.D.E. McIntyre, S.Srinivasan and F.G.Will, The Electrochemical Society, Inc., Pennington, NJ, 1977, p. 682.

[35] A.O. Isenberg, Proceedings of the Symposium on Electrode Materials and Processes for energy Conversion and Storage, edited by J.D.E. McIntyre, S. Srinivasan and F.G.Will, The Electrochemical Society, Inc., Pennington, NJ, 1977, p. 572.

[36] S. P.Jiang, L. Christiansen, B. Hughan, K. Foger, J. Mat. Sci. Lett. 20 (2001) 695.

[37] The State-of-the-Art in Sealing Technology for Solid Oxide Fuel Cells, K. Scott Weil, JOM August 2006.

[38] B.C.H. Steele and A. Heinzel *Nature* 414(6861) (2001), 345–352.

[39] K. Eichler, G. Solow, P. Otschik and W. Schaffrath , J. European Ceramic Soc. 19(6/7) (1999)1101–1104.

[40] Z.G. Yang, K.S. Weil, D.M. Paxton, K.D. Meinhardt and J. W. Stevenson (2003)Considerations of glass sealing solid oxide fuel cell stacks, *in:* J.E. Indacochea, J.N DuPont,T.J. Lienert, W. Tillmann, N. Sobczak, W.F.Gale and M. Singh (Eds),Joining of Advanced and Specialty Materials V (ASM) International, Materials Park, OH, (USA), 40–48.

[41] Z.G. Yang, K.S. Weil, K.D. Meinhardt, J.W. Stevenson, D.M. Paxton, G.-G. Xia and D.S. Kim (2002) Chemical compatibility of barium-calcium-aluminosilicate

base Sealing glasses with heat resistant alloys, *in:* J.E. Indacochea, J.N. DuPont, T.J. Lienert, W.Tillmann, N. Sobczak, W.F. Gale and M. Singh (Eds), Joining of Advanced and Specialty Materials V (ASM International, Materials Park, OH, (USA)116–124.

[42] S.P. Simner and J.W. Stevenson (2001) Compressive mica seals for SOFC applications, J. Power Sources 102(1/2) 310–316.

[43] E. Pippel, J. Woltersdorf, P. Colombo and A. Donato (1997) Structure and Composition of interlayers in joints between SiC bodies, J. European Ceramic Soc.17(10) 1259–1265.

[44] C.W. Fox and G.M. Slaughter (1964) Brazing of ceramics, Welding J. 43(7) 591–597.

[45] J.P. Rice, D.M. Paxton and K.S. Weil (2002) Oxidation behavior of a commercial gold based braze alloy for ceramic-to-metal joining, in: H.-T. Lin and M. Singh (Eds), Proceedings of 26th Annual Conference on Composites, Advanced Ceramics, Materials and Structures: B (American Ceramic Society, Westerville, (OH, USA).

[46] J.W. Stevenson, T.R. Armstrong, R.D. Carneim, L.R. Pederson and W.J. Weber J. Electrochem. Soc. 143(9) (1996) 2722–2729.

[47] J.S. Hardy, J.Y. Kim and K.S. Weil, J. Electrochem. Soc. 152 (2005) 52–58.

[48] Z.B. Shao, K.R. Liu, L.Q. Liu, H.K. Liu and S.-X. Dou (1993) Equilibrium phase diagrams in the systems PbO–Ag and CuO–Ag, J. American Ceramic Soc. 76(10) 2663–2664

2.1 Background

As mentioned in the previous chapter glass and glass ceramics are essential and important part of planar design of solid oxide fuel cells (SOFC). Due to high working temperature and other stringent conditions for SOFC, sealing material should have some basic properties for their application as a seal material in planar design of SOFCs. Additionally the glass seal forms different interface with various parts of SOFCs as shown in fig. 2.1.

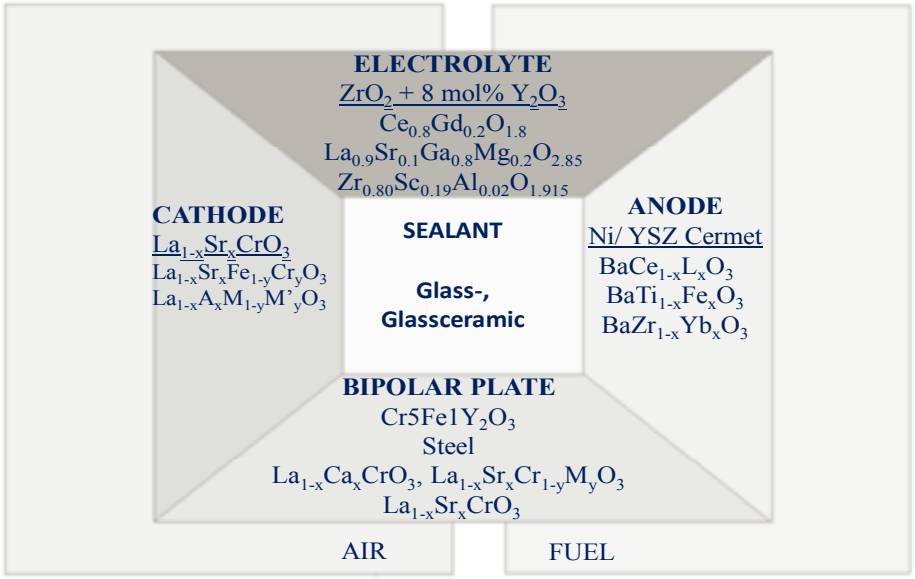

Figure 2: Components and possible interfaces of Solid Oxide Fuel Cells.

According to these requirements the glass transition temperature and melting temperature must be lower and higher than operating temperature of SOFCs, respectively. Apart from this, sealing materials should be electrically insulated and chemically stable up to operating temperature of SOFCs. Moreover, during operation of SOFCs glass gets converted to the glass ceramic and may form some detrimental crystalline phases which

are responsible to deteriorate the overall performance of the SOFC. Above mentioned properties are very sensitive to initial constituents of glasses, their mol% and chemical nature of the glass components. Lot of research has been carried out all over the world to find appropriate sealing glass and glass ceramics for SOFCs. In this chapter, the various influencing factors for sealing properties, related results and advancements in the field of glass sealants are summarized.

2.2 Various factors and their influence on sealing properties

2.2.1 B_2O_3/SiO_2 ratio

Independent studies of glass have shown that the B_2O_3/ SiO_2 ratio is a dominant factor for determining the glass transition temperature, T_g and the viscosity. Glasses with high B_2O_3/ SiO_2 ratios exhibit higher T_g as compared to glasses with lower fraction of B_2O_3/ SiO_2 ratio [1, 2, 3]. This can be explained on the basis of the property of formation of boron-oxygen triangle by B_2O_3, which deteriorate the strength of basic tetrahedral Si-O glass network. Due to this reason, viscosity of glass decreases which furthermore leads to the enhancement in wetability of glasses. Ley et al. [1] have reported that small amount of La_2O_3 have a stronger influence on viscosity than the B_2O_3/SiO_2 ratio. An increase in La_2O_3 amount in glass composition leads to decrease the viscosity of the glass. Similarly, Sohn et al. [2] studied the controlled effect of La_2O_3 on the viscosity of glass and reported that higher content of BaO increases the thermal expansion coefficient (TEC). On the other hand, Al_2O_3 content in glass prevents the rapid crystallization of glass during heat-treatment. Lara et al. [3] have also reported a decrease in TEC of the glasses on increasing the SiO_2 content. Additionally, in borosilicate glasses, boron reacts with a

humidified hydrogen atmosphere to form the gaseous species $B_2(OH)_2$ and $B_2(OH)_3$ at the operating temperature of SOFC. Therefore, high boron glass may get corroded in a humidified hydrogen environment. Moreover, B_2O_3 containing glasses have shown weight loss in the humidified hydrogen environment up to 20 % and extensive interactions with other components of SOFC in both oxidizing and reducing atmosphere [4].

2.2.2 Effect of additives

Several additives are used to optimize the properties of the glass sealants. However, the choice of additives is restrictive as they do not influence just one property of the sealant but also the other properties of glasses. Al_2O_3, for instance, improves flux, thus making for better joining behavior. On the other hand, higher content of Al_2O_3 decreases the thermal expansion coefficient, as it promotes the formation of a detrimental crystalline phase, which exhibit low thermal expansion coefficient [5]. Similarly, Na_2O acts as the most effective flux, but it makes the glass soluble in water. Na_2O can be replaced by K_2O but K^+ cations enhance the volatility of chromium [6, 7] thus, poisoning the cathode and also react vigorously with the other components of fuel cell leading to the formation of undesirable low TEC phases [3, 8-10]. Bloom et al. [11] evaluated, Corning 0080, a commercial glass for possible use as sealants for the SOFC. It is a soda-lime glass, with TEC of 9.35 x 10^{-6} $^oC^{-1}$. It produced good bonds with YSZ but it shows unacceptable chemical and/or physical interactions with the various interconnect materials. The effects of various additives on the different properties of sealants are listed in Table 2.1.

Table 2.1 Effect of additives on various properties of glasses [1, 7, 10, 12-18]

Additive	Effect
Al_2O_3	Improves flux. Prevents rapid crystallization of glass during heat treatment and also increase surface tension of glass. Too much Al_2O_3 decreases thermal expansion as it promotes the formation of crystalline phase with low TEC.
Na_2O, K_2O	Act as effective flux but the alkali cations react vigrously with the fuel cell components like cathodes; have undesirable TEC. Increases conductivity
La_2O_3, Nd_2O_3, Y_2O_3	Increase TEC, T_g, T_M
B_2O_3	Improves flux, reduces T_g, surface tension and stability of glass
ZnO, PbO	Improves flux, reducing agent
Cr_2O_3, V_2O_5	Reduces surface tension
NiO, CuO, CoO, MnO	Improves adhesion
TiO_2, ZrO_2, SrO, MgO, Cr_2O_3, Ni	Stimulates crystallization
Sb_2O_5	Oxidizing agent
P_2O_5	P_2O_5 decreases volatilization, reduce TECs and mechanical strength

The effect of small additions of TiO_2 and P_2O_5 has been studied by several researchers. These agents enhance the nucleation of crystalline phase in the glasses and induce phase separation in glasses. Presence of Al_2O_3 has a marked effect to prevent the crystallization. If Al_2O_3 concentration is less than 5 mol % it does not exhibit any phase separation. However, if Al_2O_3 content increases, it leads to phase separation. The structural role of Al^{3+} for its deviation in nature is because of variation in coordination number of Al^{3+}. Higher coordination number connectivity of Al^{3+} cations leads to phase separation [13].

Tomozawa [19] explained the greater tendency of phase separation of P_2O_5 over TiO_2 as a result of higher ionic potential (Z/r) of phosphorous than titanium ions. TiO_2 is quite readily soluble in silicate glasses and leads to lowering of viscosity considerably. A number of other oxides have been used as nucleating agents. Among these are zirconium, chromium, vanadium, iron, zinc and nickel. Their field strength played important role in the phase separations among the glasses.

Larsen et al. [14] revealed a number of challenging problems with glasses particularly P_2O_5 rich glasses. At high temperature, the phosphate volatilized and reacted with the Ni/yttria-stabilized zirconia-based anode to form nickel phosphide and zirconium oxyphosphate. Additionally, when de-vitrified these phosphate glasses typically form meta- or pyrophosphates, both of which exhibit low stability in humidified fuel gas at temperatures greater than 700^{o}C.

Nucleating agent containing glass is often heat treated in two stages. Initially glass is given a lower temperature heat treatment (nucleation treatment) and in second stage heat treatment which leads to the controlled crystallization within glass matrix. The separation between these two processes is not distinguishable since in some cases crystallization probably occurs during nucleation treatment itself [20].

At least three different mechanisms have been proposed for the action of nucleating agents. Their role can be classified such as crystallization agent, catalysts of phase separation, and reduction of interfacial tension. However, very few reports have appeared in the literature on the role of first two actions of nucleating agents. After rejecting the other possibilities, Hillig [21] suggested that these agents lower the interfacial tension, between the crystallites and the glass matrix, thus increasing the rate

of nucleation. This idea has been confirmed by measurements of crystal numbers as a function of time in lithium aluminosilicate glasses containing different amounts of titania as nucleating agent [22]. The change in titania concentration was too small to change the heat of fusion appreciably, so the increase in nucleation rates must result from a reduction in the interfacial energy. Ions of high field strength can possibly act as "surface active agents" to lower the interfacial energy. Barry et al. [23] have extended this idea in developing a detailed model for the enhancement of crystalline nucleation by titania in lithium aluminosilicate glasses. According to them, Ti^{4+} ions associate with the non-bridging oxygen ions, causing these ions and alkalis to concentrate at the edge of domains enclosing bridging oxygens. Based on this hypothesis, the effect of initial composition on nucleation of the different crystalline phases in the glasses can be explained.

2.2.3 Crystallization of glasses

Glass crystallization is advantageous for several reasons: the resulting material is typically stronger than the starting glass and by controlling the kinetics of crystallization and the product phases that form, it is possible to tailor the properties. During SOFCs operation the glass gets converted into glass ceramic and forms some crystalline phases. Glass ceramics also exhibit superior mechanical properties than the glasses. On the other hand, nucleation of different crystalline phases sometimes leads to decrease or increase the TEC. Therefore, it is worthwhile to study the crystallization kinetic of the glasses. Basically understanding the fundamental mechanisms of glassy state is impossible without understanding the nucleation and growth process of crystalline phases in glass matrix [6, 8, 9, 12, 24, and 25]. As mentioned in previous paragraph glass–ceramics,

possess superior mechanical properties and have very different thermal expansion coefficients (TEC) compared to glass, due to nucleation of different crystalline phases in different volume fractions. The crystallization behavior of the glasses can be classified into two types, namely, slow crystallization which leads stable crystallization with the long-term operation of SOFCs. On the other hand, the second type is rapid crystallization. The rapid crystallization of glasses is thought to be unsuitable for long-term operation of SOFC [26]. Moreover, rapid crystallization of glass sealants during cell operation can deteriorate the fluidity of the glasses because of a significant decrease of the residual glass matrix. It can also lead to thermal expansion mismatch, especially if the TEC value of the increasing crystalline phase differs significantly from that of the parent glass. Lot of work has been carried out on glass and glass ceramics to check their suitability as a sealant for solid oxide fuel cells. Various glass-forming systems have been considered as pSOFC sealants, including those based on phosphates, borates, and silicates. However, prior work has shown that phosphate and borate glasses are not sufficiently stable in the humidified fuel gas environment, tending to undergo significant corrosion through the formation of volatile species as well as reacting with and degrading the various cell materials [27-29]. To date, the best results have been obtained using compositions based on silica with various modifiers added to increase TEC and improve adhesion and joint strength. In the following paragraphs most common glass systems are discussed with their suitability as sealing materials for SOFCs.

2.3 Selection criteria of glass sealants

Alkaline earth metals based glasses have been studied extensively for sealing properties. These systems are important from sealing point of view; their binary phase diagram is

given in figure 9. The preference of alkaline earth metals over alkali silicate glasses is due to later's tendency to interact detrimentally with the cell materials [30]. The use of alkaline-earths to form systems such as $BaO\text{-}CaO\text{-}SiO_2$ [31] and $BaO\text{-}Al_2O_3\text{-}SiO_2$ [32] yield glass-ceramics with much higher chemical resistance and far less reactivity toward other stack components [33-34].

This strategy has been used to prepare sealants that have been tested beyond 1,500 hours of continuous operation of SOFC. There are several challenges in developing an acceptable glass-ceramic for pSOFC sealing. First is achieving the proper balance of material properties that results in a consistent and repeatable sealing process. By control of crystallization, the viscosity of the sealant can be raised slowly so that it attains the proper stiffness after wetting to minimize excessive flow or "squeeze out." In addition to viscosity, several other key material parameters must be simultaneously controlled to achieve a robust sealing process, including T_g, T_s (the temperature at which the glass first softens), TEC, wetting behavior, and bulk strength. These factors can be optimized in one of two ways. The first involves tailoring the initial glass composition and the heating schedule employed during sealing [35, 36] to control the rate of crystallization, which primarily affects viscosity and wetting behavior, and the nature of the crystalline phases, which impacts TEC, T_g, T_s, and sealant strength. Listed in table 2.1 are compositional

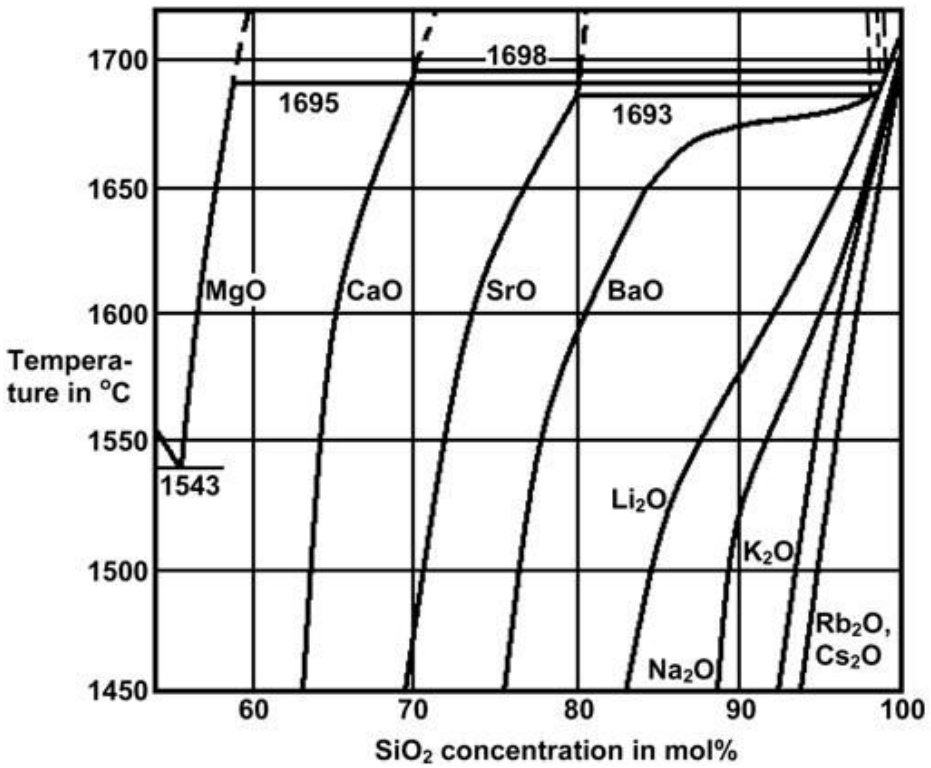

Figure 2.1: Immiscibility in binary alkali earth silicate glasses [37].

modifiers that are commonly added to alter the initial bulk properties of the glass with no incipient leakage [38, 39]. In the second method, either an inert or reactive filler material (i.e., powder or fiber) [40, 41] is added directly to a fluid glass matrix to increase viscosity and raise the TEC of the resulting composite. The fillers also act as nucleation sites, thereby influencing the kinetics of subsequent crystallization. To date, this strategy has met with less success than the former. The second key challenge in developing a useful glass-ceramic sealant is to stabilize the material's TEC as a function of time and temperature. If the TEC changes too much, the bonded joint becomes susceptible to cracking during thermal cycling. The primary culprit for the time-dependent reduction in TEC is the transformation of a key crystalline phase, celsian, from its metastable, high-TEC structure (hexacelsian) to its stable, low-TEC form (monocelsian). It is possible to

stabilize the long-term TEC properties of glass-ceramics by again modifying the starting glass composition or by incorporating filler additions [41, 42]. Several glass-ceramic formulations prepared using the former approach have been reported to survive over 30 thermal cycles in full-scale stacks at slow-to-moderate heating/cooling rates (i.e., ~2–5°C/min)[40, 43]. Alternatively, there are new concepts to develop glass-based systems that can withstand some degree of thermally induced cracking by self-healing when re-heated [44].

La_2O_3 is reported to increase the thermal expansion considerably, similar to SrO and BaO [45]. It should be investigated if La_2O_3 offers advantages over SrO and BaO. The rare earth oxides and Y_2O_3 are reported to have similar properties [46]. Glass formation and thermal expansion increase with increasing ionic radius, while viscosity decreases. Therefore, among the rare earth oxides, Nd_2O_3 and Pr_2O_3 may be preferred. However the rare earth oxides do not seem to offer advantages as compared to SrO and BaO. Among alkali oxides Cs_2O is reported to cause comparable or less ion diffusion than alkali earth oxides [47, 37, 48]. On the contrary its chemical stability in water, evaporation [49], and its strong basicity are major disadvantages.

It becomes very clear from above discussion that constituents of glass composition influence the sealing properties remarkably. Therefore in preceding section of this chapter the details of development of alkaline earth metal glasses are given in different sub-sections.

2.3.1 Magnesium silicate system

The crystallization of glass in this system is extremely complex because of the large number of phases, many of them metastable, which can be crystallized form the glass.

Barry et al. [50] demonstrated that the sequence of crystallization can vary from non stoichiometric to stoichiometric cordierites depending upon the nucleating agents (i.e. titania or titania plus zirconia).

A typical sequence of crystallization for a near-stoichiometric cordierite glass-ceramic containing approximately 11 wt. % TiO_2 as the nucleating agent would proceed in the following manner. During heat-treatment, initially glass undergoes amorphous phase separation preceding the precipitation of [(Mg, Al) $(Ti, Al)_2O_5$], a pseudobrookite phase. On further heat treatment of the glass (900^oC), a metastable silicate phase is formed which is, stuffed derivative of the β-quartz solid solution phase. Subsequently, this solid solution phase breaks down to a very fine mixture of silicious quartz and spinel at slightly higher temperatures than 900 ^oC and forms cordierite and rutile phases. The formation of cordierite and rutile phases is very rapid near 1200^oC due to solid-state reaction between quartz, sapphirine, and pseudobrookite. These phases are stable at temperatures above 1250^oC.

When mixtures of TiO_2 and ZrO_2 are employed as nucleating agents, the sequence of crystallization differs in a way that β-quartz and magnesium petalite are observed in the early stages of crystallization and a minor amount of cristobalite occurs at higher temperatures, which delays the conversion to cordierite. The influence of alkaline earth metals A (A=Ba, Ca, Mg) and nucleating agents (TiO_2, ZrO_2, Cr_2O_3 and Ni) on the crystallization kinetics of $AO-Al_2O_3-SiO_2-B_2O_3$ glasses has been studied by thermal and microstructural studies [5, 7, 13, 16, 51]. The activation energy of crystal growth, E_a, was shown to be varying between 330 and 622 $kJmol^{-1}$. It was observed that E_a increases with nucleating agents except ZrO_2. Cr in the hexavalent state and Ti^{4+} ion posses a high field

strength imparting a marked ordering effect in MgO-Al_2O_3-SiO_2-B_2O_3 glasses. These may be the reasons for higher E_a values for the glasses containing ZrO_2 or without nucleating agent. An increase of the Al_2O_3 concentration induced phase separation and decrease in E_a.

The crystallization characteristics and microhardness of $CaO–Na_2O$ (MgO) $–P_2O_5–CaF_2–SiO_2$ glass–ceramics were investigated by Salman et al. [52]. Addition of MgO in replacing Na_2O in the glass composition had an effect on crystalline phases formation, microstructures of the resulting glass–ceramic. Diopside (major), wollastonite and fluoroapatite phases could be obtained with sodium calcium silicate phase. It is also observed that T_g and T_c shifts towards higher temperatures. This is attributed to increasing effect of MgO on the rigidity of these glasses by forming MgO_4 tetrahedra with the SiO_4 group. The microhardness values (5837–3362 MPa) of the investigated glass–ceramics were markedly improved by the addition of MgO at the expense of Na_2O. High microhardness was measured in glass ceramic as compared to glasses. It may be ascribed to the formation of oriented fine fibrous microstructure and crystalline phases.

Goel et al. [53] have synthesized a series of alkaline-earth aluminosilicate glass-ceramics (GCs). The parent composition with general formula $Ca_{0.9}MgAl_{0.1}La_{0.1}Si_{1.9}O_6$ was modified with Cr_2O_3 and BaO. Augite was the primary crystalline phase obtained in all the compositions after sintering. Addition of BaO led to a substantial decrease in the total electrical conductivity of the glass ceramics thus improving their insulating properties. BaO-containing glass ceramics exhibited higher (TEC) in comparison to BaO-free glass ceramics. An extensive segregation of oxides of TiO_2 and MnO_2, along with negligible

formation of $BaCrO_4$ was observed at the interface between glass ceramics /interconnects diffusion couples (Crofer 22 APU). Thermal shock resistance and gas-tightness of sealants in contact with yttria-stabilized zirconia electrolyte (8YSZ) was evaluated in air and water.

Ghosh et al. [54] have investigated magnesium lanthanum alumino borosilicate-based glass-ceramics (MA series) with incorporation of barium oxide (BMA and BM series). Casting of completely transparent and amorphous glass within these systems became possible only at the BaO content of 25 mol% (BM1 glass) without any addition of La_2O_3 and Al_2O_3. The important thermal properties such as T_g, T_d, T_c and TECs were found to depend on the BaO content of the glass. With increment of BaO content up to 30 mol% the thermal parameters decreased probably due to the conversion in B_2O_3 co-ordination from BO_3^- trigonal to a much rigid BO_4^- tetrahedral structure within the glass network. A significant change in crystallization kinetics was also observed between the different developed systems which explain the instantaneous surface crystallization for few of the developed glasses having BaO content of 5, 10 and 30 mol%, respectively (BMA1, BMA2 and BM2). Irrespective of the compositions all the developed glasses exhibit high electrical resistivity of the order of 10^6–10^7 Ohm-cm at the SOFC operation temperature (800 °C). Upon further optimization of BM series of glasses in terms of different SiO_2:B_2O_3 ratios, one particular composition BM12 (25 mol % BaO) is found to fulfill all the requirements of an SOFC sealant. The TEC value for this particular composition was found to be intermediate between that of the YSZ electrolyte (TEC: 10.8×10^{-6} °C^{-1}) and Crofer 22APU metallic interconnect (TEC: 11.8×10^{-6} °C^{-1}) and varied insignificantly as compared to the other glass-ceramic compositions when heat-treated at 800 °C for

different time durations (0–100 h). It could be due to the formation of several crystalline phases viz. barium borosilicate, barium silicate, barium magnesium silicate and magnesium silicate (forsterite) which have compatible TEC in the range of 10–12 × 10^{-6} $°C^{-1}$. This also resulted an excellent joining with adjacent SOFC components e.g., YSZ electrolyte and Crofer22APU metallic interconnect leading to a very low helium leak-rate from the corresponding seal. The extent of chemical corrosion of this sealing composition with the metallic interconnect, which is one of the major concerns for the application of high BaO containing glasses, was also found to be relatively less (2–3 μm). The Youngs modulus value (87 GPa) for this particular composition has also found to be the highest in this series and suitable for SOFC application. The superior thermal, electrical and mechanical properties along with negligible interfacial reaction with the adjoining components and lowest leak-rate qualify the investigated glass-ceramic for further experimentation as candidate SOFC sealant material.

2.3.2 Barium silicate systems

Many researchers [2, 10, 55-58] have targeted their search of sealing material on barium aluminosilicate glass and some related systems. Eichler et al. [57] characterized the crystallization properties of commercially available BAS (BaO. Al_2O_3. SiO_2) glass in order to test their suitability as sealing glass for SOFC, while Sohn et al. [2, 55] studied the thermal and chemical compatibility of glasses with yttria stabilized zirconia (YSZ) electrolyte. These systems formed two major phases during heat treatment. These phases are hexacelsian and monocelsian. The details of these two phases are given in Table 2.2

Gosh et al. [59] studied BaO–CaO–Al_2O_3–SiO_2 (BCAS) as potential SOFC sealants. It was observed that a relatively high barium oxide containing composition (BCAS4) lead

to a glass having low T_g and best matching of TEC with the Crofer22APU metallic interconnect. X-ray diffraction study of the developed glass–ceramics reveals formation of various crystalline phases. For the particular case of BCAS4, a combination of barium silicate phases along with a minor amount of hexagonal barium aluminosilicate phase is suitable one. The presence of these phases in BCAS4 glass increase TEC which is almost compatible with TEC of metallic interconnect (Crofer22APU). The shrinkage study of the glasses reveals 35–50% volume shrinkage for all the compositions. Low barium contained glass–ceramic shows relatively better electrical insulation after long term exposure in air in contact with Crofer22APU at elevated temperature (800 ^{o}C).

The increase in TEC with increasing BaO content, is believed to be associated with the highest ionic radius of Ba^{2+} among all the alkaline-earth elements in this group of the periodic table [60]. This glass series is found to have low T_g and least TEC mismatch with Crofer 22 APU (steel interconnect) even after 100 h of heat treatment at 800^{o}C. SEM study of the same glass series shows excellent adhesion with Crofer 22 APU. At the interphase it has a mixture of amorphous glassy and needle like crystallized phases after heat treatment at 800^{o}C for 20 h. Ghosh et al. [61] have reported BAS glass with lanthanum doping which shows good compatibility and less TEC mismatch with YSZ and Crofer 22 APU which ultimately leads to the thermal and thermo-mechanical stability of the sealant during long term operation. The XRD pattern of this glass shows the formation of hexacelsian phase which is desirable for SOFC due to its TEC matching with other components of SOFC. Therefore, crystallization of hexacelsian is always desirable in the preparation of glass sealant for SOFCs, whereas, rapid and progressive transformation from hexacelsian to celsian is considered undesirable because of less

value of TEC in celsian. Fortunately, the transformation of hexacelsian to celsian is very sluggish. According to Drummond et al. [62] the crystal structure of hexacelsian contains infinite two dimensional hexagonal sheets consisting of two layers of $(Al,Si)O_4$ tetrahedra. Celsian consists of three dimensional feldspar structure in which all four corners of silica tetrahedra are shared forming a three dimensional network. The transformation of hexacelsian to celsian would require the creation of a three dimensional network from a two dimensional structure of hexacelsian as well as rearrangement of the Ba-sites. This would require breaking and forming of Al–O and Si–O bonds. Due to this kinetic barrier, the transformation of hexacelsian to celsian is very slow.

Sea-Fue Wang [63] also studied the glass-ceramic composites consisting of BaO-Al_2O_3-SiO_2-B_2O_3 glass and ceramic fillers for use as sealing materials of SOFCs. The softening temperature of glasses strongly depends on the SiO_2 content in the glass. TECs of the glasses decrease with the increase in SiO_2 content and increase with the rise in BaO content. Composites containing MgO additive show little change in TEC at high temperature while demonstrating a high structural stability with the change in time. Wettability of the glass on the YSZ substrate strongly depends on the BaO content in the glass and the soaking temperature.

In an another study on barium aluminosilicate glasses (BAS) [13], it was found that BAS glasses exhibit the lowest transition temperature, T_g and crystallization temperature, T_c as well as more than two exothermic peaks [figure. 2.2]. Moreover, glass BAS showed 100% crystallization when heated at $\geq 800^oC$. Obviously, the crystallization energy of glass BAS is significantly smaller that of the other glasses.

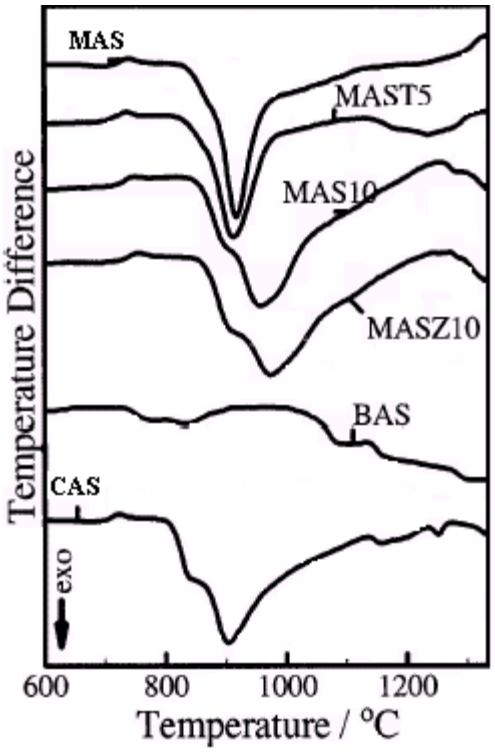

Figure 2.2: DTA thermograms determined with a heating rate of 10 $Kmin^{-1}$ for samples BAS, CAS, MAS, MAST5, MAS10, MASZ10 [13].

Smeacetto et al. [64] designed and successfully used barium- and boron-free glass to join YSZ to Crofer 22 APU alloy. The pressure less joining process at 900°C causes the partial surface induced crystallization of the glass, resulting in a glass–ceramic seal, still having a matched TEC with both YSZ and Crofer 22 APU alloy. The wettability of the seal was determined to be very good on both YSZ and as received- and preoxidised Crofer 22APU substrates. The powdered glass was applied as a sealant by both slurry coating and by EVD, in air or Ar. Thermal ageing in air (800 °C, 400 h) caused a Cr-diffusion from Crofer 22 APU alloy to the seal only when the alloy is in the as received condition, whereas the preoxidised one did not result in migration of Cr ions through the seal.

Drummond et al. [65, 66] reported that the BaO. Al_2O_3. $2SiO_2$ (BA2S) glass always crystallizes to the hexacelsian first than monocelsian. However, the transformation from the hexacelsian to monocelsian is very sluggish. These glasses (BA2S) were prepared by melting at 2000^oC. The as prepared glasses were completely crystallized to pure hexacelsian phase when heated at 1000^oC for 1h. After increasing heat treatment time duration (10hrs) and temperature (1100^oC), the hexacelsian phase began to transform to the monocelsian. The BA2S glass powders heated even at 1400^oC for 10h showed formation of both the hexacelsian and monocelsian phases although the amount of monocelsian phase was increased relative to the hexacelsian.

In another study Tao Sun et al. [67] prepared barium aluminosilicate glass by the melt–quenching method. The introduction of Al_2O_3 caused the conversion of [BO_3] units and [BO_4] units to each other. Al_2O_3 started behaving as glass network former when the addition of Al_2O_3 was up to 10 mol%. The stability of the glass increased first and then decreased as Al_2O_3 increased from 2 to 10 mol%, 5 mol% Al_2O_3 glass being the most stable. The wetting behavior of the glasses indicates that excess Al_2O_3 leads to high sealing temperature. The introduction of Al_2O_3 increases the crystallization temperature of the glass. Al_2O_3 addition also helps the crystallization of $BaSiO_3$ and $BaAl_2Si_2O_8$.

In the case of barium containing glass-ceramics, the crystallization increases thermal expansion. The increase in the TEC is due to the formation of barium silicate ($BaSiO_3$), which has large TEC (9-13 x 10^{-6} $^{\circ}C^{-1}$) [68, 69-47]. On the other hand, MgO based glass ceramic exhibits the TEC in the range of 7-9 X 10^{-6} $^{\circ}C^{-1}$ due to formation of enstatite ($MgSiO_3$). Strontium forms solid solutions with barium in the celsian crystal structures and has been shown to stabilize the monocelsian phase [70]. Other alkaline earth oxides

do not dissolve in the celsian phase, but rather form other phases. Calcium oxide is often added to form barium calcium aluminosilicate (BCAS) sealants. In this case an additional phase, barium calcium orthosilicate ($Ba_3CaSi_2O_8$), with a desirably large TEC is formed during crystallization [71-74].

2.3.3 Calcium silicate systems

A great deal of emphasis has been laid over calcium based glass systems for their utility as sealants. Jinhua et al. [82] found that T_c and T_d values increase greatly with an increase in CaO content and decrease in the BaO content. The crystallization peak (T_c) of the glasses shift to higher temperature with an increase in the CaO content. The field strength of the Ca^{2+} ion is higher than that of Ba^{2+} ion, which leads to increase in T_c and T_d values. Higher field strength has been reported in glass ceramics as compared to the glass. The reason is that the atoms and ions in the melt are reset during the process of crystallizing. The original chemical bond between the atoms and ions in the melt can be destroyed when forming new bonds. When the structure changes from an unformed state to a regular crystal lattice, the stronger the original bond, the more energy needed to destroy the bond. It can be noted that the TEC values decrease with reduction in Ba^{2+}

Table 2.2 Dominant phases formed in glass sealants and their effects on the different properties.

S.No	Phase formed	Properties
1.	Hexacelsian and Celsian ($BaAl_2Si_2O_8$)	Hexacelsian is stable phase. In general it always crystallizes out first in BaO. Al_2O_3 $2SiO_2$ system after heat treatment. Since hexacelsian is more compatible with the parent glasses than the celsian, in terms of TEC mismatch, hexacelsian crystallization is considered desirable in preparation of glass-ceramic sealants for SOFCs, whereas progressive celsian crystallization is considered undesirable. TEC of the hexacelsian is relatively close to that of the stainless steel and reaction zone is quite thin, therefore, thermal expansion mismatch is not as problematic as in the case of $BaCrO_4$ formation. Thus the crystallization of celsian impairs the long term thermal stability of sealant [2, 55, 61].
2.	Cristobalite, Quartz (SiO_2)	Quartz is thermodynamically stable at the operating temperature where as cristobalite acts detrimentally in the case of thermal cycling procedures with respect to a volume change of about 8 %, caused by the change of the crystal structure of cristobalite at 200^oC [75]. Imanaka et al. [76] examined the effect of ceramic additions containing Al, such as alumina, cordierite based ceramics, aluminium nitride, mullite and spinel into the borosilicate glass for suppression of cristobalite precipitation. The results showed that formation of cordierite, mullite or aluminium nitride suppress cristobalite formation more effectively than alumina or spinel. The common factor for this suppression is the Al^{3+}. It has also been demonstrated that cristobalite prevention depends on the amount of alumina present in the composite.
3.	Cordierite ($Mg_2Al_4Si_5O_{18}$)	This phase is transparent to microwave, resistant to thermal shock and erosion. It is suggested that in the early stages of crystallization, a SiO_2 rich solid solution is formed. In the later stage, an isomorphic substitution of Mg^{2+} and Al^{3+} occurs that composition approaches to cordierite [77]. Due to low thermal expansion coefficient, it is very harmful for SOFC operation. It can be suppressed with the addition of various additives like TiO_2, Cr_2O_3 [78-80].
4.	Barium calcium orthosilicate ($Ba_3CaSi_2O_8$)	Thermal expansion of this phase is compatible to other components of SOFC. Highly desirable phase.
5.	Forsterite (Mg_2SiO_4)	Forsterite has no alkali ions in vitreous phase so that it has higher resistivity (> 10^{12} ohm.m). Formation of forsterite phase suppresses the formation of cordierite phase when the alumina content is low (5%). It has been demonstrated that Ni promotes the forsterite formation in MgO-CaO-Al_2O_3 glass system [81]. Ni in the ionic state substitutes the Mg^{2+} ion in the octahedral site of the forsterite structure.

and increase in the Ca^{2+} content when the other components in the sealant are invariable. It can be attributed to the lower field strength of the Ba^{2+} ion as compared to that of Ca^{2+} ion. For the other reason, the expansion of glass is related to the non simple harmonic vibration of particles.

A detailed characterization of calcium aluminosilicate glass sealants was carried out by Smeacetto et al. [83]. The glass–ceramic prevent adverse corrosion effects at the Crofer22APU/glass–ceramic sealant interfaces in static heat treatment at 800 °C for 300 h in humidified hydrogen. The zinc based calcium aluminosilicate glass ceramic exhibited a promising behaviour in humidified hydrogen. SEM image of this glass–ceramic and YSZ exhibit pores and crack free interface after heat treatment at 800 °C under humidified hydrogen atmosphere. Moreover, this glass–ceramic sealant does not show microstructural modification during heat treatment. The diffusion of yttrium from YSZ into glass–ceramic was negligible which confirmed the thermo-chemical compatibility of the glass–ceramic sealant and YSZ at 800 °C under humidified hydrogen atmosphere.

According to Lahl et al. [13], CAS glass sample shows a lower thermal expansion coefficient than the MAS glass though the field strength of Mg^{2+} is higher than Ca^{2+}. This may be attributed due to the higher degree of crystallization of CAS glass as compared to MAS glass during heat treatment. Also, it has been observed [13] that activation energy increases significantly as the alkaline earth metal changes from Ba-Ca- Mg. The reason to this observation has been explained on the basis of field strength. Monterio et al. [71] realized that the bulk crystallization is taking place when the SiO_2 content in CAS glasses is low. Kingery's research [84] showed that the glasses crystallize only on the surface if

the content of SiO_2 is high but, if some nucleating agents such as TiO_2, Cr_2O_3, etc., are added to the glasses, they can crystallize in the bulk. Larsen and James [85] reported that presence of Cr^{6+} in the form of $CaCrO_4$ might cause pore formation inside the seal if severe reaction takes place at the interconnect-glass interface. Lahl et al. [57] showed that CaO base glasses in contact with 8YSZ give rise to formation of m-ZrO_2, which is detrimental to SOFC. This may not only create leakage in the seal but will also reduce the mechanical strength. Gunther et al. [86] and Ley et al. [1] reported promising results for high B_2O_3 glasses in the SrO-La_2O_3-Al_2O_3-B_2O_3-SiO_2 system. Boron undergoes significant reaction with humidified hydrogen to form several gaseous species including $B_2(OH)_2$ and $B_2(OH)_3$ at operating temperature. Therefore, it can be concluded that high boron containing glass will likely undergo measurable corrosion over time in a humidified fuel environment. However, the softening temperature of these glasses was too low for SOFCs application [87]. Additionally, B_2O_3 containing glass tends to exhibit excessive volatilization in the SOFC environment.

Several studies of the interconnect alloys in oxidizing atmosphere have demonstrated that Cr vaporization might present a long-term reliability issue [6, 58]. Apart from this other studies on interconnect alloys have focused on the contact resistance of the alloys both with and without ceramic coating [57, 84, 88]. In general, the long term stability of the interconnect is critical parameter for electrical performance. But the chemical reaction for the sealing glass with an oxide scale appears to be critical for the hermiticity requirement [1].

Although silicates are the most common ceramic glass sealants, non-oxide systems synthesized from the polymer precursors have also been developed [89, 90]. However,

the stability of such systems in the oxidizing environment of the SOFC cathode creates as additional challenge to their implementation as a sealing material.

Nonetheless, barium calcium aluminosilicates have been used successfully in fuel cells [91]. In addition, the success of glass sealants has led to their use for bonding interconnects to the frames [92].

Smeacetto [64] have designed a new barium and boron free glass of composition SiO_2-Al_2O_3-CaO-Na_2O and successfully used that glass to join YSZ to Crofer 22 APU alloy. The pressure less joining process at 900^oC causes the partial surface induced crystallization of the glass, resulting in a glass–ceramic seal, still having a matched TEC with both YSZ and Crofer 22 APU alloy. The wettability of the seal was determined to be very good on both YSZ and as received and preoxidised Crofer 22 APU substrates. Thermal ageing in air (800 ^oC, 400 h) caused a Cr-diffusion from Crofer 22 APU alloy to the seal only when the alloy is in the as received condition, whereas the preoxidised one did not show Cr ion diffusion into the glass.

Smeacetto et al. [93] have also studied the performance and characterization of glass-ceramic sealant with metallic interconnects YSZ and anode-supported-electrolyte. During experimentation a barium-free silica-based glass was used. This glass crystallized by heat treatment after being deposited on substrate by the slurry technique. The joined ceramic/seal/metal sample was characterized and tested for 400 h in air and hydrogen atmosphere. They claim that the glass exhibit excellent adhesion with ceramic electrolyte and metallic interconnect with minimum diffusion at the interfaces.

2.3.4 Strontium silicate systems

Mahapatra et al. [94] reported the thermo physical properties and devitrification behavior of $SrO–La_2O_3–Al_2O_3–B_2O_3–SiO_2$ based glass system. In spite of the potential to have high electrostatic bond strength (0.5 in octahedral coordination and 0.75 in tetrahedral coordination), Al^{3+} tends to be tetrahedrally coordinated in the glass network [95]. This is supported by the enriched Al^{3+} concentration in the residual glass phase and small concentration of Al^{3+} in the crystalline phase in the thermally cycled samples. Absence of SrB_2O_4 phase and appearance of $SrAl_2SiO_7$ phase in all the compositions except for SrO free sample indicates that there is a critical Al_2O_3 concentration to suppress the formation of SrB_2O_4. Suitable increase of Al_2O_3 stabilizes the glass by suppressing devitrification. La_2O_3 and B_2O_3 contribute to devitrification by forming $LaBO_3$.

In a theoretical study Pramuanjaroenkij et al. [96] have developed the mathematical transport model for planar solid oxide fuel cells. In this model SOFC being operated at 500, 600, 800 & 1000^oC and reversible cell voltage is obtained by the use of modified Nernst equation. They have also compared the electrolyte material i.e. YSZ and CGO (gadolinium-doped ceria) and found that YSZ electrolyte shows higher power density than the CGO electrolyte at higher temperatures than 750^oC.

In another study by Zhang et al. [97] thermodynamic calculations and experimental results of volatility of borate glass for SOFC have been reported. They have observed that the glasses containing 20 mol % B_2O_3 have 10 times greater weight loss than the glass containing 2 mol % of B_2O_3 under the same condition. The activation energy of volatilization was calculated to be 371 ± 86 and 372 ± 65 kJ/mol for this category of glasses.

Ley et al. [98] reported on $SrO–La_2O_3–Al_2O_3–B_2O_3 –SiO_2$ glass systems. These glasses are bonded well to the electrolyte, anode, and cathode of the SOFC. The interfaces could not show any failure during thermal cycling. The performance of the glass was checked in simple zirconia-based oxygen concentration cells. It shows no change in permeation coefficients during experiment.

Chou et al. [99] synthesized a novel composite glass Sr-Ca-Ni-Y-B with 10 vol% NiO which was tested for sealing standard coupons of Ni/YSZ anode-supported YSZ electrolyte bilayer and metallic interconnect Crofer22APU at various temperatures. The leakage rate of the samples was close to hermetic seals with 3 of the samples having leakage rate in the range $3\text{-}9x10^{-3}$sccm/cm at 1000 °C. Interestingly, seal showed lowest leakage rate at 1050°C that was even smaller than the background leakage. The parent glass was hermetic when sealed at 950-1000°C. Adding the inert NiO particles required higher temperatures for hermetic sealing as observed in this study. After leak testing, the samples sealed at 1050 °C were selected for reduction tests which involved exposure to a wet reducing environment (30% H_2O/70% H_2) followed by 10 thermal cycles in the same environment. The exposed samples were again tested for leakage at room temperature. The leakage rate was in the range of $\sim1\text{-}2x10^{-4}$ sccm/cm.

Lu and Mahapatra [100] studied the thermal stability of $SrO–La_2O_3–Al_2O_3–B_2O_3–SiO_2$ glass systems. The study shows that high B_2O_3 contained glasses induce BO_4 and SiO_4 structural unit ordering, increases localized homogeneity, decreases glass network connectivity, and causes devitrification. Glass modifiers interact with either silicon- or boron-containing structural units and form different devitrified phases at different B_2O_3: SiO_2 ratios. B_2O_3-free glass shows the best thermal stability among all the studied

compositions. The results of their findings highlight that B_2O_3-free composition, remains stable after thermal treatment for 200 h at 850 °C.

Based on literature review some glass compositions were selected to study the effect of different intermediate oxides on sealing properties particularly in oxidizing atmosphere. The structural, thermal and crystallization kinetic studies were done on the proposed glasses to check their applicability and suitability as a sealing material of SOFCs.

2.4 CHOICE OF ELECTROLYTES FOR PLANAR STACK CONFIGURATION

In order to make SOFC an operational unit, a number of stack technologies have been designed and tested. This includes an overall ceramic planar SOFC stack design and hybrid stack design. The separate stack design was developed using the cell as a basis and fitting gas manifolding, flow structures and also the thermal conductivity factors around the cell. The focus for planar SOFC technology is based upon electrolyte-supported cells. Generation 3 (1998-2000) stacks were also used as a platform to test anode-supported thin electrolyte cells developed in parallel [101].

Fig 2.3: A 3-kW stacks assembly [101].

The substance in which conduction takes place through movement of ions is called ionic conductor. Ionic conductivity is observed in those solids in which defects (vacancies) exist. Ionic conductivity is a critical property of a solid electrolyte which determines the efficiency and operating temperature of electrochemical cells. In order to obtain a material that is a pure ion conductor (solid electrolyte), the level of electronic contribution to the total electrical conductivity (ionic + electronic) must be negligible. Solid electrolyte must exhibit high ionic conductivity at the operating temperature to allow efficient transfer of ions from the cathode to anode and also a low electronic conductivity to prevent electron leakage across the cell [102].

There are several criteria that the electrolyte has to meet. It must be:

- Dense and leak tight
- Stable in reducing and oxidising environments
- A good ionic conductor at operating temperatures
- Non-electron conductor
- Thin to reduce ionic resistance
- Extended in area for maximum current capacity
- Thermal shock resistant
- Economically processable.

Table 2.3 Different electrolytes for planar SOFC with their characteristics [103].

Electrolyte	Structure	Characteristics
doped ceria (CeO_2)	flourite	• useful for lower temperature applications • electron conductor in the reducing environment at the anode and hence short-circuiting is a problem.
doped lanthanum gallate ($LaGaO_3$)	perovskite	• High ionic conductivity
doped barium zirconate ($BaZrO_3$)	perovskite	• structure is very tolerant and can accommodate large concentrations of dopants
yttria-stabilised zirconia (YSZ)	flourite	• abundance, chemical stability, non-toxicity and economics make it the most suitable material at present • high thermal expansion coefficient

2.4. GAPS IN THE STUDY

On the basis of above discussion, it can be concluded that glasses and glass ceramics, in principle can meet most of the requirements of an ideal sealant by selecting the suitable constituent components of the glasses in their defined stoichiometric proportion. The MgO based glasses are found to be very stable and suitable due to their minimum

reaction with other components of SOFC whereas, BaO based glasses exhibit good bonding. However, the following drawbacks are found in these glasses:

- MgO based glasses are very prone to form cordierite ($Mg_2Al_4Si_5O_{18}$) phase, which is detrimental due to their lower thermal expansion as compared to other components of SOFC.
- Formation of cristobalite (SiO_2) phase during long run operation of SOFC.
- Similarly, BCAS glasses showed the formation of detrimental $BaCrO_4$ phase on interaction with the interconnect materials.
- Formation of detrimental $BaCrO_4$ in the regions exposed to oxidizing environment.

However, the formation of these phases can be avoided by suitably choosing the starting composition and the nucleating agent. Therefore, to develop suitable sealing materials, which can suppress the formation of cordierite and $BaCrO_3$ phase with higher TEC, is an urgent need, which can work at 800° -1000°C for longer duration without deteriorating the properties of other components of SOFC.

2.5 OBJECTIVES

Based on the studies above, our aim is to choose carefully a composition for studying long term crystallization behaviour of glasses. Y, Al, La, Cr have been chosen as the intermediates whose cationic radii are in the same range. The main objectives of our work are

- To prepare a glass series SiO_2- B_2O_3-A_2O_3-MO, A= (Y, La, Al, Cr), M= (Mg, Sr, Ca, Ba) using conventional melt-quenching technique
- To investigate long term behaviour of glasses in oxidizing atmosphere and study crystallization kinetics for various phases formed.
- To study activation energy and thermal expansion coefficient of the glass series.

Summary

An extensive literature survey was done mainly in Strontium, Magnesium, Calcium and Barium based glass systems. An extensive work has been recently done in this field by F.Smeacetto, C. Lara and S.Ghosh. Careful review of literature to select a glass series which did not form detrimental phases during heat treatment was the main objective.

References:

[1] K. Ley, M. Krumplet, R. Kumar, J. Meiser, I. Bloom, J. Mat. Res. 11, 1489 (1996).

[2] S.-B. Sohn, S.-Y. Choi, G.-H. Kim, H.-S. Song and G.-D. Kim, J. Non-Cryst. Solids 297, 103(2002).

[3] C. Lara, M. J. Pauscal, A. Duran, J. Non-Cryst. Solids 348, 149 (2004).

[4] K. D. Meinhardt, J. D.Vienna, T. R. Armstrong, L. R. Pederson, U. S. Pat. 6430966 (2002).

[5] D. Bahadur, N. Lahl, K. Singh, L. Singheiser, K. Hilpert, D. Bahadur, J. Electrochem. Soc. 151, A558 (2004).

[6] S. P.Jiang, L. Christiansen, B. Hughan, K. Foger, J. Mater. Sci. Lett. 20, 695 (2001).

[7] N. Lahl, L. Singheiser, K. Hilpert, K. Singh, D. Bahadur, in "Solid Oxide Fuel Cells-VI" edited by S. Singhal, M. Dokiya (Electrochemical Society, Pennington, NJ, PV 99-19, 1999) p. 1057.

[8] D. Stolen, E. Monreal, W. Miller in Fuel Cell Seminar Abstracts, Tucsan, AZ, 1992, p. 53.

[9] Y. Harufuji, Jpn Kokai Tokyo JP 04-47, 672 (Feb. 17, 1992).

[10] Z. Yang, J. W Stevenson and K. D. Meinhardt, Solid State Ionics 160, 213 (2003).

[11] I. D. Bloom, K. L. Ley, U.S. Pat. 5453331 (Sept. 26, 1995).

[12] I. Gutzow and J. Schmelzer, The Vitreous State (Springer, Berlin, 1995).

[13] N. Lahl, K. Singh, L. Singheiser, K. Hilpert, D. Bahadur, J. Mater. Sci. 35, 3089 (2000).

[14] P. H. Larsen, F. W. Poulsen, R. W. Berg, J. Non-Cryst. Solids 244, (1999) 16.

[15] Robert A Meyers "Encyclopedia of Physical Science and Technology" (Academic Press Inc. 1987) Vol. 6.

[16] N. Gupta, K. Singh, O. P. Pandey in Proceedings of the National Conference on Materials and Related Technologies held at Thapar Institute of Engineering & Technology, Patiala during September 19-20, 2003 p. 141.

[17] K. Singh, N. Gupta, O. P. Pandey, J. Mater. Sci. 42, 6426 (2005).

[18] S. Ghosh, P. Kundu, A.D. Sharma, R. N. Basu, H. S. Maiti, J. Eur. Ceram. Soc. 28 69 (2008).

[19] M. Tomozawa, in Advances in Crystallization and Nucleation in Glasses (American Ceramic Society, 1971) p. 41.

[20] Robert H. Dooremus in Glass Science (Second Edition) (John Wiley & Sons, Inc. New York, NY, 1994) p. 85.

[21] W. B. Hillig, in Proceedings of Symposium on Nucleation and Crystallization in Glasses and Melts (American Ceramic Society, Columbus, OH, 1962) pp. 77.

[22] U. Schiffner and W. Panhorst, Glastech. Ber., 60, 239 (1987).

[23] T. J. Barry, D. Clinton, L. A. Ray, R. A. Mercer, and R. P. Miller, J. Mater. Sci. 4(1969) 496; 5 117 (1970).

[24] Glasses, The Physics Hypertextbook, 1998-2007 by Glenn Elert -- A Work in Progress

[25] D. R. Uhlmann, J. Non-Cryst. Solids 38 & 39, 693 (1980).

[26] M. Abdel-Satar, M. A. Abdel-Rahim, Int. J.of Pure and App. Phy. 3, pp. 59–68(2007).

[27] F. Tietz*, Ionics*, 5 (1999), p. 129.

[28] P. Larsen et al., *Solid Oxide Fuel Cells IV* (Pennington, NJ: Electrochemical Society, (1995).

[29] K.A. Nielsen et al., *Ceramic Engineering & Science Proceedings, Vol. 25* (Westerville, OH: American Ceramic Society, 2004), p. 309.

[30] T. Schwickert et al., *Proceedings of the 1st International Brazing and Soldering Conference* (Materials Park, OH: ASM International, 2000), p. 116.

[31] K. Eichler et al., *J. Europ. Ceram. Soc.,* 19 (1999), p. 1101.

[32] K.D. Meinhardt et al., U.S. patent 6,430,966 (2002).

[33] S.-B. Sohn et al., *J. Non-Cryst. Sol.,* 297 (2002), p. 103.

[34] C. Lara, M.J. Pascual, and A. Duran, *J. Non-Cryst. Sol.,* 348 (2004), p. 149.

[35] M.B. Volf, *Chemical Approach to Glass: Glass Science and Technology,* Vol. 7 (New York: Elsevier, 1984).

[36] Y.-N. Sung, *J. Mater. Sci.*, 31 (1996), p. 5421.

[37] P. J. Melling, C. S. Vempati, A. R. Allnatt, P. W. M. Jacobs: "Tracer diffusion in and electrical conductivity of a natural volcanic glass: rhyolite"; Phys. Chem. Glasses 1981, vol. 22, no. 3, p 49

[38] S. Mukerjee et al., *Solid Oxide Fuel Cells IX,* Vol. I (Pennington, NJ: Electrochemical Society, 2005), p. 48.

[39] L. Blum et al., *Solid Oxide Fuel Cells IX,* Vol. I (Pennington, NJ: Electrochemical Society, 2005), p. 39.

[40] K.G. Ewsuk and L.W. Harrison, *Sintering of Advanced Ceramics, Ceramics Transactions Vol. 7* (Westerville, OH: American Ceramic Society, 1990).

[41] M. Brochu et al., J. Amer. Ceram. Soc., 89 (2006), p.108

[42] K.D. Meinhardt et al., Joining of Advanced and Specialty Materials VII, Proceedings from Materials Solutions 2004 (Materials Park, OH: ASM International, 2005), p. 124.

[43] J. Zizelman, "Development Update on Delphi's Solid Oxide Fuel Cell System: from Gasoline to Electric Power" (Paper presented at the 4th Annual Solid State Energy Conversion Alliance Workshop, 15–16 April, 2003, Seattle WA), www.delphi.com/pdf/fuelcells/sofc_update_apr03.pdf.

[44] www.netl.doe.gov/publications/proceedings/05/SECA_PeerReview/posters/UCinn%

[45] G. W. Cleek, C. L. Babcock: "Properties of glasses in some ternary systems containing BaO and SiO_2"; National Bureau of Standards Monograph 135, Library of Congress Catalog No. 73-600135, Sept. 1973

[46] J. E. Shelby, J. T. Kohli: "Rare-earth aluminosilicate glasses"; J. Am. Ceram. Soc., vol. 73 (1990), no. 1, p 39-42 J. E. Shelby: "Rare-earths as major components in oxide glasses"; Key Engineering Materials, vol. 94-95 (1994), p 1-42

[47] I. A. Ivanov, V. M. Sedov, A. N. Gulin, S. V. Stefanovskii, V. M. Shatkov; Fizika i Khimiya Stekla, vol. 17 (1991), no. 2, p 351

[48] O. V. Mazurin: "Phase separation in glass", North-Holland, 1984.

[49] Gmelin's handbook of inorganic chemistry, Verlag Chemie, Weinheim, Germany

[50] T. I. Barry, J. M. Cox and R. Morell, J. Mater. Sci. 13, 594 (1978).

[51] N. Lahl, K. Singh, L. Singheiser, K. Hilpert, D. Bahadur, J. Electrochem. Soc. 149A607 (2002).

[52] S.M. Salman, S.N. Salama, H. Darwish and E.A. Mahdy Cer Int. 36 (1) 55-61 (2010)

[53] Ashutosh Goel, Dilshat U. Tulyaganov, Vladislav V. Kharton, AlekseyA.Yaremchenko and José M.F. Ferreira Journal of Power Sources 195 (2), 522-526 (2010).

[54] Saswati Ghosh, A. Das Sharma, A.K. Mukhopadhyay , P. Kundu and R.N. Basu Int Journal. Hyd . Energy 35 (1), 272-283 (2010).

[55] S.-B. Sohn, S.-Y. Choi, G.-H. Kim, H.-S. Song and G.-D. Kim, J. Am. Ceram. Soc.87 (2), 254 (2004).

[56] M. G. Nicholas, "Joining Structural Ceramics" In Designing Interfaces forTechnological Applications, edited by S. D. Peteves, (Elsevier Appl. Science, Amsterdam, 1989) p. 49.

[57] K. Eichler, G. Solow, P. Otschik and W. Schaffrath, J. Eur. Ceram. Soc. 19, 1101(1999).

[58] Z. Yang, K. D. Meinhardt, J. W. Stevenson, J. Electrochem. Soc. 150 A1095 (2003).

[59] Saswati Ghosh, A. Das Sharma, P. Kundu, S. Mahanty, R.N. Basu J. Non-Crys Sol 354 (34) 4081-4088 (2008).

[60] S. Ghosh, A. Das Sharma, P. Kundu, R.N. Basu, H.S. Maiti, Electrochem. Soc. Trans. 7, 2443 (2007).

[61] S. Ghosh, P. Kundu, A.D. Sharma, R. N. Basu, H. S. Maiti, J. Eur. Ceram. Soc. 28 69 (2008).

[62] C. H. Drummond, W. E. Lee, N. P. Bansal, and M. J. Hyatt, Ceram. Eng. Sci. Proc, 10(9-10), 1485 (1989).

[63] Sea-Fue Wang, Yuh-Ruey Wang, Yung-Fu Hsu and Ching-Chin Chuang Int Journal. Hyd . Energy (19), 8235-8244 (2009).

[64] F. Smeacetto, M. Salvo, M. Ferraris, J. Cho and A.R. Boccaccini J. Eur. Ceramic. Soc 28, 61–68 (2008).

[65] C. H. Drummond III and N. P. Bansal, Ceram. Eng. Sci. Proc. 11, 1072 (1990).

[66] M. J. Hyatt and N. P. Bansal, J. Mater. Sci. 31, 172 (1996). Tao Sun , Hanning Xiao, Wenming Guo, Xiucheng Hong Ceramics Internationa 36, 821–826 (2010).

[67] Tao Sun, Hanning Xiao, Wenming Guo, Xiucheng Hong Ceramics International 36, (2010) 821–826.

[68] W. Holland, G. Beall in "Glass-Ceramics Technology" The American Ceramic Society, Westerville, OH, 2002.

[69] K. Scott Weil, John E Deibler, John S Hardy, Dong Sang Kim, Guan Guang Xia, LA Chick and Chris A Coyle, J. Mat. Eng. Perf. 13(3), 316 (2004).

[70] D. Bahat, J. Mater. Sci. 7, 198 (1972).

[71] Y. S. Touloukian (Ed.), Thermophysical Properties of High Temperature Solid Materials, vol. 4, Oxides and Their Solutions and Mixtures, (The MacMillan Co., New York).

[72] C. Lara, M. J. Pascual, J. M. Prado, A. Duran, Solid State Ionics 170, 201(2004).

[73] K. S. Weil, J. Mater. Eng. Perf. 13, 309 (2003).

[74] N. P. Bansal, E. A. Gamble in Proceedings of Electrochemical Society 2005-07(SOFC IX).

[75] T. Schwickert, R. Sievering, P. Geasee and R. Conradt, Mat.-wiss.u. Werkstofftech.33, 363 (2002).

[76] Yoshihiko Imanaka, Shigenori Akoi, Nobuo Kamehara and Koichi Niwa, J. Am. Ceram. Soc. 78, 1265 (1995).

[77] W. Zdaniewski, J. Am. Ceram. Soc. 58, 163 (1975).

[78] J. W. Stevenson, T. R. Armstrong, R. D. Carneim, L. R. Pederson and W. J. Weber, J. Electrochem. Soc. 143, 2722 (1996).

[79] J. S. Hardy, J. Y. Kim and K. S. Weil, J. Electrochem. Soc. 151, J43 (2004).

[80] J. Kim, A. Virkar, in, "Solid Oxide Fuel Cells-VI" , edited by S. Singhal, M. Dokiya (Electrochemical Society, Pennington, NJ, PV 99-19, (1999) p. 830.

[81] L. Barbieri, A. M. Ferrari, C. Leonelli, T. Manfredini, G. C. Pellacani, S. Bruni and F. Cariatti, Phys. Chem. Glasses 36, 176 (1995).

[82] Piao Jinhua, Sun Kening, Zhang Naiqing, Chen Xinbing, Zhou Derui J. Rare Earths 25, 434- 438 (2007)

[83] F. Smeacetto, M. Salvo, F.D. D'Hérin Bytner, P. Leone and M. Ferraris 30 (4), 933-940 (2010).

[84] W. D. Kingery, P. B. Vandiver, I. W. Huang, J. Non-Cryst. Solids 54, 163 (1983).

[85] P. H. Larsen and P. F. James, J. Mater. Sci. 33, 2499 (1998).

[86] C. Gunther, G. Hofer, W. Kleinlein, Proceedings of the Fifth International Symposium on Solid Oxide Fuel Cells, vol. 97-18, The Electrochemical Society,1997, p. 746.

[87] F. Teitz, Ionics 5, 129 (1999).

[88] S. P. Simner, J. W. Stevenson, J. Power Sources 102, 310 (2001).

[89] C. A. Lewinsohn, S. Elangovan, S. M. Quist, Ceram. Eng. Sci. Proc. 25, 315 (2004).

[90] C. A. Lewinsohn, S. Elangovan, Ceram. Eng. Sci. Proc. 24, 317 (2003).

[91] L. G. J. de Haart, I. C. Vinke, A. Janke, H. Ringel, F. Tietz in, Proceedings of Electrochemical Society 2001-16 (SOFC VII) (2001) 111.

[92] L. Blum, H. P. Buckhkremer, L. G. J. de Haart, H. Habielek, J. W. Quadakkers, U.Reisgen, R. Steinbrech, F. Tietz, I. Vinke, Ceram. Eng. Sci. Proc. 25 (2004) 219.

[93] F. Smeacetto, M. Salvo, M. Ferraris, V. Casalegno, P. Asinari and A. Chrysanthou, J. Eur. Ceram. Soc. 28, 2521 (2008).

[94] M.K. Mahapatra K. Lu and W.T. Reynolds Jr. J. Power Sources 179 (1), 106-112 (2008).

[95] E.M. Levin and S. Block, J. Am. Ceram. Soc. 41, 49–54 (1958).

[96] A. Pramuanjaroenkij, S. Kakac and Xiang Yang Zhou Int. Jour Hyd Energy, 33 2547 (2008).

[97] T. Zhang, W. G. Fahrenholtz, S. T. Reis and R. K. Brow, Am. Ceram. Soc., 912564 (2008).

[98] K. L. Ley et al.: Glass-ceramic sealants for solid oxide fuel cells: Part I. J.Mater. Res., 11(6), (1996).

[99] Yeong-Shyung Chou, Jeffry W. Stevenson, Robert N.Gow J.Power Sources 170, 413-418 (2007).

[100] K. Lu and M. K. Mahapatra J. Appl. Phys. 104, 074910 (2008).

[101] K. Foger, J.G. Love, Solid state ionics 174, 119-126 (2004).

[102] R. Kant, K. Singh and O. P. Pandey, Ionics 16, 277-282 (2010).

[103] J.H Hirschenhofer, D. V. Stauffer, R. R. Engleman and M. G. Klett, Fuel Cell Handbook Parsons Corp (1998) 134.

3.1 Glass sample preparation

The brief details of sample processing and characterization techniques which were adopted during the course of the present investigations are presented in this chapter. Glass samples were prepared by mixing the raw materials in the form of SiO_2, B_2O_3, Y_2O_3, Al_2O_3, La_2O_3, Cr_2O_3 and SrO/MgO/BaO/CaO using conventional melt-quenching techniques. The purity of constituent oxides which were used to prepare the samples was ≥ 99 %. All the chemicals were procured from Sigma Aldrich or CDH India. Each batch was prepared by mixing an appropriate mole fraction of well desired initial ingredients. Sample compositions with their label are given in table 3.1.

Table 3.1 Glass compositions (mol %) with their label.

Sample	SiO_2	B_2O_3	SrO	MgO	BaO	CaO	Y_2O_3	La_2O_3	Al_2O_3	Cr_2O_3
VS1	40	20	30	0	0	0	10	0	0	0
VS2	40	20	30	0	0	0	0	10	0	0
VS3	40	20	30	0	0	0	0	0	10	0
VS4	40	20	30	0	0	0	0	0	0	10
VM1	40	20	0	30	0	0	10	0	0	0
VM2	40	20	0	30	0	0	0	10	0	0
VM3	40	20	0	30	0	0	0	0	10	0
VM4	40	20	**0**	30	0	0	0	0	0	10
BaY	40	20	30	0	30	0	10	0	0	0
BaLa	40	20	30	0	30	0	0	10	0	0
BaAl	40	20	30	0	30	0	0	0	10	0
BaCr	40	20	30	0	30	0	0	0	0	10
CaY	40	20	30	0	0	30	10	0	0	0
CaL	40	20	30	0	0	30	0	10	0	0
CaAl	40	20	30	0	0	30	0	0	10	0
CaCr	40	20	30	0	0	30	0	0	0	10

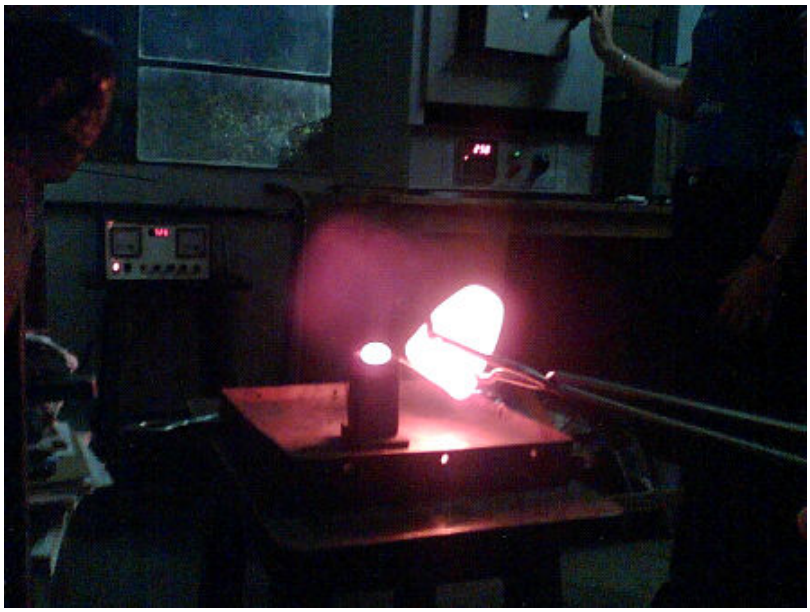

Figure 3.1: Sample preparation by melt quenching technique.

3.1.1 Synthesis of glass sample

For each system, required amount of raw materials as per the stoichiometry ratio were taken. The mixture was ground to break agglomerate particles. After grinding the mixture was further transferred to ball mill and ground for two hours in wet medium (acetone). The ball milling was done using porcelain balls in porcelain jar (Retsch, Germany, Model S 1000). The powder to ball ratio for each system was 1:2 which was kept constant for each milling. The resulting mixture was dried in air. The ground powder was transferred in recrystallized alumina crucible and melted in an atomized Molybdenum Disilicide ($MoSi_2$) high temperature furnace. The powders of the samples were initially heated at 1000ºC for 2 h to facilitate the calcination. During calcination process moisture is released. After that the temperature was increased upto 1200 ^{o}C and kept at this temperature for 0.5 h to facilitate the fusion and melting process. Then, system was reheated at 1550ºC and kept at this temperature for 1.5 h to achieve homogeneous molten materials. The schedule followed for melting of samples is also shown in figure 3.2. The molten mass was poured in a preheated graphite mold. The remaining melt was poured on the flat copper plate and

quenched by other copper plate in air to obtain flakes. All the samples were prepared using the same route as described above. Before melting, the furnace was calibrated and the temperature fluctuation in hot zone was ± 2 ^{o}C. The details of the sample preparation and other relevant information about preparation and characterization are given in the flow chart (figure 3.3).

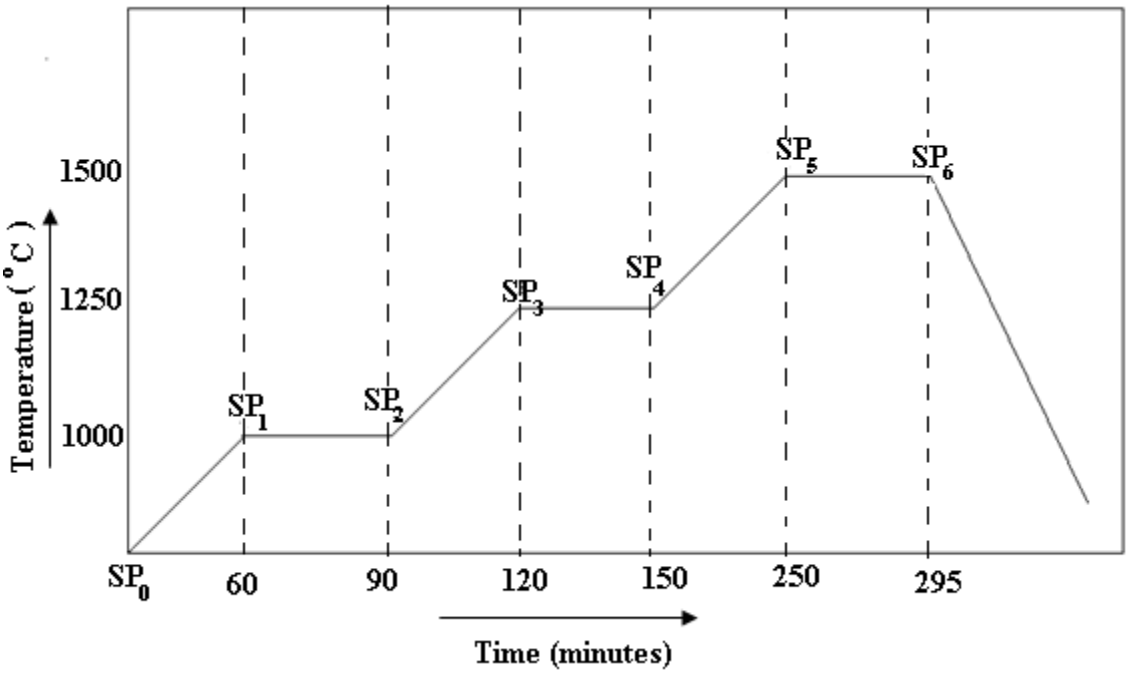

Figure 3.2: Typical schedule followed for the melting of the glass samples.

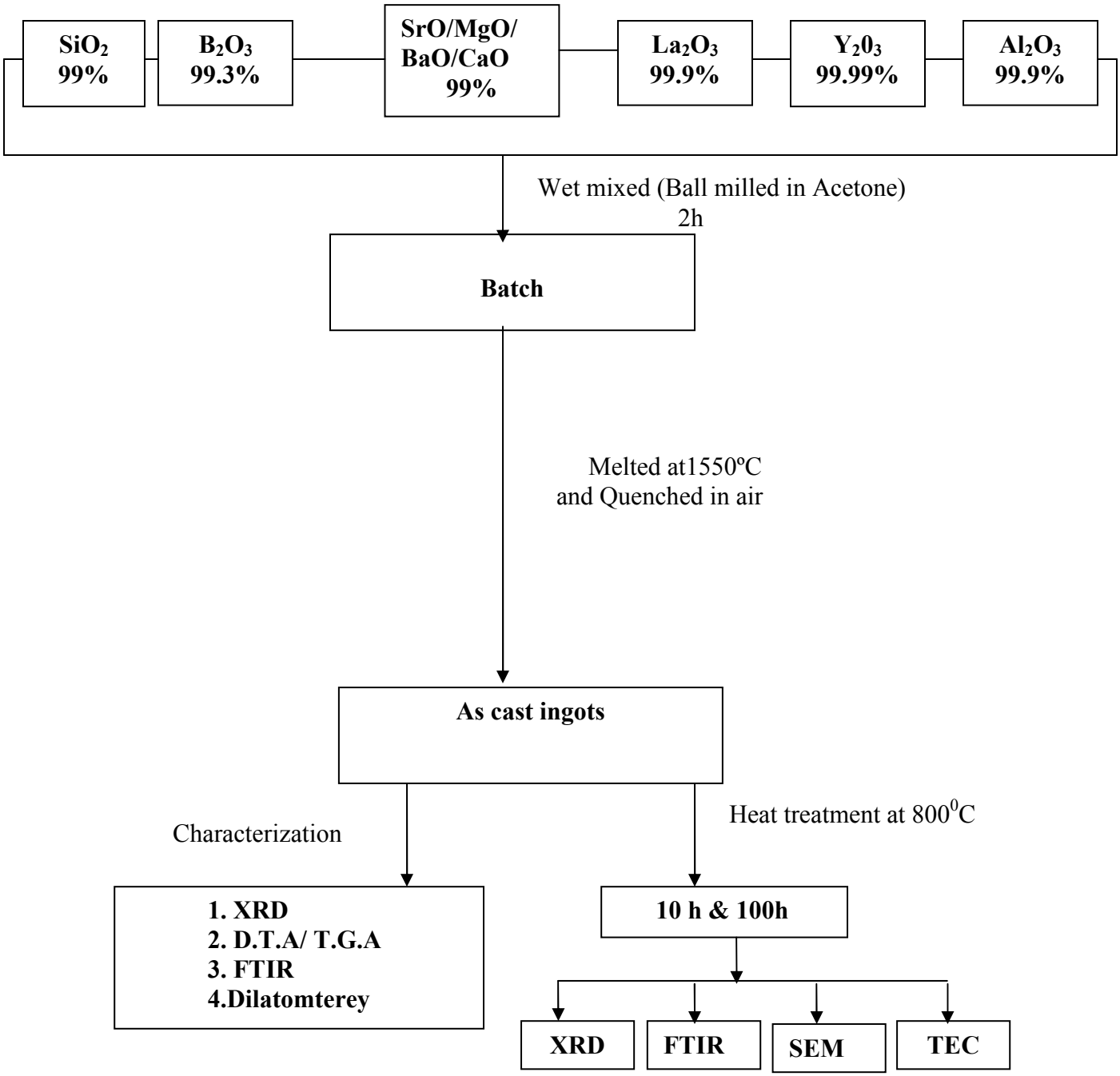

Figure 3.3: Typical flow chart showing the procedure of glass synthesis and their characterization techniques.

3.1.2 Sample preparation for chemical interaction

In order to visualize the sealing capability of the glasses chemical interaction of strontium based glass samples with doped bismuth vanadate DBiV was done. For this study the ratio of glass and doped bismuth vanadate were 3:1 (wt %), respectively. The powders of both the components were ground in wet media for 1 h by mortar and pestle. The ground powder was kept in recrystallized alumina crucible and heated at 800°C for 1, 10 and 100 h. The temperature variation of furnace at 800 °C was ± 5 °C. Many researchers have tried to develop high ionic conducting electrolytes in intermediate temperature range (600-800^{o}C) to reduce the working temperature of SOFC. High ionic conductivity has been reported in doped bismuth vanadate (DBiV). The basic aim of this experiment was to determine the nature of chemical interaction between glass sealants and doped bismuth vanadate (DBiV) in order to visualize the sealing capability of the glasses.

3.2 Characterization of materials

The present samples have been characterized using various techniques to check their applicability and suitability as sealing materials for SOFCs. The X-ray diffraction technique was used for structural characterization of glass and glass ceramics. Differential thermal analysis (DTA)/ Thermo gravimetric analysis (TGA) have been done to study thermal properties and stability of glasses. The thermal expansion coefficient is very important parameter in view of TEC mismatching among various components of SOFCs. Therefore, TEC was measured by Dilatometer. Micro structural analysis was carried out on some selected glass ceramic samples by scanning electron microscope (SEM). The details of these techniques are described below:

3.2.1 X-Ray diffraction

X-ray diffraction (XRD) is a versatile, non-destructive technique that reveals detailed qualitative and quantitative information about the crystalline phases and crystallographic structure of natural and synthetic materials. X-ray powder diffraction pattern were recorded at room

temperature by Rigaku model Geiger diffractogram with CuK_α radiation (λ = 1.5418 Å) obtained from a copper target using an inbuilt Ni filter. The XRD pattern are taken generally in the range of $10° \leq 2\Theta \leq 80°$ for most of the samples. Samples are analyzed as powders with grains in random orientations to insure that all crystallographic directions are sampled by the beam. Monochromatic X-rays are used to determine the interplanar spacing of the unknown samples using Bragg's law.

$$2d\text{Sin}\Theta = n\lambda \tag{3.1}$$

Where d = interplanar spacing, λ = wavelength of incident X-ray, θ = diffraction angle, n = integer. The data obtained from XRD is indexed by standard powder diffraction files provided by International Centre for Diffraction Data ICDD.

3.2.2 Density measurement

The density of glass samples was measured by Archimedes principle using microbalance with xylene as buoyant. Density data was used to calculate the molar volume (V_m), excess volume (V_e), oxygen molar volume (V_o) of as cast glasses using the following equation:

$$V_m = \frac{M}{\rho} \tag{1}$$

M denotes the molar mass of the investigated glass.

$$V_e = V_m - \sum_i x_i V_m(i) \tag{2}$$

Here, $V_m(i)$ is the molar volume of each oxide constituent, x_i is the molar concentration of every oxide in glass composition. The molar volume of the oxygen contents V_o of the glasses was calculated using equation (3) below.

$$V_o = \frac{\sum_i x_i M_i}{\rho \sum_i n_i x_i} \qquad (3)$$

Where, M_i and n_i is the molar weight of the oxide and oxygen content in the i^{th} oxides respectively.

3.2.3 Differential thermal analysis (DTA)

Differential thermal analysis (DTA) is a thermo analytic technique, similar to differential scanning calorimetry which gives information about the phase transformation behavior of the sample. In DTA, the thermal event of sample is observed with respect to the inert reference sample in heating or cooling cycle under identical conditions. This differential temperature is then plotted against time, or against temperature (DTA curve). Changes in the sample, either exothermic or endothermic, can be detected relative to the inert reference. Thus, a DTA curve provides data on the transformations that have occurred, such as glass transitions, crystallization and melting. In the present work differential thermal analysis of the powdered samples was done by DTA, Perking Elmer (Diamond TG/DTA) in nitrogen atmosphere (figure 3.4) using platinum crucibles at different heating rates from room temperature to 1000 ^{o}C. In the present investigations Al_2O_3 is taken as reference sample. The endothermic peaks exhibit the glass transition temperature and melting of the glass samples. On the other hand exothermic peaks denote crystallization of the glasses. The DTA sensitivity depends upon the heating rate. It is reduced with the slower rates because temperature for a particular event decreases with decreasing heating rate. The thermal stability of the glasses was investigated using thermo gravimetric analysis (TGA). The temperature and weight loss detection limit are ± 1ºC and 0.001 mg respectively during DTA/TGA measurements. The stability of glass at higher temperature can easily be predicted by TGA in terms of weight loss. B_2O_3 based glasses are known to be volatile at higher temperatures, the TGA can predict the degree of volatility in a particular glass accurately.

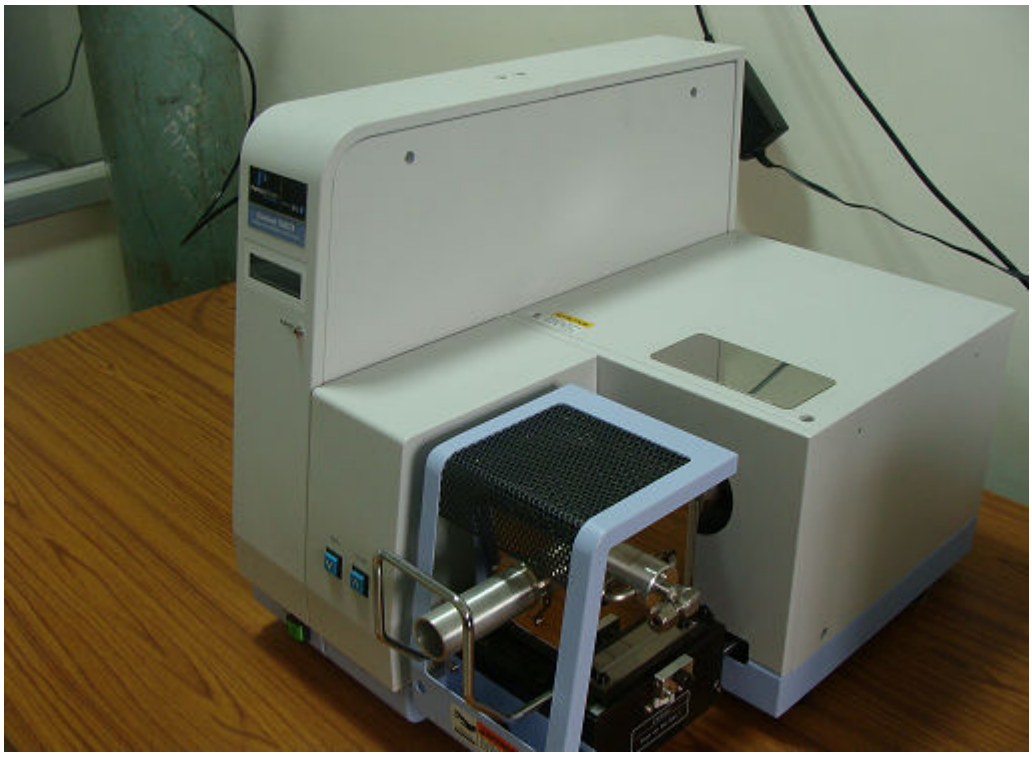

Figure 3.4: Differential Thermal Analyzer (DTA).

3.2.4 Dilatometric measurement

Thermal dilatometric analysis (TDA), often called "dilatometry", measures the dimensional change of a material (ceramics, glasses, metals, composites and others) as a function of temperature or time. This test determines both reversible and irreversible changes in length (expansion and shrinkage) during heating and cooling, and pinpoints the temperature where reactions occur due to expansion or contraction. The dilatometer is used to determine TEC, softening point, glass transition temperature, Curie point, crystalline transformation, phase transition, shrinkage, warping, bloating, sintering rate, isothermal creep and stress relaxation. In the present context dilatometry is important and essential tool to know the TEC of glasses, glass ceramics and diffusion couple (Crofer + glass). Crofer 22 APU is a high temperature ferritic stainless steel specially developed for application in solid oxide fuel cells. In principle, a dilatometer has simple

arrangement where the sample is kept between two rods. These rods extend outside of the heated region as shown in figure 3.5. The sample pushes the two rods (A and B) during heating. The sample will expand an amount shown by the shaded area, ΔL_S. By examining the experimental model, it becomes immediately clear that this configuration will not produce the desired ΔL_S. It is inevitable that these rods will also expand (ΔL_A and ΔL_B respectively) since portions of both rods A and B are in the controlled environment. Thus, the measured value of (ΔX_A+ΔX_B) will contain (ΔL_A+ΔL_B) in addition to ΔL_S. The sample's length change, ΔL_S, can therefore be written as:

$$\Delta L_S = (\Delta X_A - \Delta L_A) + (\Delta X_B - \Delta L_B) \qquad (2)$$

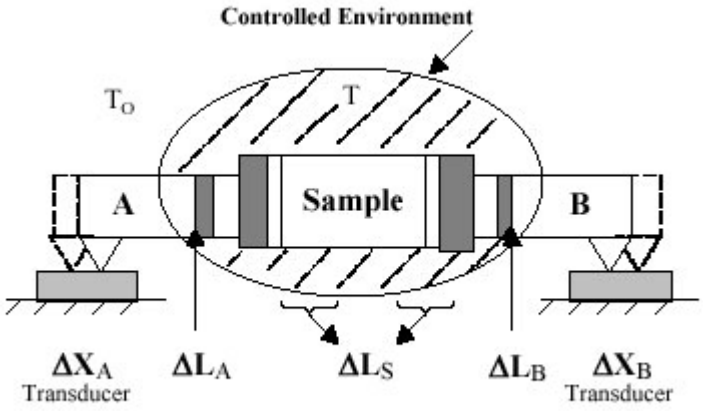

Figure 3.5: Diagrammatic representation of sample holder (top view).

The most tempting prospect is to minimize the magnitudes of ΔL_A and ΔL_B in comparison to ΔL_S and then to neglect them. If the material of rods A and B do not expand appreciably compared to the sample, or not at all, the conditions become favourable to obtain results with reasonable accuracy. A good example of this would be to use light beams that do not expand when entering the controlled environment in place of rods A and B. More frequently, very low expansion

materials such as fused silica are used for rods A and B, and, for many applications, this is enough to reduce inaccuracies to a small fraction of the measured values when high expansion materials such as plastics are tested.

In the present work dilatometery of the well polished glass frits was done by dilatometer, Netzsch (DIL 402 PC) in air using alumina kit including alumina push rod at a heating rate of 5^{o}C/min (figure 3.6) from room temprature to a glass transition temperature. Thermographs have been taken between temperature and percentage change in length of the sample. Thermal expansion coefficient of all the glass samples was measured at various temperature ranges. Apart from glass TEC of a diffusion couple consisting of glass and doped bismuth vanadate (electrolyte) was also measured. The diffusion couple made by pressing a glass fret (1.5 x 2) mm over a pellet of bismuth vanadate (diameter 2 mm and 1.5 mm thick) and heated in resistance furnace for 1 h at 800°C to determine its thermal expansion coefficient**.** During the experiment the heating rate was 5 °C in oxidizing atmosphere and the temperature range was from room temperature to 650°C.

If a temperature change from T_o to T has caused expansion in a sample of initial length L_o, the average coefficient of linear thermal expansion can be calculated as follows

$$a = (\Delta L_S / \Delta L_o)/(T - T_o) \qquad (3)$$

This coefficient, often referred to as TEC, is only true for the temperature range T_o to T.

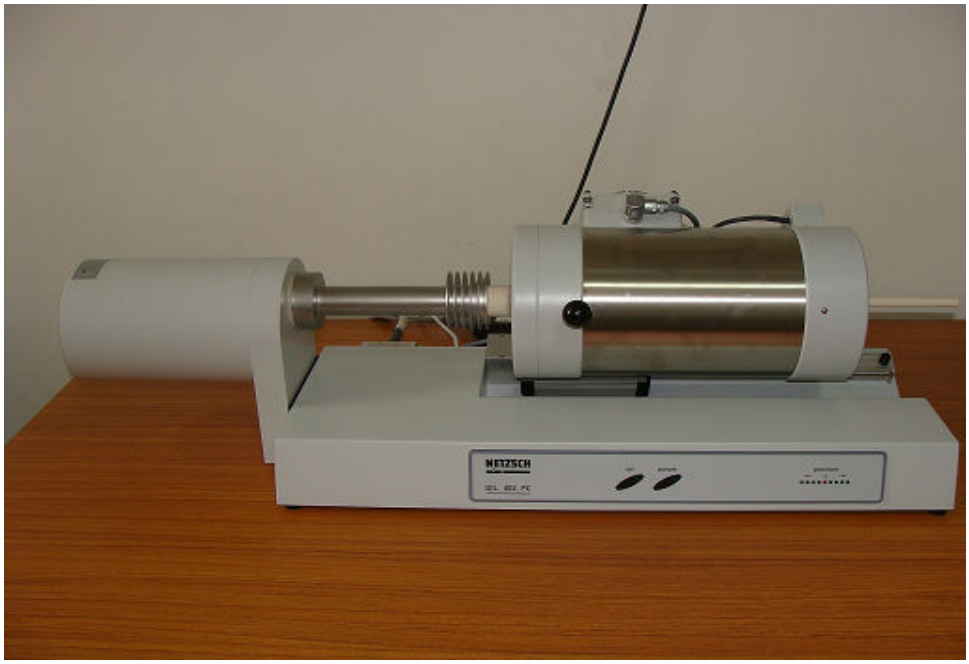

Figure 3.6: Thermal Dilatometric Analyzer (TDA)

3.2.5 Scanning Electron Microscopy (SEM)

The scanning electron microscope (SEM) is a very powerful tool to study the morphological features of the samples using a high-energy beam of electrons. The electrons interact with the samples and produce signals that contain information about the sample's surface topography, composition and morphology of crystalline phases. The types of signals that are produced by the SEM include secondary electrons (SE), back scattered electrons (BSE), characteristic X-rays, light (cathodoluminescence), specimen current and transmitted electrons. The detection of these signals require specialized detectors for their detection that are located at different places in the machine. Scanning electron micrographs of the selected samples were taken by using JEOL 840, JSM and Hitachi TM 1000 scanning electron microscope. Before SEM analysis, the samples were gold plated to make them conducting. The SEM was done either on fractured surface or on polished surface topography.

In order to see the morphology of the phases present and to study the interaction between glass and Crofer 22APU (interconnect) SEM along with EDX analysis was done. The specimen for this study was prepared by mixing finely powdered glass in 2% PVA (poly vinyl alcohol) to form a paste. This paste was applied uniformly over the surface of interconnect. Once the paste dried in air, this combination of glass sealant and interconnect was placed in high resistance furnace in air and given a heat treatment for 1h at a temperature of 1000 ºC. The selection of glass for interaction study was made on the basis of its high melting point compared to other glasses. All other glasses exhibited melting point in the range of 800 ºC - 850 ºC which made them suitable for sealing below 800 ºC. After the heat treatment the system was mounted, polished and etched by 2% HF for SEM studies.

3.2.6 Fourier transform infrared spectroscopy (FTIR)

Infrared spectroscopy is very important technique for materials analysis since last century. An infrared spectrum represents a fingerprint of a sample with absorption peaks which correspond to the frequencies of vibrations between the bonds among the atoms. Each material is a unique combination of atoms (including bond length, size of atoms and bonding etc.), so no two compounds can produce the exact infrared spectrum. Therefore, infrared spectroscopy can result in a positive identification (qualitative analysis) of various materials. In addition, the size of the peaks in the spectrum is a direct indication of the amount of material present. With modern software algorithms, infrared is an excellent tool for quantitative analysis, it is the absorption measurement of different IR frequencies by a sample positioned in the path of an IR beam. The main goal of IR spectroscopic analysis is to determine the chemical functional groups in the sample. Using various sampling accessories, IR spectrometers can accept a wide range of sample types such as gases, liquids, and solids. Thus, IR spectroscopy is an important and popular tool for structural

elucidation and compound identification. For most common materials, the spectrum of an unknown can be identified by comparison to a library of known compounds.

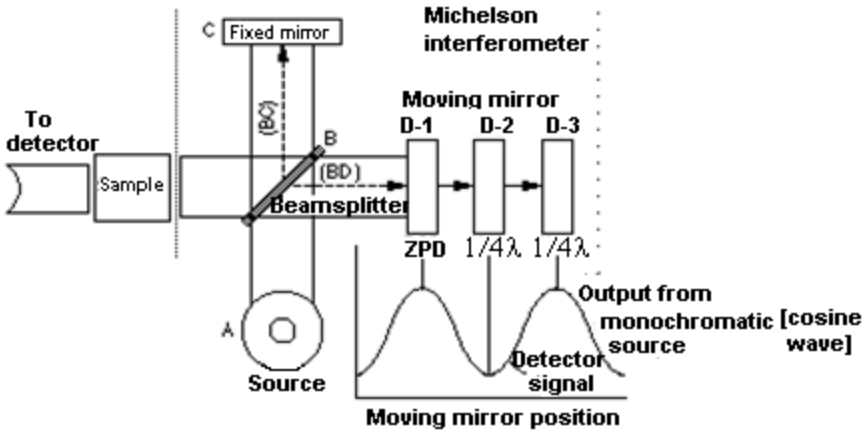

Figure 3.7: Simplified optical layout of a typical FTIR spectrometer.

3.2.6.1 Components of FTIR spectroscope

There are three basic spectrometer components in an infra-red spectroscope: radiation source, interferometer, and detector. A simplified optical layout of a typical FTIR spectrometer is illustrated in figure. 3.7. The same types of radiation sources are used for both dispersive and Fourier transforms spectrometers. However, the source is more often water-cooled in FTIR instruments to provide better power and signal stability. In contrast, a completely different approach is taken in an FTIR spectrometer to differentiate and measure the absorption at component frequencies. The monochromator is replaced by an interferometer, which divides radiant beams, generates an optical path difference between the beams, and then recombines them in order to produce repetitive interference signals measured as a function of optical path difference by a detector. As its name implies, the interferometer produces interference signals, which contain infrared spectral information generated after passing through a sample. The most commonly used interferometer is a Michelson interferometer. It consists of three active components: a moving

mirror, a fixed mirror, and a beam splitter (Fig.3.7). The two mirrors are perpendicular to each other. The beam splitter is a semi reflecting device and is often made by depositing a thin film of germanium onto a flat KBr substrate. Radiation from the broadband IR source is collimated and directed into the interferometer, and impinges on the beam splitter. At the beam splitter, half the IR beam is transmitted to the fixed mirror and the remaining half is reflected to the moving mirror. After the divided beams are reflected from the two mirrors. These beams are recombined at the beam splitter. Due to changes in the relative position of the moving mirror to the fixed mirror, an interference pattern is generated. The resulting beam then passes through the sample and is eventually focused on the detector.

During the present investigations FTIR spectra were recorded in the range 400 cm^{-1} to 1500 cm^{-1} using a Perkin Elmer- Spectrum RX-1. A spectral resolution of FT-IR spectroscopy was 1cm^{-1}. 2 mg of each sample was mixed with 200 mg of KBr in an agate mortar and then pressed into 13 mm diameter pellets. The FTIR spectrum was recorded on these samples. For each sample, the FTIR spectrum represents an average of twenty scan, which were normalized to the spectrum of the standard KBr pellet.

IR Frequency Range and Spectrum Presentation

Infrared radiation spans a section of the electromagnetic spectrum having wave numbers from roughly 13,000 to 10 cm^{-1}, or wavelengths from 0.78 to 1000 μm. It is bound by the red end of the visible region at high frequencies and the microwave region at low frequencies. IR absorption positions are generally presented as either wave numbers or wavelengths (λ). Wave number defines the number of waves per unit length. Thus, wave numbers are directly proportional to frequency, as well as the energy of the IR absorption. The wave number unit (cm^{-1}) is more commonly used in modern IR instruments that are linear in the cm^{-1} scale. In contrast, wavelengths are inversely proportional to frequencies and their associated energy. At present, the recommended

unit of wavelength is μm (micrometers), but μ (micron) is used in some older literature. IR absorption information is generally presented in the form of a spectrum with wavelength or wave number on the X-axis and absorption intensity or percent transmittance on the Y-axis.

I. $BaO\text{-}40SiO_2\text{-}20B_2O_3\text{-}10A_2O_3$ (A= Y, La, Al, Cr) system

The glassy nature of the samples of above series was investigated using TG/DTA. The curves of all the glasses were taken with different heating rates of 10, 20, 30, 40 ºC min^{-1} to calculate the activation energy for crystallization. The quenched samples were examined to confirm their amorphous nature using X-ray diffraction technique. Furthermore, the X-ray diffraction (XRD) study was also done on heat treated sample to identify various crystalline phases. The dilatometer study was performed using Netzsch DIL 402 PC in the temperature range 100-650 ºC to determine the thermal expansion coefficient (TEC) of glasses and glass ceramics to study the effect of crystalline phase formation on TEC.

4.1 Differential thermal analysis

Fig. 4.1(a) shows the typical DTA curves of all Ba based glasses. The DTA curve for BaY, BaLa and BaAl glasses show the typical transition temperature (T_g), crystallization temperature (T_c) and melting temperature (T_m) of all the glasses. The transition and melting peaks are represented by the endothermic peaks whereas an exothermic peak represents crystallization in glases. The numerical values of (T_g), (T_c) and (T_m) are given in table 4.1. The activation energy of glass samples was calculated by heating glass powders at different heating rates.

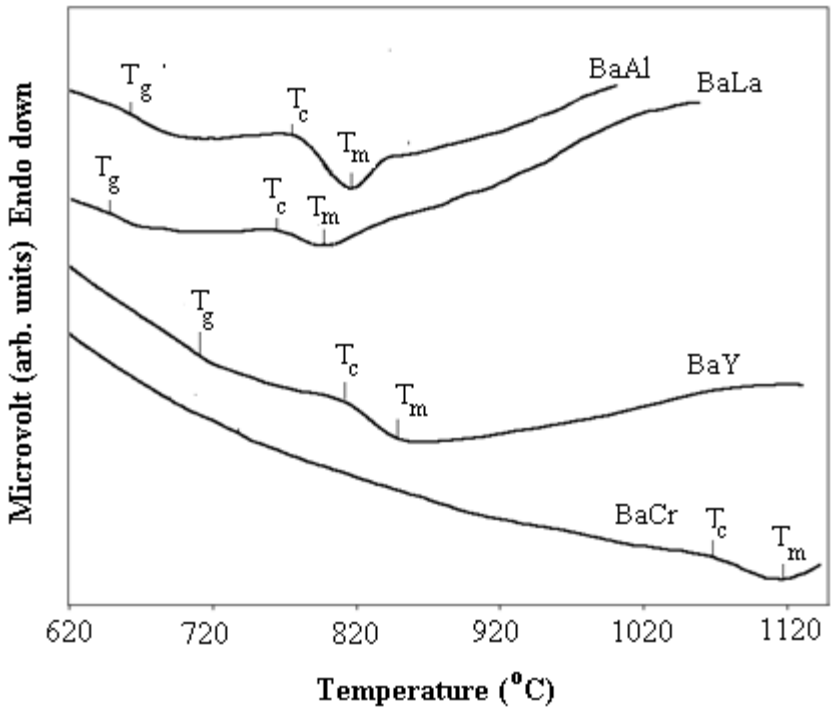

Figure 4.1(a): Differential thermal analysis (DTA) of fine powders of glass samples at 10 ºC min^{-1}.

The crystallization peaks (T_c) were observed to shift towards higher with respect to the increasing heating rate in all the glasses which is because of delay in attaining thermal equilibrium. A typical representative diagram showing increase in crystallization temperature with heating rate is given in figure 4.1(b). Ray et al. [1] have reported that T_g is related to the density of covalent cross linking, number and strength of co-ordinate links formed between oxygen atoms and the cations and the oxygen density of network. Higher values of these factors correspond to higher T_g. In case of BaY glass, Y^{3+} might be acting as network former where it may have higher number of covalent cross linking. The non bridging oxygen due to modification of glass network by Ba^{2+} might be bonded by Y^{3+} cations which lead to the higher T_g of this particular glass as compared to the BaLa and BaAl glasses. Interestingly, the cation field strength might not be playing very important role to

govern the glass transition temperature since the field strength of Al^{3+} has high value as compared to the $Y^{3+}$and La^{3+}cations. Thermal data obtained from DTA

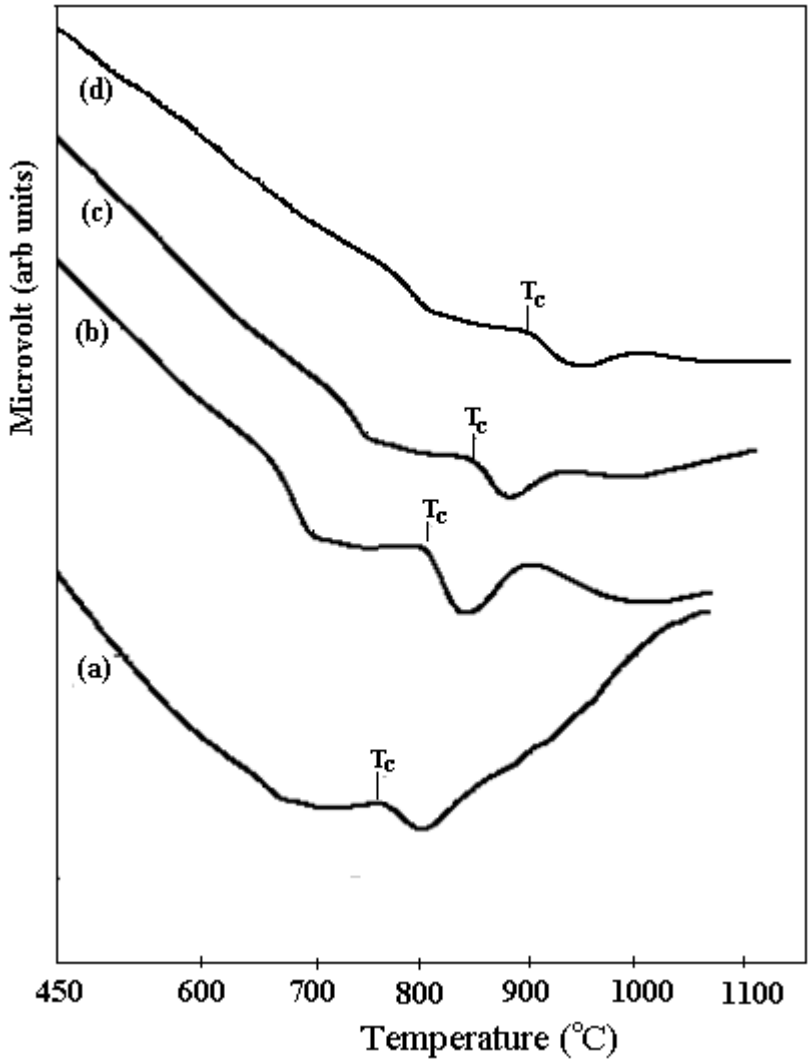

Figure 4.1(b): A typical DTA plot of BaAl glass at different heating rates (a) 10 $^{\circ}C\ min^{-1}$ (b) 20 $^{\circ}C$ min (c) 30 $^{\circ}C\ min^{-1}$ and (d) 40 $^{\circ}C\ min^{-1}$.

measurement of these glasses was used to calculate the thermal stability and activation energy for crystallization.

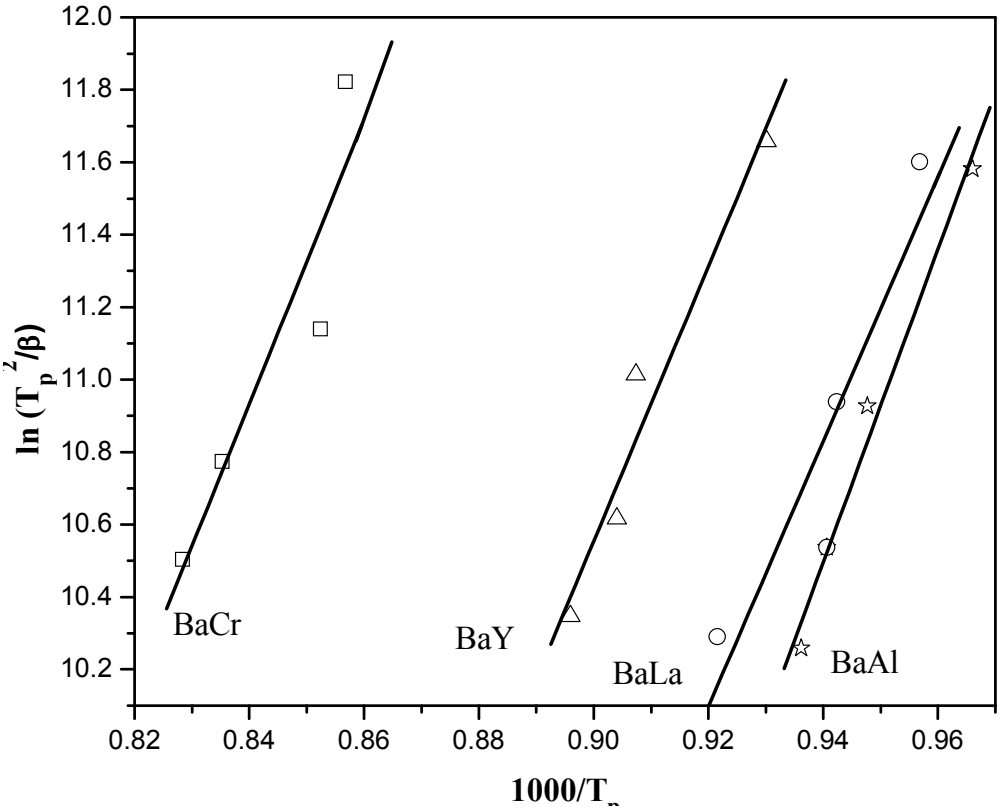

Figure 4.2: Kissinger plot of BaY, BaLa, BaAl and BaCr glass samples.

The activation energy of all the glasses were calculated using Kissinger equation [2, 3]

$$\ln(T_p^2/\beta) = (E_p/RT_p) + \text{constant} \quad (1)$$

where β is heating rate, T_p is crystallization temperature and R is gas constant. From the experimental data a graph between ln (T_p^2/β) versus $(1000/T_p)$ was plotted, slope of this graph gives the activation energy of crystallization. The Kissinger plot for activation energy of BaY, BaLa, BaAl and BaCr glasses is shown in Fig 4.2. The highest activation energy is observed in BaCr glass followed by BaAl, BaY and BaLa glasses as summarized in Table 4.1. It is observed that the as prepared BaCr glass exhibit small portion of unreacted crystalline Cr_2O_3 phase which is described in next section.

Table 4.1 Glass transition, crystallization and melting temperature along with activation energy for crystallization and fragility index of glasses.

Sample Name	T_g (ºC) (Dilatometer)	T_g (ºC) (DTA)	T_c (ºC)	T_m (ºC)	% Wt.loss 50-1000 (ºC)	A.E ($kJmol^{-1}$)
BaY	690	707	810	850	1.25	316
BaLa	656	670	775	815	1.5	303.5
BaAl	650	664	766	800	1.3	359.54
BaCr	-	-	1074	1120	6.5	573.75

Presence of microcrystalline Cr_2O_3 phase in glass matrix provides higher strength in local regions, so the formation of new crystalline phase requires higher activation energy as compared to other glasses. On the other hand, higher field strength cation such as Al^{3+} exhibit higher activation for crystallization followed by other cations as Y^{3+} and La^{3+}. The field strength of Al^{3+} which act as intermediate is highest and due to this it holds the glass matrix tightly. Because of this fact it requires higher activation energy for crystallization as compared to Y^{3+} cation followed by La^{3+} which has the least value of field strength [4]. Moreover, Al_2O_3 addition in glass is well known to prevent the crystallization and control the viscosity of the glasses [5].

4.2 X-ray diffraction for crystallization study

Glass–ceramics, as-prepared by controlled crystallization of glasses, exhibit superior mechaniCal properties than glasses and can have various TEC values depending on the type of precipitated crystalline phases and their volume fraction in the glass matrix. Glass–ceramics also show higher chemiCal stability than glasses, especially, under SOFC operating conditions. Therefore, the glasses developed in the present investigation were subjected to long-term heat-treatment, namely 10–100 h at 800 ºC to study their crystallization behavior and to examine any structural changes that may occur during prolonged thermal operation. All the as prepared glasses were found to be amorphous and exhibited two broad halos in the X-ray diffractogram except BaCr glass in which unreacted Cr_2O_3 phase is present. During heat treatment, glass modifier (BaO) competes with intermediates oxides (Y, La, Al, Cr) to enter into the silicate network. BasiCally, during initial stage of crystallization silica rich phase is formed and in the later stage of heat treatment other cations diffuse from glass matrix to form the stable crystalline phases [4].

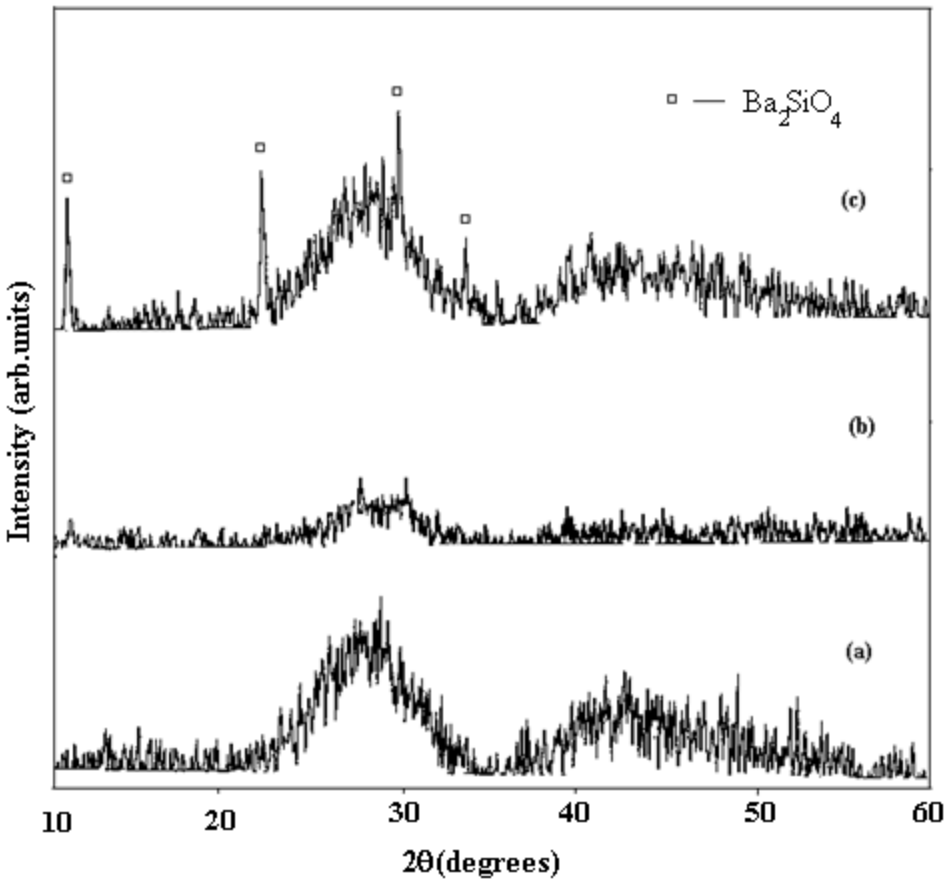

Figure 4.3: XRD patterns of BaY (a) pristine (b) 10 h and (c) 100 h heat treated at 800 ºC.

The BaY glass, has the highest glass transition temperature because of higher cross link density and higher field strength of Y^{3+}cation than Ba^{2+} which makes it possible for the modifier (Ba^{2+}) to enter into the glass network and form barium silicate (Ba_2SiO_4) phase instead of yttrium rich phase even after 100 h heat treatment as shown in Fig. 4.3. It is possible that Y_2O_3 is associated with B_2O_3 instead of SiO_2 network former which may prevent formation of boron and yttria rich crystalline phases in this glass. Our earlier reports [6, 7] also indicated that the addition of Y_2O_3 in any glass composition increase the stability of the glasses without forming any detrimental phase during the heat treatment.

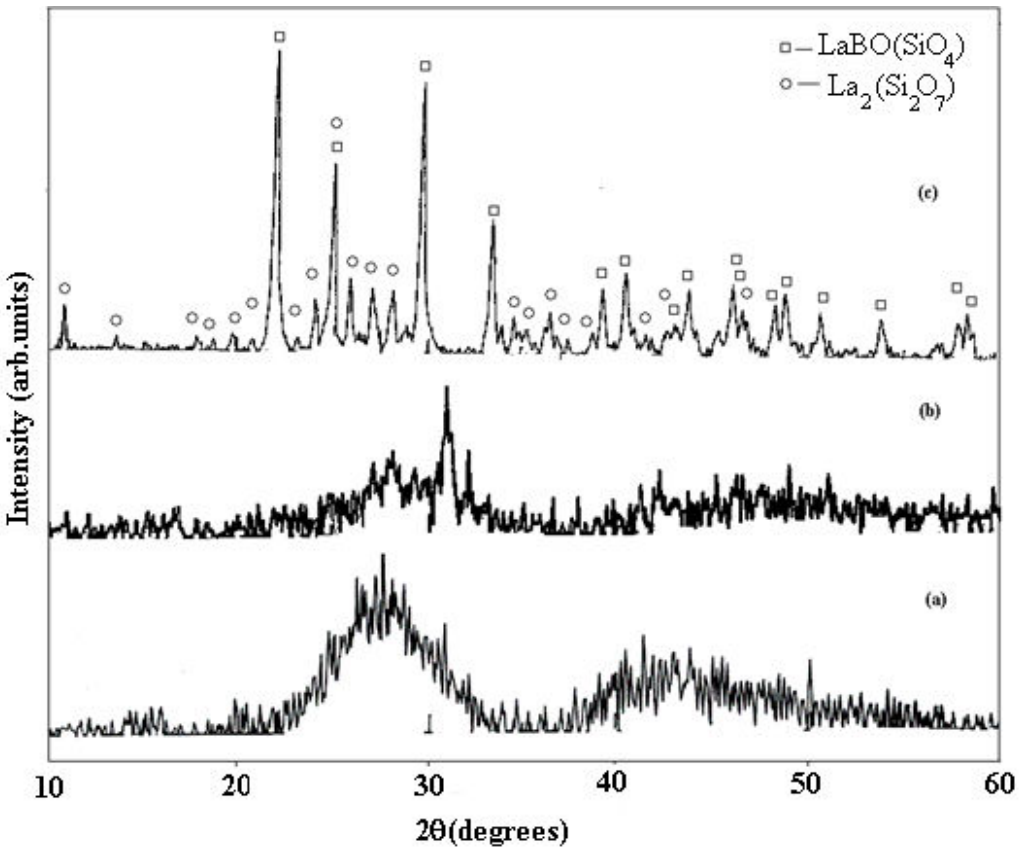

Figure 4.4: XRD patterns of BaLa (a) pristine (b) 10 h and (c) 100 h heat treated at 800 ºC.

In case of BaLa glass (Fig. 4.4), no significant change is observed after 10 h heat treatment, however at 100 h heat treatment lanthanum boron silicate $LaBO(SiO_4)$ and lanthanum silicate $La_2(Si_2O_7)$ phases are formed. It can be explained on the basis of small size difference between intermediate cation La^{3+}(1.22 Å) and modifier Ba^{2+} (1.43Å). Therefore, most likely La_2O_3 is acting as glass modifier which leads to lower activation energy of crystallization with lower glass transition temperature of La_2O_3 containing glass.

The ionic radii of Al^{3+} (0.54Å) in BaAl glass allows it to fit easily in either tetrahedral or octahedral sites in an oxygen structure. If it is connected as tetrahedrally it works as a network former otherwise it acts as modifier. It is well reported in the literature, that less than 5 mol%

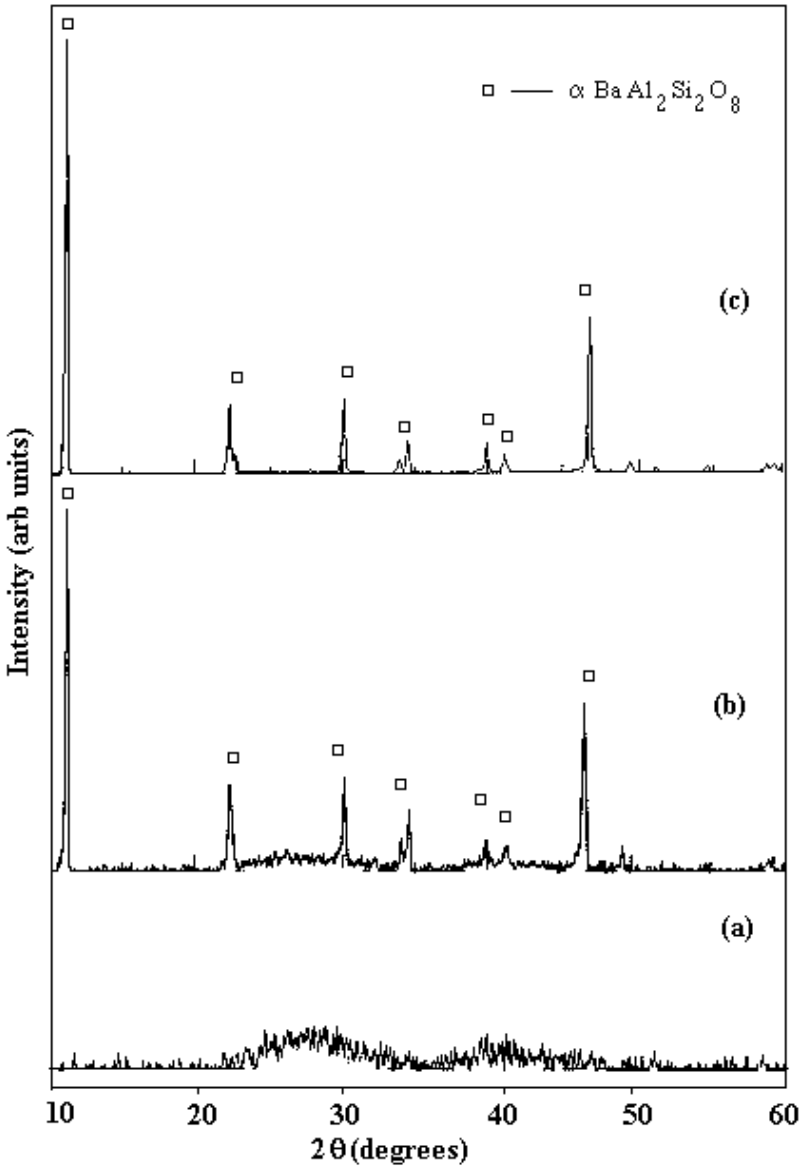

Figure 4.5: XRD patterns of BaAl (a) pristine (b) 10 h and (c) 100 h heat treated at 800 ºC.

Al_2O_3 in glass composition acts as glass former and above that it acts as modifier. Al^{3+} along with Ba^{2+} enters into the glass network and form hexacelsian phase as shown in fig 4.5. Although the density of hexacelsian phase (3.29 gcm^{-3}) is less than parent BaAl glass (3.5 gcm^{-3}). However, the

difference is not very large to produce appreciable thermal stress in seal during operation for longer duration. TEC of hexacelsian phase is 8 x 10^{-6} K^{-1} which lies within the limit required for SOFC application [8]. Moreover, Ghosh et al. [9] have mentioned hexacelsian as a desirable crystalline phase.

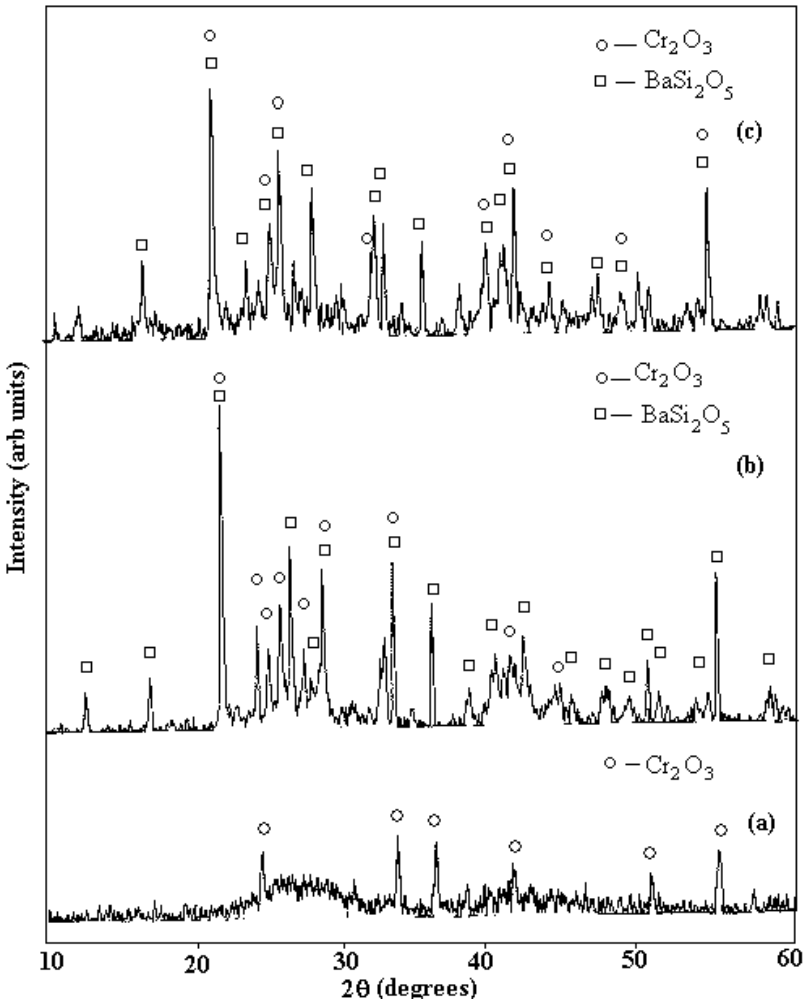

Figure 4.6: XRD patterns of BCr (a) pristine (b) 10 h and (c) 100 h heat treated at 800 ºC.

On the other hand BaCr glass exhibit unreacted Cr_2O_3 phase as shown in Fig. (4.6a). The presence of Cr_2O_3 in glass matrix is clearly shown in scaning electron micrograph Fig. (4.6 d). During 100 h heat treatment, barium enters into glass network preferentially and form $BaSi_2O_5$.

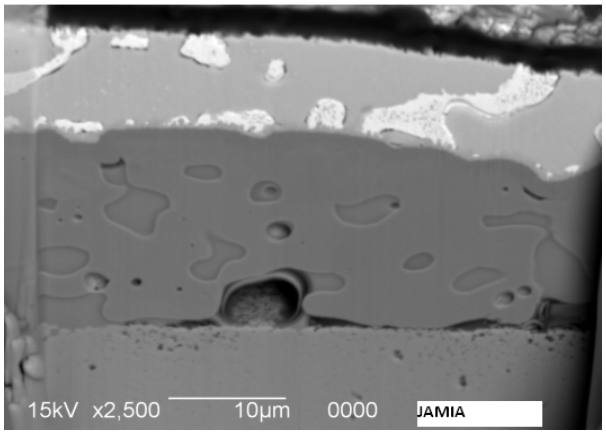

Figure 4.6 (d): Micrograph of as prepared BaCr sample.

Conclusively, BaY glass is more stable as compared to BaAl and BaLa samples. In all the samples BaLa and BaAl crystallized fully and did not form any detrimental crystalline phase(s) even after 100 h heat treatment in air.

4.3 FT-IR investigation

FTIR transmittance spectra of 100 h heat treated glass ceramics shows the structural rearrangement undergone compared to as prepared glasses shown in Figs. 4.7- 4.10. All the spectra exhibit three broad transmittance bands i.e. 300-600 cm^{-1}, 600-800 cm^{-1} and 1300-1500 cm^{-1}.These diffused bands are indicative of the general disorder in the silicate network mainly due to a wide distribution of Qn units (polymerization in the glass structure, where n denotes the number of bridging oxygen) occurring in these glasses. However, after heat treatment the diffused bands become sharp with splitting. This change in bands might be associated with definite crystalline phases [5].

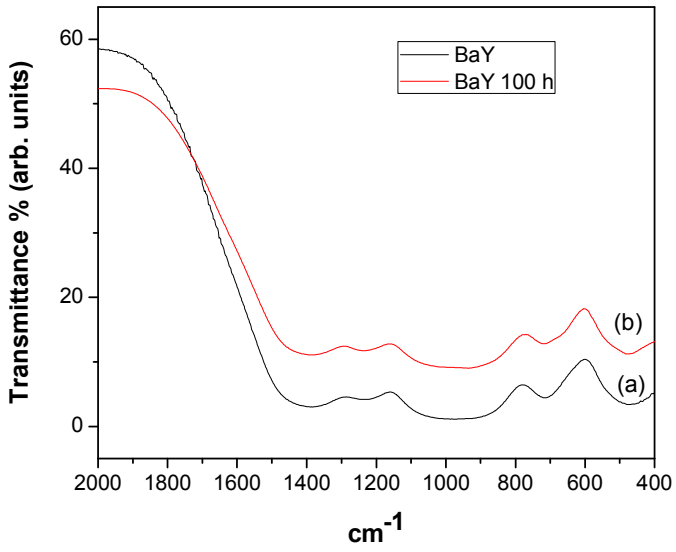

Figure 4.7: FTIR spectra of (a) BaY as prepared (b) BaY 100 h heat treated at 800 ºC.

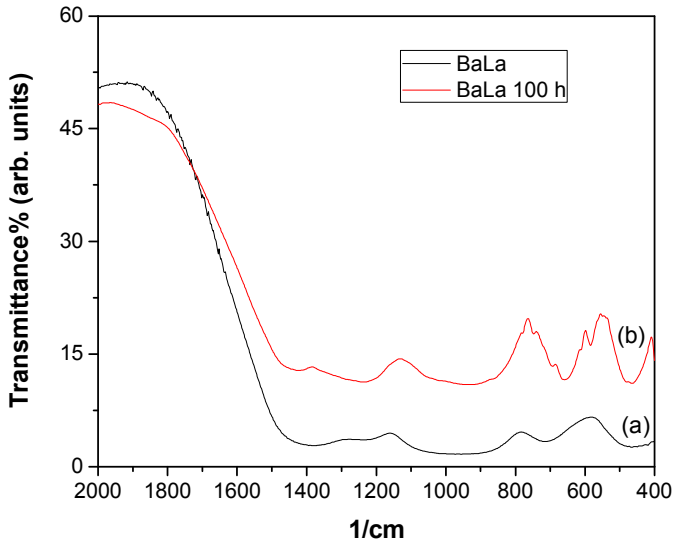

Figure 4.8: FTIR spectra of (a) BaLa as prepared (b) BaLa 100 h heat treated at 800 ºC.

The bands in the 300–600 cm^{-1} region are due to bending vibrations of Si–O–Si linkages. The transmittance band in the 650–800 cm^{-1} region in the glasses is attributed to the bending vibrations of bridging oxygen between trigonal boron atoms and it is also related to the stretching vibrations of the A–O bonds with A^{3+} ions in four-fold coordination (A=Y, Cr , La, Al) [10]. The band in the

region 1350–1500 cm^{-1} corresponds to B–O vibrations in BO_3 triangle. Borate glasses show two characteristic bands derived from the B–O bonds in the BO_3 triangles about 1300–1500 cm^{-1} and the BO_4 tetrahedra about 1000 cm^{-1} [11]. These bands get shifted under the influence of surrounding cations, the extent and the direction of this shift depends on the type of cation. FTIR spectra of the glasses under investigation show that in these glasses boron primarily occurs in the form of BO_3 triangles (1396 cm^{-1}).

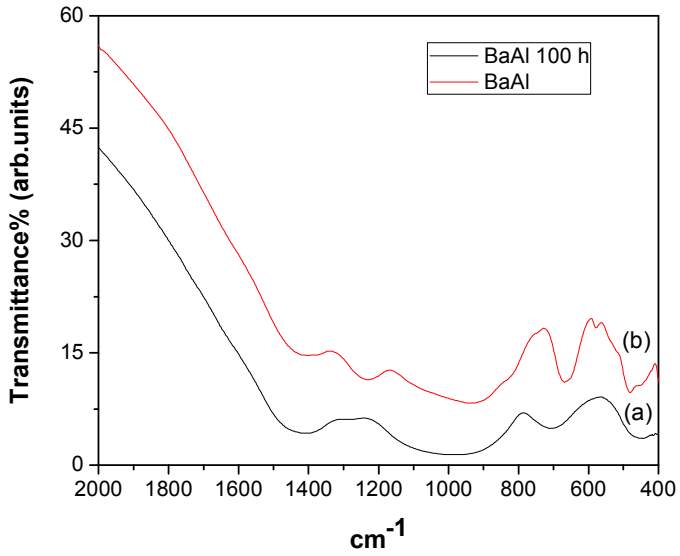

Figure 4.9: FTIR spectra of (a) BaAl as prepared (b) BaAl 100 h heat treated at 800 ºC.

However, the presence of BO_4 tetrahedron in the glass structure cannot be neglected. Since the IR band for BO_4 tetrahedron about 1000 cm^{-1} overlaps with that of stretching vibrations of SiO_4, therefore, it could not be observed [12]. The broad band in the 800–1300 cm^{-1} is assigned to the stretching vibrations of the SiO_4 tetrahedron with different number of bridging oxygen atoms [13, 14]. For heat treated glasses, these bands shift towards lower wave numbers implying towards the decrease in the connectivity of the silicate glass network. The FTIR spectrum of BaY sample is shown in Fig. 4.7 (a) and 4.7(b) for glass and glass ceramic, respectively. Glass ceramic sample

shows slight change in sharpness of bands at 800-1300 cm^{-1} as compared to glass indicating small amount of rearrangement in silicate chains leading towards an ordered pattern. On the other hand, La_2O_3 containing glass as shown in Fig. 4.8 (b), a special band centered appears at 1120-1320 cm^{-1} which is due to boroxol rings and borate stretching [5]. Apart from this, the lower wave number band (500-1000 cm^{-1}) in glass ceramics becomes sharper and split indicating that crystalline phase is formed. Similar phenomenon was also reported by Fatma et al. [5]. The FT-IR spectra of BaAl glass are shown inFig. 4.9 (a) and (b). The heat treated glass exhibit an additional band around 1200 cm^{-1} which is due to hexacelsian [10].

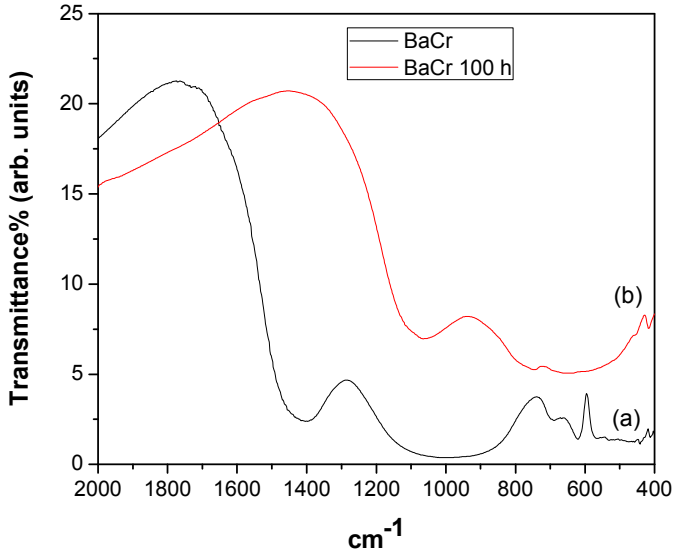

Figure 4.10: FTIR spectra of (a) BaCr as prepared (b) BaCr 100 h heat treated at 800 ºC.

In case of BaCr glass and glass ceramic Fig. 4.10, both the spectra exhibit sharp bands. Additionally, a sharp peak is observed at 800 cm^{-1} in heat treated samples which is due to SiO_4 tetrahedron indicating presence of barium silicate also observed in XRD study as shown in Fig 4.6. In all the four samples, the BaY and BaCr could not show any appreciable change in the FTIR spectra of glass and glass ceramics except higher sharpness of bands in heat treated sample.

Obviously, there is not too much change in the basic units. On the other hand BaLa and BaAl sample show remarkable differences in glass and glass ceramic due to regrouping in Si-O-Si and BO_4 structure. Additionally, the shift of the bands at lower wave number in glass ceramic also indicates that these systems have more stability than their glass counterpart.

4.4 Thermal expansion coefficient (TEC)

In present investigation the BaLa glass has the highest TEC value among all the studied glasses as shown in table 2. The higher TEC in this glass as compared to other glasses can be associated with the higher ionic radii of La^{3+}. After heat treatment when it turns into glass ceramic the TEC value increases, this is due to the formation of crystalline phases which improve the TEC of this glass.

Table 4.2 Thermal expansion coefficient (10^{-6}/K) Calculated from R.T. to T_g for glass and R.T. to 650 ºC for glass ceramics.

Sample Name	Glass	Glass ceramic (10h)	Glass ceramic (100h)	% change in TEC after100 h heat treatment
BaY	7.58	7.69	7.80	3
BaLa	7.71	7.67	8.10	5
BaAl	6.98	7.81	7.67	10
BaCr	6.84	7.57	8.08	18

*R.T – Room temperature

BaY glass does not show much variation in TEC with heat treatment as very limited amount of crystallization takes place in this glass which indicates that glass matrix has undergone very little structural rearrangement. The formation of hexacelsian phase, which has a relatively higher TEC value of ~ $8x10^{-6}$ K-1 [14] greatly, improves the TEC of BaAl glass after heat treatment. The change in TEC after heat treatment of this glass is observed around 10%. In case of BaCr the as prepared glass was already in crystalline form and its TEC has low value of 6.8 x 10^{-6} K^{-1}.

However, after heat treatment for 10 h the crystallization of $BaSi_2O_5$ in the glass matrix increased the TEC value (7.6 x 10^{-6} K^{-1}). With further increase in volume fraction of $BaSi_2O_5$ phase due to 100 h heat treatment the TEC value again increased to 8.1x10^{-6} K^{-1}. In this sample, formation of $BaSi_2O_5$ phase might be having high TEC which leads to higher % change in TEC. It might also be attributed that crystalline phase ($BaSi_2O_5$) do not exhibit the intermediate cations which may be responsible for low change in TEC due to small ionic radii as compared to the Ba^{2+} (1.49Å)

The maximum value of TEC was recorded after 100 h heat treatment of the glasses. These heat treated glass ceramics had TEC in the range of 7.67-8.10 x 10^{-6} K^{-1} which is lower than Crofer (11.5 x 10^{-6} K^{-1}). However, it is close to the permissible limit required for SOFC operation (9-12 x 10^{-6} K^{-1}) [8, 15].

4.5 Interaction study

The scanning electron microscopy (SEM) was done using Hitachi TM 1000 to study the interaction between BaCr glass and APU crofer sample. For this finely powdered glass was mixed in 2% PVA (poly vinyl alcohol) to form a paste. This paste was applied uniformly over the surface of interconnect. This combination of glass sealant and interconnect was placed in high resistance furnace in air and given a heat treatment for 1h at a temperature of 1000 ºC. The selection of BaCr glass for interaction study at such a high temperature was due to its high melting point as shown in figure 4.1. All other glasses exhibited melting point in the range of 800 ºC - 850 ºC which made them suitable for sealing below 800 ºC. After the heat treatment the system was mounted, polished and etched by 2% HF for SEM studies.

The BaCr sample exhibit Cr_2O_3 crystalline phase as shown in Fig. 4.6 (a). The DTA curve of this sample could not show any clear cut endothermic peak. Therefore, this sample was heat treated

around (T_c) i.e 1000 ºC for 1h to study the change in crystallinity. The SEM microphotograph of BaCr glass heat-treated at 1000 ºC for 1 h is shown in Fig. 4.11.

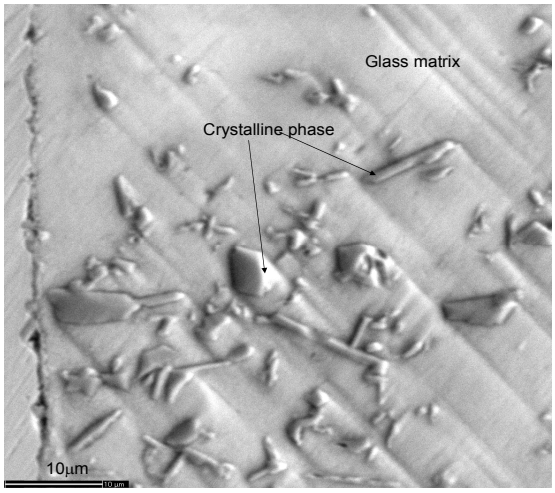

Figure 4.11 SEM of BaCr glass.

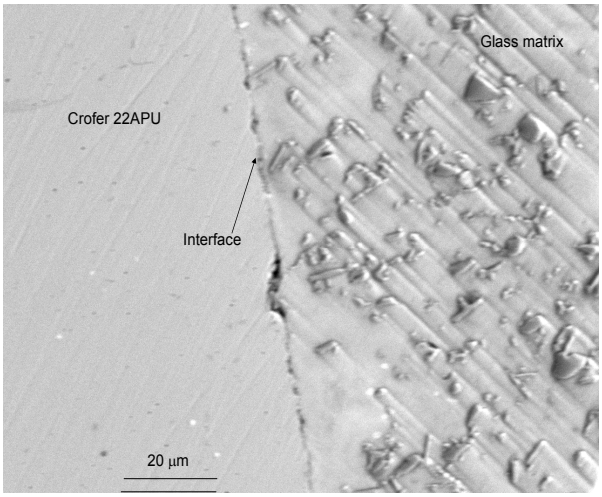

Figure 4.12 Interface of BaCr glass and Crofer 22 APU.

It can be clearly seen that after heat-treatment for 1h, some crystals grow as small floral patterns embedded in glass matrix. These floral patterns have been formed by combination of small needle shaped crystals of barium silicate phase as reported by Bansal [14]. This sample showed highest change in TEC after 100 h heat treatment at 800 ºC. Moreover due to the presence of Cr_2O_3 in glass as well as in Crofer 22 APU this glass was selected to study its bonding characteristics with Crofer 22 APU. A highly uniform and homogenous interface is formed as indicated in Fig.4.12. However, the small voids of the order of few micrometers, which are visible in the micrograph, are due to chipping out of glass during grinding and polishing while preparation of sample for SEM. Preliminary studies clearly indicate good adhesion without any gap at the interface**.** Based on preliminary results, the compatibility study was extended for 20 h to study the growth of interface by elemental analysis as shown in Fig.4.13 (a) and Table 4.3.

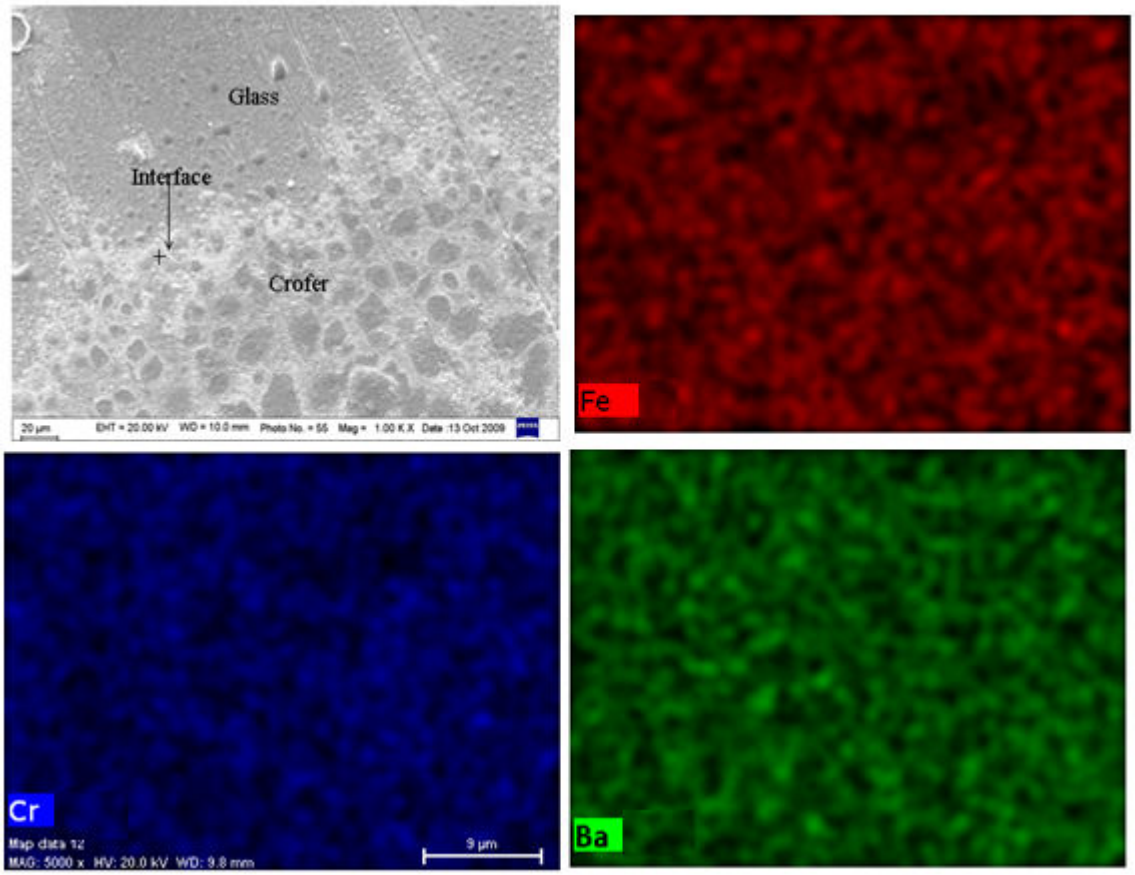

Figure 4.13(a): Microstructure (SEM) of interface between Crofer 22 APU and BaCr glass developed after 20 h heat treatment at 1000 ºC along with X-ray dot mapping.

The interface is devoid of any crack and with the increase of heat treatment time it becomes smoother and shows good adherence to the Crofer. The major elements present at the interface are Fe, Cr and Ba. The interdiffusion of Fe and C from the Crofer and Ba from the glass took place at the interface whereas Cr interdiffused from the glass as well as the Crofer

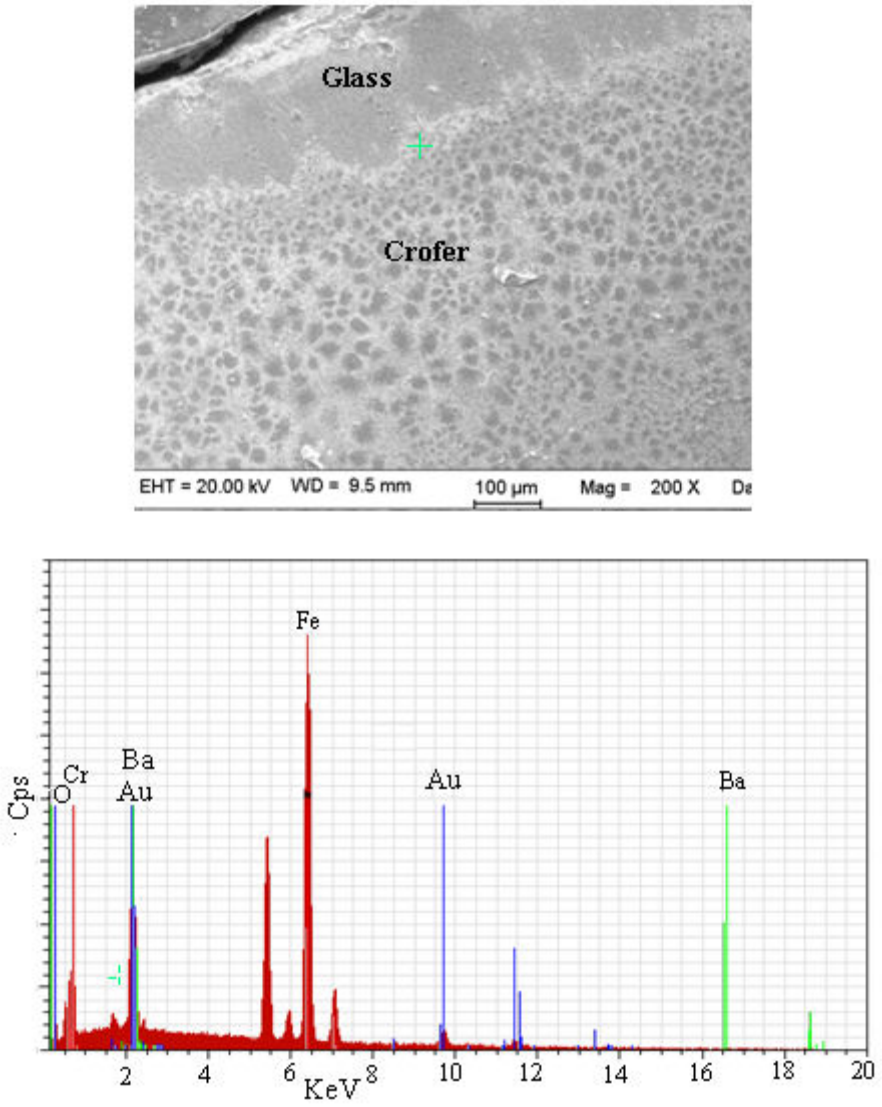

Figure 4.13(b): SEM and EDS of interface between Crofer 22 APU and BaCr glass**.**

However, Si was not present at the interface which means it could not diffuse out from the glass matrix. Barium containing glass ceramic and Cr containing ferritic steels are known to form $BaCrO_4$ which has been extensively reported in literature, especially at high sealing temperatures (950°C). The EDS analysis figure 4. 13 (a) shows a fair amount of Ba, Cr and O present at the interface which indicate the presence of $BaCrO_4$ at the interface which is common phase as reported in literature.

II. $30CaO\text{-}40SiO_2\text{-}20B_2O_3\text{-}10A_2O_3$ (A= Y, La, Al, Cr) system

4.6 X-ray diffraction

The as prepared glasses were found to be amorphous and exhibited two broad halos in the X-ray diffractogram. It is possible that Y_2O_3 is associated with B_2O_3 and SiO_2 network simultaneously. The two humps as shown in Fig 4.14 are due to silicate and borate network which are trying to grow simultaneously in the matrix. Glass–ceramics, as-prepared by controlled crystallization of glasses, exhibit superior mechanical properties than glasses which depend upon nature of nucleated phase. These exhibit various TEC values depending on the type of nucleated crystalline phases and their volume fraction in the glass matrix. Glass–ceramics also show higher chemical stability than glasses, especially, under SOFC operating conditions. The present glasses were subjected to different heat-treatment, namely 10–100 h at 800 ºC and 1–10 h at 900 ºC. The CaY glass has the highest glass transition temperature because of higher cross link density and higher field strength of Y^{3+}cation.

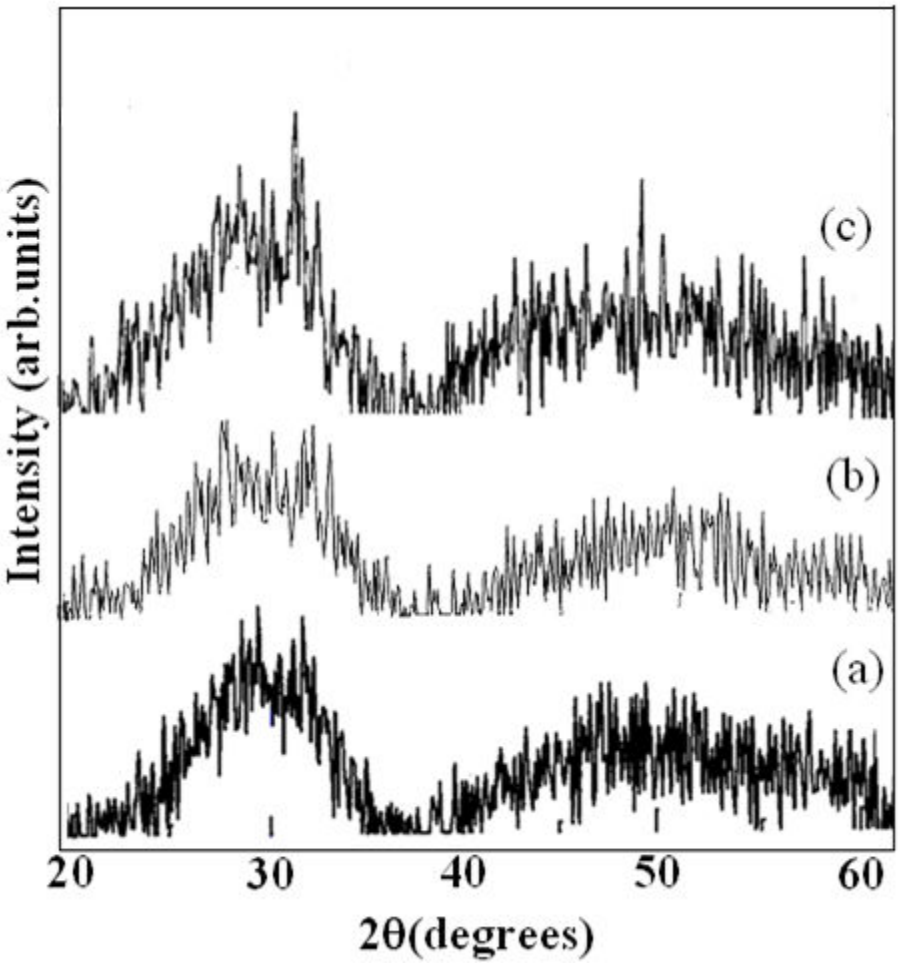

Figure 4.14: XRD pattern of CaY (a) pristine (b) heat treated at 800°C for 10 h and for (c) 100h.

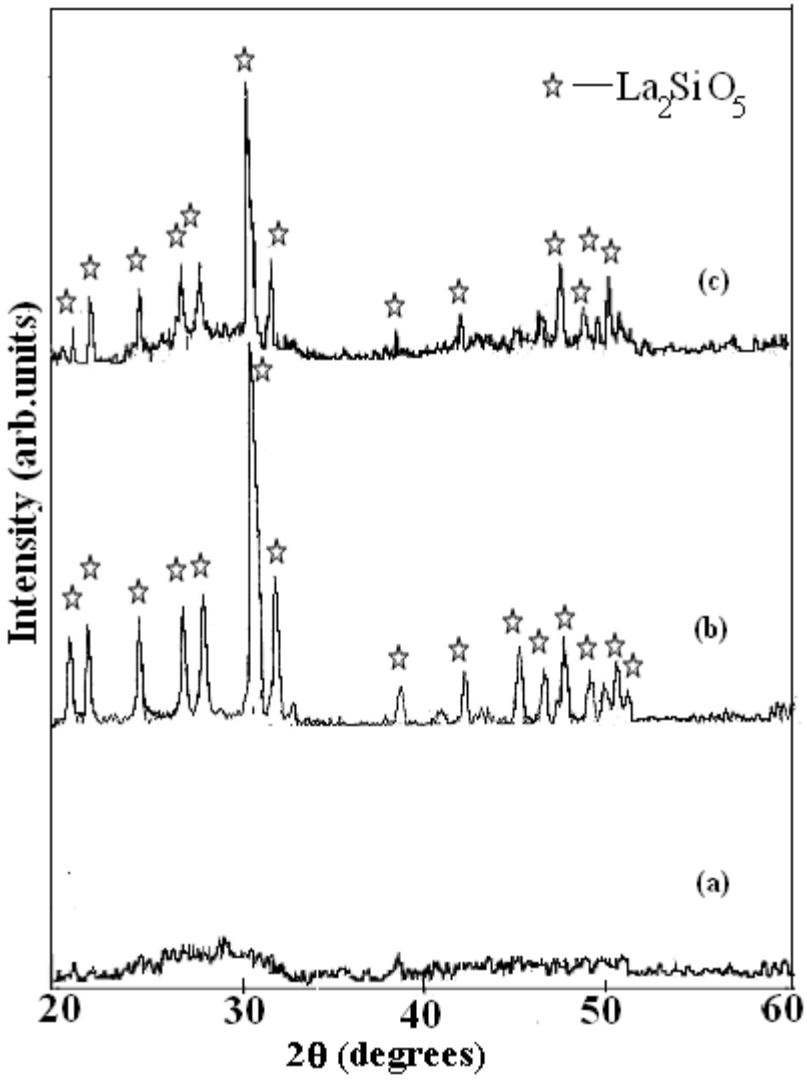

Figure 4.15: XRD pattern of CaLa (a) pristine (b) heat treated at 800°C for 10 h and for (c) 100h.

The intentional addition of intermediate oxide might lead to phase separation in glass network. Phase separation is common phenomenon in alkaline borosilicate glasses [6]. CaY glass could not form any crystalline phase even after heat treatment. As shown in table 4.5, this glass exhibit higher activation energy compared to CaLa glass (278 $kJmol^{-1}$). In our earlier reports [6, 7] it is observed that the addition of Y_2O_3 in any glass composition increases the stability of the glasses without forming any detrimental crystalline phase during the heat treatment. As mentioned earlier it is possible that Y_2O_3 is associated with B_2O_3 and SiO_2 network. The high field strength of Y^{3+}

compared to B_2O_3 and SiO_4 pulls the borate and silicate network thus producing a strain in the matrix, however, when heat treatment is given to glasses it provides sufficient energy (which further depends on duration of heat treatment) to cations for movement in the glass matrix. As the time duration of heat treatment increases the stress relaxation in the matrix takes place.

The XRD patterns of CaLa glass are shown in Fig.4.15. Most likely La_2O_3 is modifying the silicate network which leads to formation of monoclinic La_2SiO_5 crystalline phase after heat treatment. Even after 100 h heat treatment at 800°C (Fig.4.15(c)) no new phase has formed. However, the full width at half maxima (FWHM) of peaks decreased with increase in time duration of heat treatment. Fig.4.15 (a) shows small humps in XRD pattern which indicate the amorphous content in glass. This amorphous content is completely consumed by crystalline phase La_2SiO_5 as shown in Fig.4.15 (b) and (c) due to increase in time duration of heat treatment. In case of CaAl glass we find initiation of crystallization of Al_2SiO_5 phase in glass matrix after 10 h heat treatment at 800°C. The volume fraction of this phase increases with time duration as seen in figure 4.16(c). Conclusively the addition of Y_2O_3 prevents crystallization, it might be better than Al_2O_3 in suppressing crystallization.

In case of CaCr composition the sample was not glassy in nature; this has been confirmed by XRD diffraction pattern shown in Fig.4.17. Calcium and chromium interact with silicate network thus forming Calcium silicate and chromium silicate. During the heat treatment the volume fraction of these phases increases which is shown by the increase in intensity of crystalline peaks.

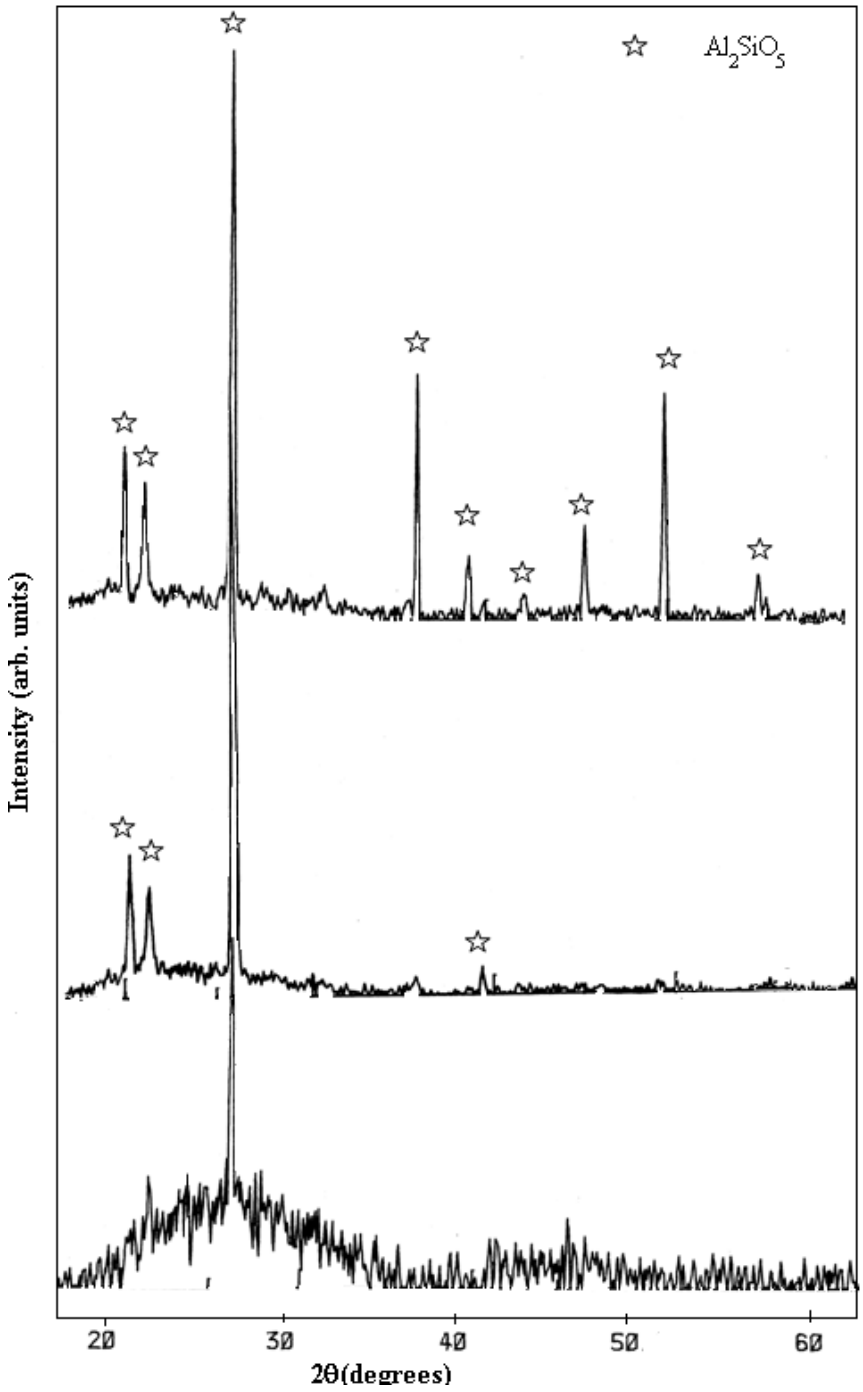

Figure 4.16: XRD pattern of CaAl (a) pristine (b) heat treated at 800°C for 10 h and for (c) 100h.

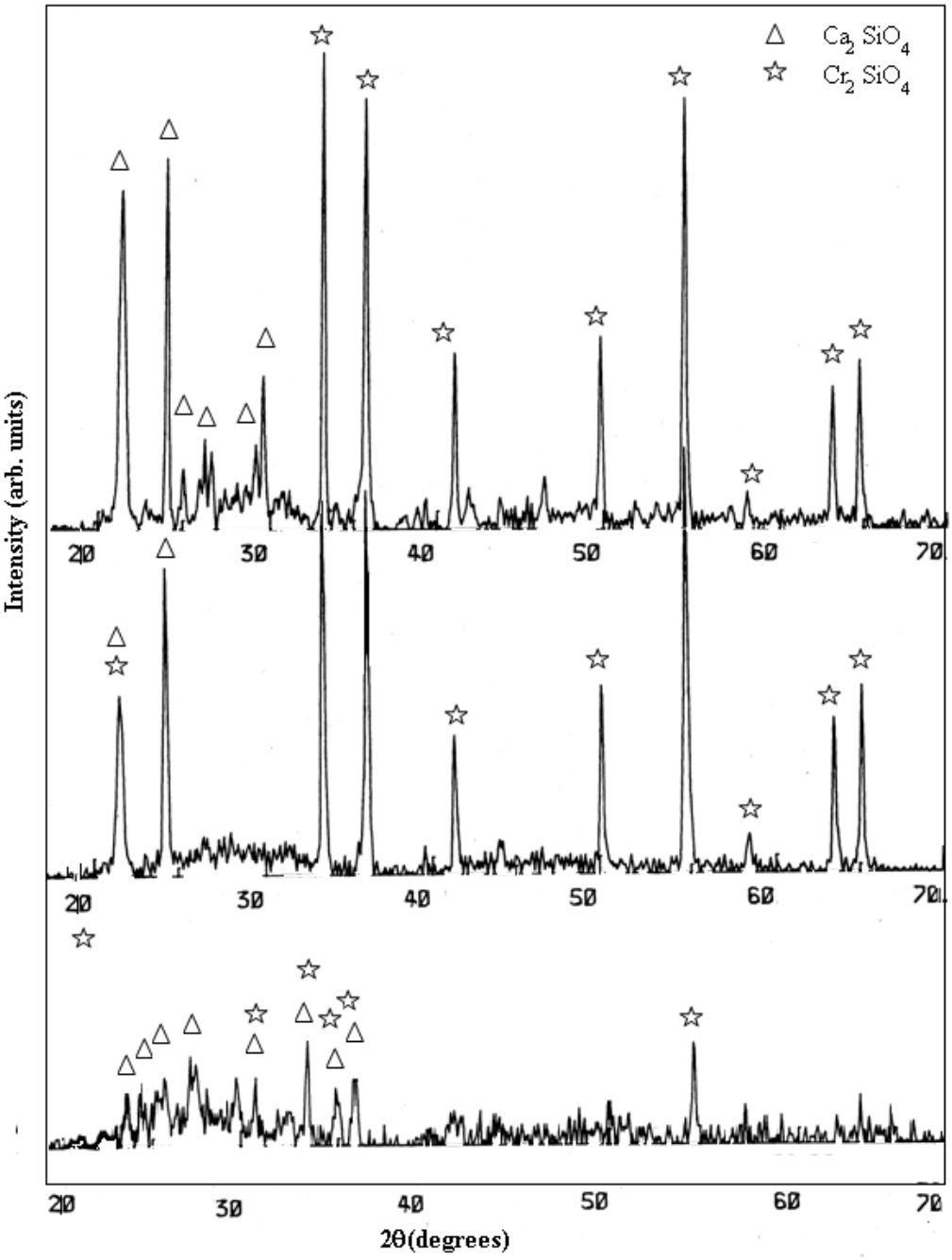

Figure 4.17: XRD pattern of CaCr (a) pristine (b) heat treated at 800°C for 10 h and for (c) 100h.

4.7 FT-IR investigation

As observed in case of barium, strontium and magnesium based glasses the FTIR spectra of Calcium based glasses also exhibit three broad transmittance bands at 300-600 cm^{-1}, 600-800 cm^{-1} and 1300-1500 cm^{-1}. It has been observed that silicate and borate groups play a dominant role in the spectra. Although alkaline earth metals are also present as modifier in the glass network but their presence is not highlighted by FTIR. The spectra shows the changes brought about in the silicate and borate network before and after different heat treatments.

In case of as prepared glasses spectra does not have sharp characteristic peaks, instead it exhibits diffused bands which are indicative of the general disorder in the silicate network arising mainly due to a wide distribution of Qn units (polymerization in the glass structure, where n denotes the number of bridging oxygen) occurring in these glasses. The bands in the 300–600 cm^{-1} region are due to bending vibrations of Si–O–Si linkages. The transmittance band in the 650–800 cm^{-1} region in the glasses is attributed to the bending vibrations of bridging oxygen between trigonal boron atoms and is also related to the stretching vibrations of the A–O bonds with A^{3+} ions in four-fold coordination (A=Y, La, Al) [10]. The band in the region 1350–1500 cm^{-1} corresponds to B–O vibrations in BO_3 triangle. Borate glasses show two characteristic bands derived from the B–O bonds in the BO_3 triangles which appears at 1300–1500 cm^{-1} and the BO_4 tetrahedra at 1000 cm^{-1} [11]. The broad band in the 800–1300 cm^{-1} is assigned to the stretching vibrations of the SiO_4 tetrahedron with different number of bridging oxygen atoms [12, 13]. These bands get shifted under the influence of surrounding cations, the extent and the direction of this shift depends on the type of cation present in the glass matrix.

The bands becomes little broader in glass ceramic sample which indicate some rearrangement in glass matrix. Apart from some common bands in FTIR spectra of CaLa glass as shown in Fig.4.18

a special band centered at 1120-1320 cm^{-1} appears which is due to boroxol rings and borate stretching [14]. This band might be attributed to BO_4 stretching which shifts to lower wave number. Moreover, the intensity decreases as time duration for heat treatment increases. Similarly a transmission band observed at 1450-1500 cm^{-1} correspond to B-O vibrations of various borate groups and intensity of this peak decreases as the time duration of heat treatment increases. No additional transmission band formation takes place after increasing time duration of heat treatment. However, after heat treatment the transmission peaks shift towards lower wave number.

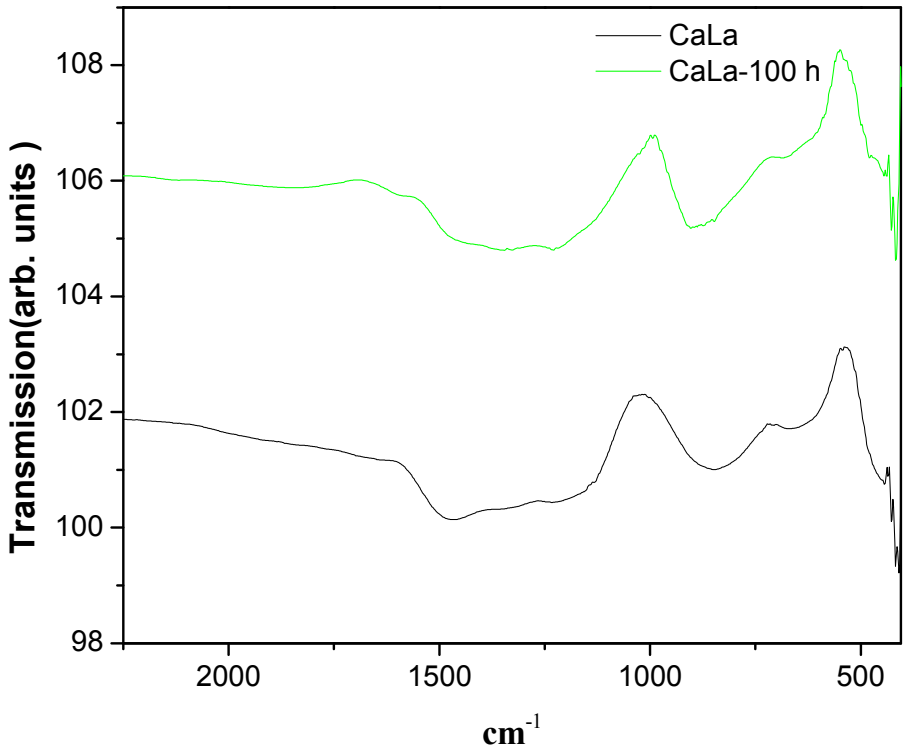

Figure 4.18: FTIR spectra of CaLa glass and glass ceramic heat treated for 1h and 10 h at 900°C.

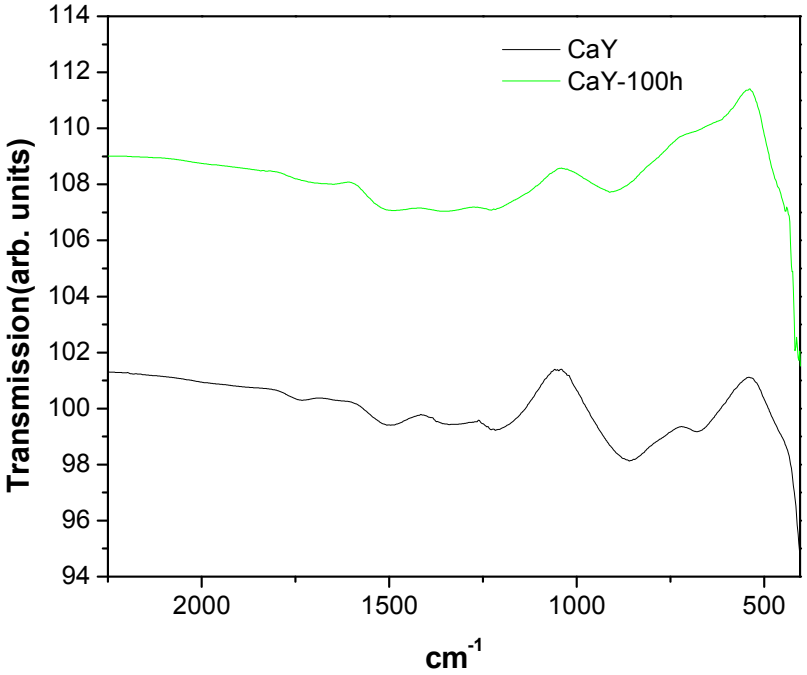

Figure 4.19: FTIR spectra of CaY glass and glass ceramic heat treated for 100 h at 800°C.

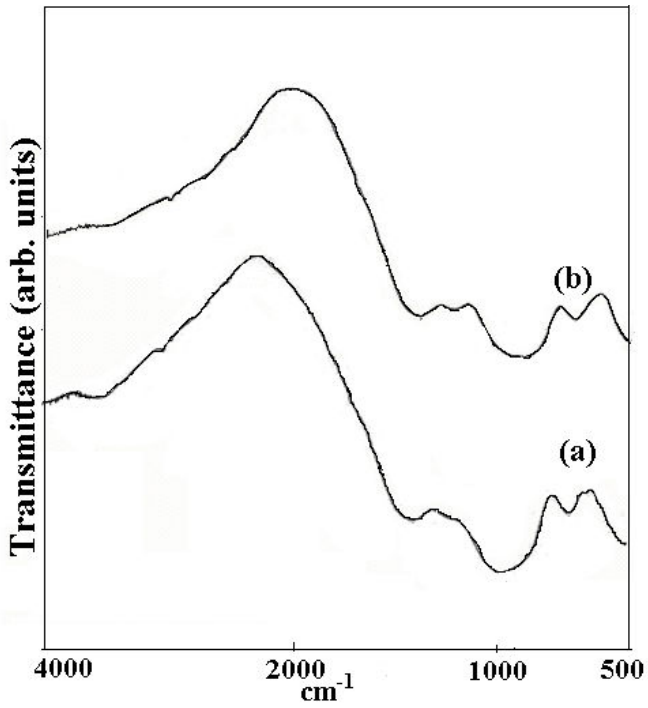

Figure 4.20: FTIR spectra of (a) CaAl glass and (b) CaCr.

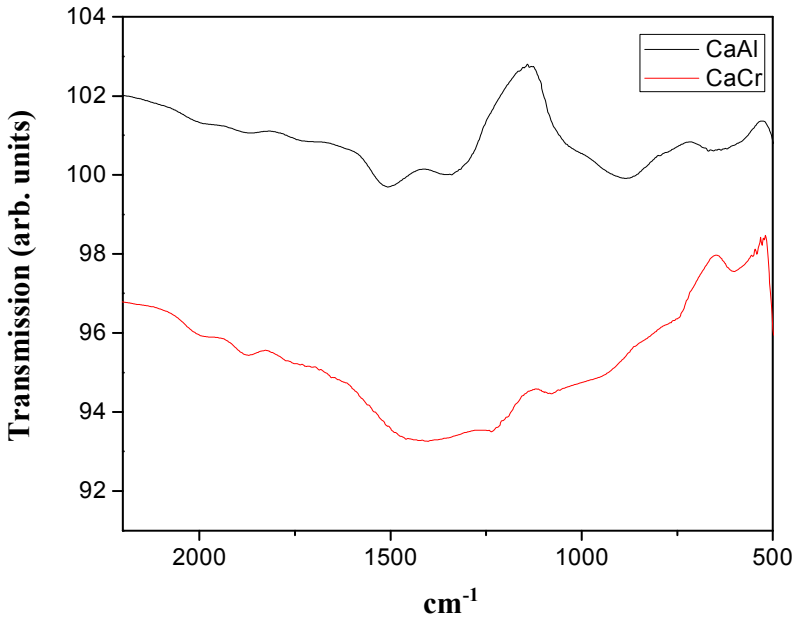

Figure 4.21: FTIR spectra of (a) CaAl and (b) CaCr glass ceramic heat treated at 800°C for 100 h.

The transmission band or peak within the frequency range 460-650 cm^{-1} signifies the bending vibrations of the Si-O-Si and O-Si-O bending modes and the region from 750-820 cm^{-1} is due to the formation of Si-O-Si symmetric stretching of bridging oxygen and there is little bit of decrease in peak intensity from parent glass to 1 hr heat treatment to 10 hrs. On the other hand, La_2O_3 containing glass, a special band centered appears at 1120-1320 cm^{-1} which is due to boroxol rings and borate stretching [14]. This peak might be attributed to BO_4 stretching which shifts to lower wave number with decreased intensity as time duration for heat treatment increases. There is another peak at 1328 cm^{-1} which is also due to boroxol rings and borate stretching. The transmission spectra of CaY (Fig.4.19) glass shows band in the frequency range of 638-726 cm^{-1} due to the vibrations of oxygen bridge between trigonal boron atoms. Another band is observed at

814-982 cm^{-1}. It is due to Si-O stretching with two non- bridging oxygens [5]. The transmission band at 1150-1240 cm^{-1} and the peak at 1328 cm^{-1} are due to the presence of borate groups (tri, tetra, pentaborate groups). Furthermore, a transmission band at 1450-1500 cm^{-1} is ascribed to B-O vibrations of various borate groups.

CaY could not show any appreciable change in the FTIR spectra (Fig 4.19) of glass (amorphous) and glass ceramics (100h). On the other hand CaLa sample shows remarkable difference in glass and glass ceramic due to regrouping in Si-O-Si and BO_4 structure. In case of CaAl glass (Fig 4.20) bands centered at 1504 cm^{-1} and 1340 cm^{-1} are due to borate group the ones at 874 cm^{-1} and 666 cm^{-1} are indicative of silicate network [11, 5]. The silicate band centered at 900 cm^{-1} is more intense before heat treatment. However, after heat treatment (Fig 4.21) the round contour of this band changes to a sharp peak. This indicates that diffused network of silicate in CaAl glass is getting ordered after heat treatment. Overall there is increase in sharpness of bands once a glass transforms into glass ceramic after heat treatment. Additionally, the shift of the bands at lower wave number in glass ceramic also indicates that these systems have more stability than their glass counterpart. The peaks centered at 1300 cm^{-1} and 1500 cm^{-1} are more intense for all amorphous glass except CaCr. The spectra for CaCr (Fig 4.20) does not show distinctive peaks or bands representative of borate and silicate network. Unlike other glasses CaCr was already crystalline in the as prepared form. The FTIR spectra before and after heat treatment for sample CaCr do not show much of a change.

4.8 Thermal expansion coefficient (TEC)

The thermal expansion coefficient of the splat-quenched and annealed glass is given in table 4.4. The transition point (T_g) and the softening point (T_s) of the investigated glass was calculated from the dilatometric curve. From the slope of the linear part of thermal expansion curve (i.e. 100-650°C) as shown in Fig 4.22 and Fig 4.23, the thermal expansion coefficients (TEC) of the glass and glass ceramics was calculated. The thermal expansion of parent glasses and glass ceramics is very close to required value for the sealant [15].

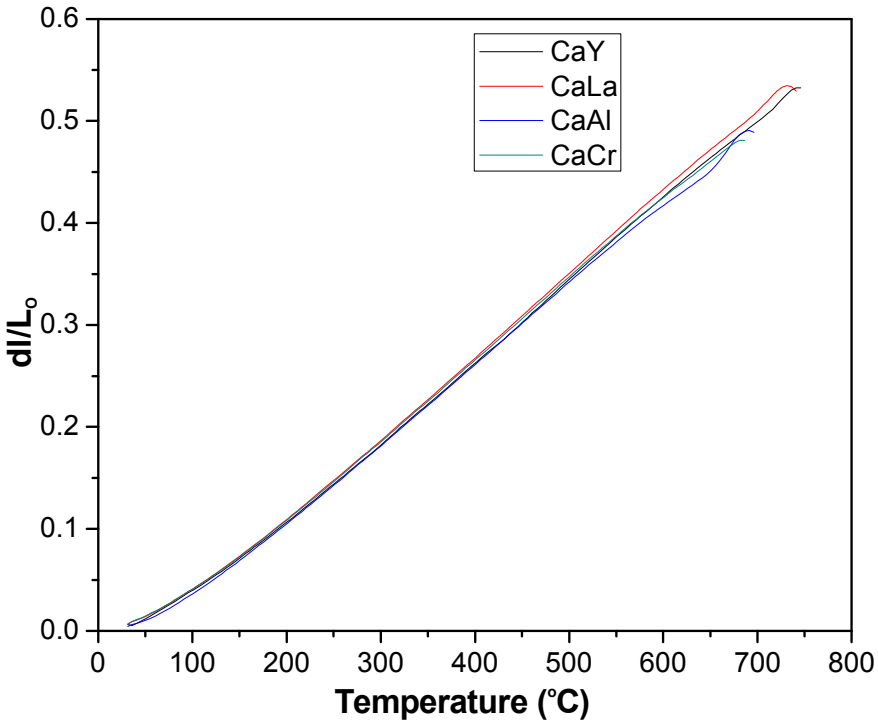

Figure 4.22: Thermal expansion curve of as prepared Calcium borosilicate glasses.

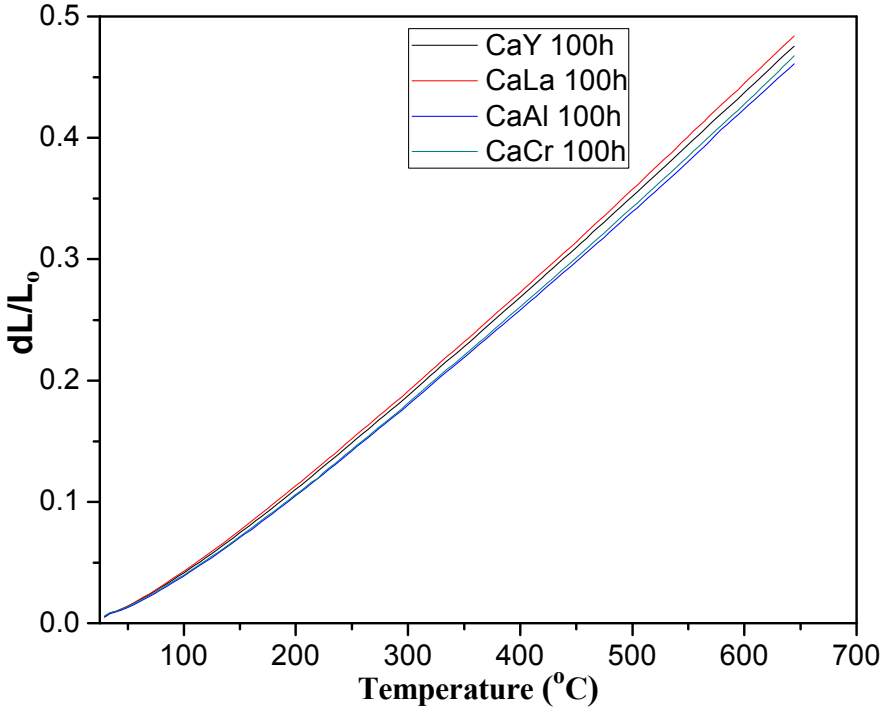

Figure 4.23: Thermal expansion curves of Calcium borosilicate glass ceramics after 100h heat treatment at 800°C.

Table 4.3 TEC for linear part of the curve 100-650 ºC.

Sample Name	TEC(10^{-6}/K) Glass	TEC(10^{-6}/K) Glass ceramic 800 ºC 10h	TEC(10^{-6}/K) Glass ceramic 800 ºC 100h
CaY	7.94	8.22	8.21
CaLa	8.06	8.43	8.42
CaAl	7.6	7.7	7.8
CaCr	7.6	7.8	7.8

The CaLa glass exhibited higher TEC value than all other glasses in present investigation. The higher TEC in this glass as compared to other glasses can be associated with the higher ionic radii of La^{3+}. Another important factor could be that after heat treatment when glass turns into glass ceramic the formation of crystalline phases may increase the TEC value. Although, crystalline phases have formed in CaAl sample as well but their volume fraction is more in case of CaLa glass ceramic. It is important to note that higher TEC value is observed in case of glass ceramics which were heat treated at 800°C for 10 and 100h as shown in table 4.4. This means TEC value improves when glass is heat treated in its crystallization range i.e. ≈ 800°C, where glass matrix undergoes maximum structural rearrangement.

4.9 Calculation of viscosity of glasses from dilatometer data

Mott and Gurney [16] proposed a simple liquid theory which established a relationship between pseudo-critiCal temperature (T_k) and the absolute melting point (T_m):

$$\frac{T_k}{T_m} = \frac{2}{3} \qquad (1)$$

Later on Beaman [17] proposed that eqn (1) can also be used for glasses and polymers. The modified equation can be written as [18]:

$$\frac{T_g}{T_l} = \frac{2}{3} \qquad (2)$$

The viscosity values of glasses are fixed and independent of materials [9]. These values are given in equation (3)

$$T_g \rightarrow \eta_g = 10^{12}\ \mathrm{d}Pa\ s,$$

$$T_s \rightarrow \eta_s = 10^{6.6}\ \mathrm{d}Pa\ s,$$

$$T_m \rightarrow \eta_m = 10^{4}\ \ \mathrm{d}Pa\ s \qquad (3)$$

According to the Vogel–Fulcher–Tamman (VFT) equation [19]:

$$\log \eta = A + \frac{B}{T - T_o} \tag{4}$$

where A, B and T_0 are constants. Using Eq. (3), these constants can be obtained by resolving coupled equations for the investigated glasses. The values of thermal expansion coefficient (TEC), transition temperature (T_g), softening temperature (T_s) and viscosity are obtained from dilatometer data. These values are used to calculate the viscosity of CaY, CaLa and CaAl glasses using VFT equation.

$$\log \eta = 4.18 + \frac{1020.11}{T - 935} \tag{5}$$

$$\log \eta = 4.42 + \frac{1015}{T - 832.29} \tag{6}$$

$$\log \eta = 3.77 + \frac{115}{T - 919} \tag{7}$$

Fig 4.24 shows viscosity versus temperature curves of CaY, CaLa and CaAl glasses using Eq. (5-7) respectively. The viscosity values of $10^{11.6}$dPa.s, $10^{8.6}$dPa.s and $10^{4.6}$dPa.s for CaY, CaLa and CaAl glasses at working temperature of SOFC i.e. 800°C are well within the required range for sealing material [20].

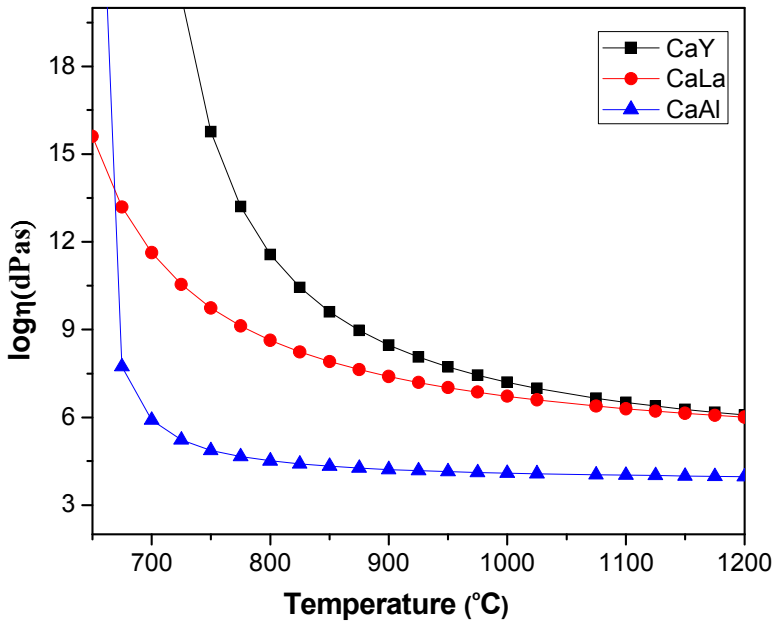

Figure 4.24: Plot of viscosity vs temperature for CaY, CaLa and CaAl glass.

4.10 Differential thermal analysis

The transition, crystallization and melting temperature of all the glasses are given in table 4.5. The crystallization peaks were observed to shift towards higher temperature with respect to the increasing heating rate in all the glasses which is because of delay in attaining thermal equilibrium. The activation energy of all the glasses were calculated using Kissinger equation [2, 3]

$$\ln(T_p^2/\beta) = (E_p/RT_p) + \text{constant} \qquad (8)$$

where β is heating rate and R is gas constant. From the experimental data a graph between ln (T_p^2/β) versus $(1000/T_p)$ was plotted as shown in Fig.4.25. The slope of this graph gives the activation energy (A.E) of transition. The A.E of transition for CaY glass is very high as compared to CaLa glass (table 4.5).

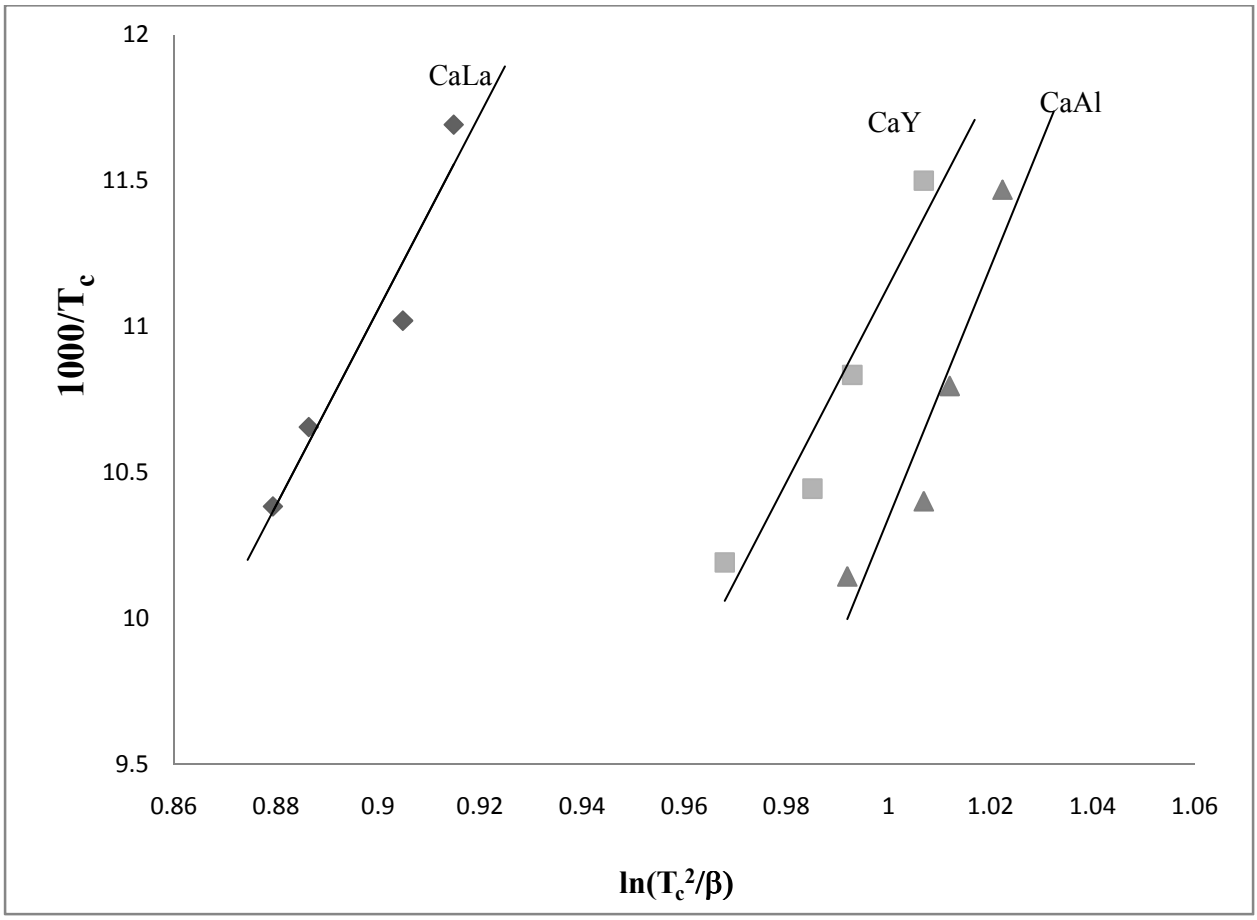

Figure 4.25: Kissinger plot of CaY, CaLa and CaAl glass.

Ray et al. [1] have reported that T_g is related to the density of covalent cross linking, number and strength of co-ordinate links formed between oxygen atoms and the cations and the oxygen density of network. Higher values of these factors correspond to higher T_g. In case of CaY glass, Y^{3+} might be acting as the network former where it may have higher number of covalent cross linking. The non bridging oxygen due to modification of glass network by Ca^{2+} might be bonded by Y^{3+} cations which lead to the higher T_g of this particular glass as compared to the CaLa glass. However, CaAl glass has the highest activation energy (A. E). The trend followed for A.E CaAl > CaY > CaLa is similar to the trend followed in case of barium based glasses. CaLa glass shows maximum volume fraction of crystalline phases after heat treatment because of lower A.E for

crystallization. Although difference in A.E for CaLa and CaY glass is not very large still CaY glass does not crystallize. According to our earlier reports also, presence of yttria in glass is known to inhibit or suppress crystallization. However, in case of CaAl glass the presence of 10 mol% Al_2O_3 makes it to act as glass modifier which results in enhanced connectivity in glass network thus increasing its A.E. Thermal data obtained from DTA measurement of these glasses was used to calculate the fragility index and activation energy for transition.

Table 4.4 Transition (T_g), crystallization (T_c), melting (T_m), T.G.A, activation energy and fragility index of glasses.

Sample name	T_g (ºC) Dilatometer	T_g (ºC) (DTA)	T_c (ºC)	T_m (ºC)	% Wt.loss 50-1000 (ºC)	A.E ($kJmol^{-1}$)	Fragility Index
CaY	710	690	810	910	2.5	278	40.4
CaLa	700	710	720	882	0.45	273	26.7
CaAl	660	640	705	870	1.3	312	19.3

4.10.1 Fragility index (F)

Generally, strong glass formers show Arrhenius type behavior in viscosity versus temperature curve. On the other hand non Arrhenius behavior is manifestation of fragile glass former [1]. Moreover, fragile glass exhibit weak interatomic/intermolecular bonding. For the present glasses, the fragility index value is calculated using the following relation [21, 22]:

$$F = \frac{E_g}{RT_g \ln 10} \qquad (9)$$

Where E_g is the activation energy for glass transition.

It is reported that fragility index for strong and fragile glass former varies from F=16 to F=20 respectively [23-24]. On the basis of calculations CaAl (F = 19.3) has strong glass forming liquid followed by CaLa (F = 26.7). Moreover, CaY (F = 40.4) is not a strong glass former compared to CaLa and CaAl glass.

4.11 Interaction study

The CaLa glass sample exhibited highest TEC among all the other glass samples. During heat treatment of this glass at 800 °C no detrimental crystalline phases were formed. Based on this CaLa glass was selected for interaction study with Crofer 22 APU. CaLa glass was cut into a thin rectangular slice having dimensions (10mm x 8mm x 1mm) using diamond cutter. This rectangular slice of glass was pressed between rectangular pieces of Crofer (10mm x 8mm x 2mm) and heated in tubular furnace for 25 h at 800 °C. The SEM microphotograph of CaLa/Crofer22APU diffusion couple heat-treated at 800 °C for 25h is shown in figure.4.26. The interface was analysed using SEM after the diffusion couple was cross-sectioned on the central part. The glass-ceramic exhibits fairly homogenous microstructure. Interface in the interior area was characterized by the formation of porosity of the order of few micrometers although the sealing glass was well bonded to crofer. The pores would have likely been created due to the formation of vapour species via the interaction of alloy element especially chromium with alkaline oxide in the glass.

EDS area analysis conducted at the marked point revealed the presence of Cr apart from Ca, Si and La. Chromium has diffused out of crofer into the glass. This observation further revealed that no undesired reactions took place and no corrosion products were formed.

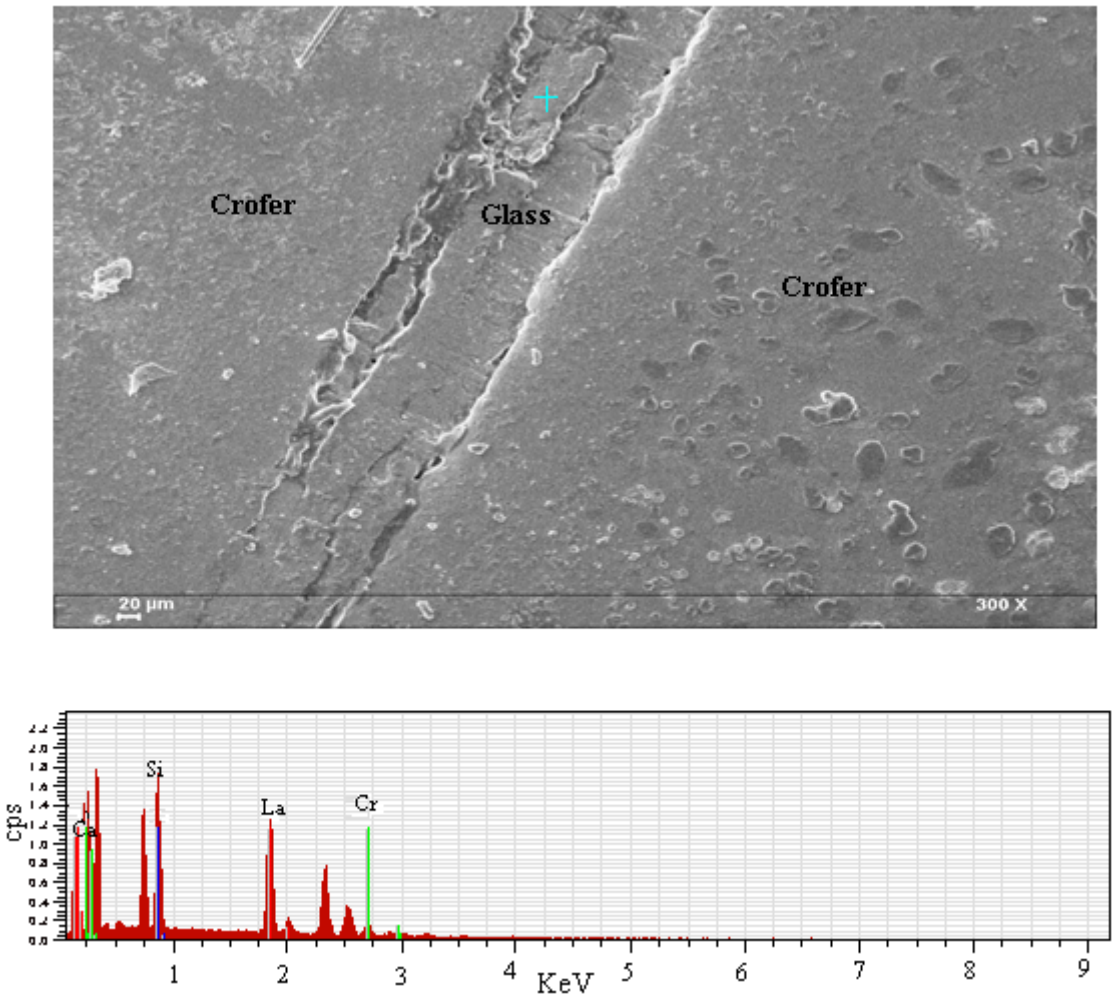

Figure 4.26: SEM microphotograph and EDS analysis of glass/ Crofer diffusion couple.

Summary

BaLa glass has the highest TEC value than BaAl, BaCr and BaY glasses. The highest activation energy is observed in BaCr glass followed by BaAl, BaY and BaLa glasses. BaLa and BaAl crystallized fully and did not form any detrimental crystalline phase(s) even after 100 h heat treatment in air. In Calcium borosilicate glasses, the phase separation tendency is more in CaLa glass as compared to CaY and CaAl glasses. The TEC has not changed appreciably for all the glass samples even after heat-treatment. Among the glasses examined in the present work, CaLa showed the best fluidity. A seal based on CaLa glass showed a good interface formation. The morphological analysis showed integrity of the seal/Crofer22APU joint region.

References

[1] N. H. Ray, J. Non-Cryst. Solids, 15 (1974) 423-434.

[2] H. S. Chen, J. Non-Cryst. Solids, 27 (1978) 257.

[3] H. E. Kissenger, Ann. Chem. 29 (11) (1957), p. 1702.

[4] Vishal Kumar, Anu Arora, O.P Pandey and Kulvir Singh, Int. J. Hydrogen. Energy, 33 (1) (2008) 434.

[5] Fatma H.A. Elbatal , Magda M.I. Khalil, Mater. Chem. Phy, 82 (2) (2003) 375.

[6] K .Singh, N. Gupta and O .P. Pandey, J. Mater. Sci, 42 (2007) 6426.

[7] A. Arora, E.R. Shaaban, K. Singh and O.P. Pandey, J. Non-Cryst. Solids, 354(33) (2008) 3944.

[8] M. K. Mahapatra, K. Lu, R. J. Bodnar, Appl Phys A, 95 (2009) 493-500.

[9] Saswati Ghosh, P. Kundu, A. Das Sharma, R.N. Basu and H.S. Maiti, J. Eur. Ceram. Soc, 28 (2008) 69–76.

[10] Ashutosh Goel , Dilshat U. Tulyaganov, Essam R. Shabaan , Christopher S.Knee, Sten Eriksson and Jose M.F. Ferreira, Acta Materialia, 56(13) (2008) 3065.

[11] L. Stoch and M. Sroda, J. Mol. Struct, 77–84 (1999) 511–512.

[12] S.-L. Lin and C.S., J. Non-Cryst. Solids, 202 (1996) 61–67.

[13] J.T. Kohli, J.E. Shelby, J.S. Frye, Phys. Chem. Glasses, 33 (1992) 73–78.

[14] N. P. Bansal and E. A. Gamble, J. Power Sources, 147 (2005) 107–115.

[15] F.Tietz, Ionics 5 (1999) 129.

[16] N. F. Mott and R. W. Gurney, Rep. Prog. Phys. 5 (1938), 46.

[17] R. G. Beaman, J. Polym. Sci. 9 (1952), 470.

[18] S. Sakka, and J. D. Mackenzie, J. Non-Cryst. Solids 6 (1971), 145.

[19] G. S. Fulcher, J. Am. Ceram. Soc.8 (1925), 39.

[20] L. Blum, R. Fleck and Jansing, US Patent 6165632, 2000

[21] R. Bohmer, K.L. Nagi, C.A. Angell and D.J. Plazek, J. Chem. Phys. 99 (1993), 4201.

[22] K. Chebli, J.M. Saiter, J. Grenet, A. Hamou and G. Saffarini, Physica B 304 (2001), 228.

[23] T.A. Viglis, Phys. Rev. B 47 (1993), 2882.

[24] A. Arora, A. Goel, E.R. Shaaban, K. Singh O.P. Pandey and J.M.F Ferreira

Physica B (2008) 403 1738.

5 Conclusions:

In this entire work four series of glasses were prepared by melt quenching technique. The chemical composition in mol % of the glasses is $40SiO_2$-$20B_2O_3$-$10A_2O_3$-30MO (A_2O_3=Y, La, Al, Cr and MO= Mg, Sr, Ba, Ca) where A represents intermediate oxides and M signifies the alkaline earth oxides. Of all the as prepared sixteen samples, only twelve were found to be glassy in nature. However, other set of glasses containing Cr as an intermediate oxide could not form glass completely.

All the as prepared samples were characterized by XRD, TGA/DTA, Dilatometer and FTIR techniques. The magnesium based glass samples exhibit higher T_g, T_c, T_m with higher thermal stability which may be due to higher field strength of Mg^{2+} than Sr^{2+}, Ca^{2+} and Ba^{2+} cations. The thermal expansion coefficient of strontium containing glasses is higher than magnesium based glasses. This is attributed to formation of a strong glass matrix due to which bonding is strong. In case of strontium based glasses TEC of VS1 sample is higher than other samples and it is also comparable to the other components of SOFC which can make it a suitable choice as sealant for SOFC applications.

In case of VS2 glass the DTA curve indicates that glass exhibits phase separation and a broad endotherm corresponding to T_m with splitting around ~895 °C and 930 °C. Based on this data, glasses were heat-treated at 900°C and 950°C for 1 and 10 h duration. The heat treated glasses exhibit the nucleation of monoclinic Sr_2SiO_4, $SrSiO_3$, orthorhombic Sr_2SiO_4 and $LaBO(SiO_4)$ phases. It was observed that less symmetric monoclinic Sr_2SiO_4 phase gets converted to more symmetric orthorhombic Sr_2SiO_4 phase. Texture coefficient parameters indicate variation in alignment of phases as temperature and time duration of heat-treatment was increased.

The SrO based glasses have lower softening temperatures so these glasses were chosen for chemical interaction with doped bismuth vanadate, which is a high ionic conducting electrolyte in intermediate temperature range (600-800 ºC). The chemical interaction studies of these glasses with $Bi_4V_{1.8}Al_{0.2}O_{11}$ electrolyte were also performed at 800°C for different heat treatment durations. Of all the three samples, VS3 glass shows higher chemical and thermal stability with doped bismuth vanadate. In all reaction products, $SrVSi_2O_7$, AVO_4 and A_2SiO_5 (A= Y, La, Al) phases are formed. Apart from this, chemical composition of $Bi_4V_{1.8}Al_{1.8}O_{11}$ electrolyte gets modified due to diffusion of V^{5+} and Bi^{3+} into glasses especially where Y_2O_3 and La_2O_3 were used as intermediate oxides in glasses. Cristobalite phase which is detrimental for SOFC application did not form in any reaction product. The FTIR spectra of all the samples exhibit three bands i.e. 400-600 cm^{-1}, 650-800 cm^{-1} and 800-1300 cm^{-1}. These spectra are assigned to bending vibrations of the Si-O-Si linkages, bending vibrations of the A-O (A= Y, La, and Al) bonds and stretching vibrations of the SiO_4 tetrahedron with the different numbers of bridging oxygen atoms. The study indicates that VS3 glass can work as a sealant for DBiV at working temperature of SOFC.

The influence of intermediate oxides (Y, Al, La and Cr) on thermal, structural and crystallization kinetics of barium borosilicate glasses has been studied. BaY glass shows higher glass transition (T_g) temperature with higher stability than BaAl and BaLa glasses. The TEC value of BaY, BaLa, BaAl glass ceramics was observed to be higher than their glass counterparts due to formation of crystalline phases. The percentage change in TEC depends on the faction of crystalline phase in glass matrix and its chemical nature and structure. The maximum value of TEC was recorded after 100 h heat treatment of the glasses. These heat treated glass ceramics had TEC in the range of 7.67-8.10 x 10^{-6} K^{-1} which is lower than Crofer (11.5 x 10^{-6} K^{-1}). However, it is close to the permissible limit required for SOFC operation (9-

12 x 10^{-6} K^{-1}). The FT-IR spectra of glass ceramics showed more sharpness with splitting in transmission bands compared to the as prepared glass due to ordered arrangement of silicate bands. After heat treatment at 800° C for 100 h, no detrimental crystalline phase is observed for SOFC application. Unlike others melting point of BaCr glass ceramic is higher than1000°C. Moreover, due to the presence of Cr_2O_3 in glass as well as in Crofer 22 APU this glass was selected to study its bonding characteristics with Crofer 22 APU. The interface between BaCr glass ceramic and Crofer 22 APU is devoid of any cracks and with the increase of heat treatment time it becomes smoother and shows good adherence to the Crofer. The major elements present at the interface are Fe, Cr and Ba.

Similar results were observed in case of calcium based glasses. The TEC value of CaL, CaAl glass ceramics was observed to be higher than their glass counterparts due to formation of favorable crystalline phases. Compared to lanthanum, yttrium as an intermediate oxide exhibited an increase in activation energy for crystallization. Thus, effectively suppressing the phenomenon of crystallization. However in case of CaAl glass the presence of 10 mol% Al_2O_3 makes it to act as glass modifier which results in enhanced connectivity in glass network thus increasing its A.E. The FTIR spectra of as prepared glasses show the presence of prominent peaks due to borate and silicate groups. The heat treated glasses show a shift in the bands towards lower wave number which indicates that these systems have more stability than their glass counterpart.

The selection of chromium as an intermediate oxide in the present sample could not form glass. In case of chromium the as prepared sample was a glass ceramic already having crystalline phase. Magnesium based sample did not form glass or glass ceramic even after heating the melt at prolonged time for 1550 °C.

Future Scope

After characterizing and studying in detail, it is observed that lanthanum and yttrium series of all glass composition exhibits suitable TEC and phase stability even at high temperature. These glasses are more stable as compared to other glasses comprising of aluminum and chromium. For more promising and favorable results the study of interaction of these glass sealants with 8YSZ and Crofer 22 APU should be done for 100 and 1000 h. In order to optimize these glasses to be used as sealants a lot of work remains to be done. The most important characterization yet to be realized for glasses as sealants is their testing in real SOFC working conditions. The new reaction surfaces or the interface thus formed should be analyzed. Apart from this, new glass series comprising of yttrium and lanthanum should be developed and studied in detail.